Orientation of Non-Native 2-Monosubstituted and 2, 3-Disubstituted 1, 4-Naphthoquinones in the A_1 Binding Site of PSI and the Effect on the Rate of Electron Transfer: An Electron Paramagnetic Resonance Spectroscopy Study

by

Sarah Anne E. Brown, B.Sc.

A thesis submitted to the Department of Chemistry

in partial fulfillment of the requirements

for the degree of

Master of Science

May, 2003

Brock University

St. Catharines, Ontario

Abstract

The process of oxygenic photosynthesis is vital to life on Earth. The central event in photosynthesis is light induced electron transfer that converts light into energy for growth. Of particular significance is the membrane bound multisubunit protein known as Photosystem I (PSI). PSI is a reaction centre that is responsible for the transfer of electrons across the membrane to reduce $NADP^+$ to NADPH. The recent publication of a high resolution X-ray structure of PSI has shown new information about the structure, in particular the electron transfer cofactors, which allows us to study it in more detail.

In PSI, the secondary acceptor is crucial for forward electron transfer. In this thesis, the effect of removing the native acceptor phylloquinone and replacing it with a series of structurally related quinones was investigated via transient electron paramagnetic resonance (EPR) experiments. The orientation of non native quinones in the binding site and their ability to function in the electron transfer process was determined.

It was found that PSI will readily accept alkyl naphthoquinones and anthraquinone. Q band EPR experiments revealed that the non-native quinones are incorporated into the binding site with the same orientation of the headgroup as in the native system. X band EPR spectra and deuteration experiments indicate that mono-substituted naphthoquinones are bound to the A_1 site with their side group in the position occupied by the methyl group in native PSI (*meta* to the hydrogen bonded carbonyl oxygen). X band EPR experiments show that 2, 3- disubstituted methyl naphthoquinones are also incorporated into the A_1 site in the same orientation as phylloquinone, even with the presence of a halogen- or sulfur-containing side chain in the position normally

occupied by the phytyl tail of phylloquinone. The exception to this is 2-bromo-3-methyl naphthoquinone which has a poorly resolved spectrum, making determination of the orientation difficult.

All of the non-native quinones studied act as efficient electron acceptors. However, forward electron transfer past the quinone could only be demonstrated for anthraquinone, which has a more negative midpoint potential than phylloquinone. In the case of anthraquinone, an increased rate of forward electron transfer compared to native PSI was found. From these results we can conclude that the rate of electron transfer from A_1 to F_X in native PSI lies in the normal region of the Marcus Curve.

Acknowledgements

First and foremost, I would like to thank my supervisor, Dr Art van der Est, who has been incredibly helpful through every step of this project. Thank you for all of the explanations, nudges in the right direction and occasional laughter at my expense! I couldn't have asked for a better supervisor. Yes, integrals build character and math is my friend...I guess.

Thank you to Dr Richardson and Dr Rothstein for the encouragement at my committee meetings, and for all the help and advice, especially with the writing of this thesis.

Thank you, Dr Bruce, for once again putting up with this 'evil chemist' invading your lab! PS, Photosystem I will always be the best Photosystem.

To Ray, Mike, Mike, Anjali, Sergej, Maryam, Yana, Ingelõg, Olena, Alfia and Yuri, thanks for all of the good times along the way, especially the annual trek to Wood's Hole.

Danke schön to Dietmar Stehlik, Julia Pushkar and Stefan Zech, our collaborators at the Free University of Berlin, for making me feel very welcome during my stay. The lab was fantastic, our discussions were very valuable and the 'field trip' to the Pergamon was amazing!

Thank you to Dr Herbert Zimmerman of Max-Planck Institute who very kindly supplied us with the perdeuterated and selectively deuterated naphthoquinones used in this study.

Lastly, I would like to thank my parents for their support. Mom and Dad, thank you for your strength during the past two years. You are very special people and have always encouraged me without pressuring me. Thank you.

> "Nature set herself the task of capturing the light flooding towards the earth and storing this, the most elusive of all forces, by converting it into an immobile force...the plant world constitutes a reservoir in which the fleeting sun rays are fixed and ingeniously stored for future use, a providential measure to which the very existence of the human race is inescapably bound"[33]
>
> Julius Robert Mayer, 1845

Table of Contents

List of Abbreviations

PSI: Photosystem I
PSII: Photosystem II
EPR: Electron Paramagnetic Resonance Spectroscopy
PhQ, VK1: Phylloquinone, Vitamin K1
P_{700}: Primary electron donor of PSI, a chlorophyll dimer
A_0: Primary electron acceptor of PSI, a chlorophyll molecule
A_1: Secondary electron acceptor of PSI, a phylloquinone molecule
F_X, F_A, F_B: Iron sulfur clusters, the terminal electron acceptors of PSI
E_M: Midpoint potential
NQ: 1, 4-Naphthoquinone
MNQ: 2-Methyl-1, 4-Naphthoquinone
ENQ: 2-Ethyl-1, 4-Naphthoquinone
AQ: 9, 10-Anthraquinone
BrMNQ: 2-Bromo-3-Methyl-1, 4-Naphthoquinone
ClMMNQ: 2-Chloromethyl-3-Methyl-1, 4-Naphthoquinone
ETMNQ: 2-Ethylthio-3-Methyl-1, 4-Naphthoquinone
OH-PhQ: Hydroxy-phylloquinone
d6-NQ: Perdeuterated NQ
d8-MNQ: Perdeuterated MNQ
d10-ENQ: Perdeuterated ENQ
d2-ENQ: Partially deuterated ENQ
PNQ: 2-phytyl-1, 4-Naphthoquinone

List of Figures

Chapter 1

Introduction

Evolution of Photosynthesis

Photosynthesis is arguably the most important process on Earth. This is a bold statement, perhaps, but consider the following: Without photosynthesis, life as we know it would not exist. Initially the atmosphere of the Earth was anaerobic and the bacteria that existed used compounds such as hydrogen sulfide, H_2S, instead of water to convert light from the sun into energy to grow[1, 2]. These anaerobic bacteria were able to survive in the oxygen-free atmosphere but it made the existence of aerobic species impossible. Then an early ancestor of modern photosynthetic organisms evolved the ability to use water as a reductant in photosynthesis, releasing oxygen as a waste product[1, 2]. Since there was abundance of water available, much more than H_2S, and water was found

literally everywhere, the oxygen-evolving bacteria thrived and in short, began to take over. The bad news was that oxygen is a strong oxidant and was poisonous to most other organisms, except for those which were able to adapt and develop defenses against its damaging effects. This was a turning point for life on Earth, as the atmosphere became oxygenated it set the stage for the development of life as we know it[2]. A few species of anaerobic bacteria retreated to sulfur springs[46] and other locations without oxygen--where they are still found today--and early aerobic bacteria began the process of evolving into modern cyanobacteria[2]. It is thought that the chloroplasts of higher plants and algae evolved by 'engulfing' oxygen-evolving bacteria, which explains why the process is so similar in eukaryotic photosynthetic organisms and oxygenic photosynthetic bacteria[2].

Photosynthesis has been around a lot longer than we have, and it is vitally important for life, yet despite its importance many details remain poorly understood. The process of photosynthesis can be described very simply in a one line equation[13]:

$$CO_2 + H_2O + \text{Light} \rightarrow CH_2O + O_2$$

However, the apparent simplicity of this reaction is deceptive. Photosynthesis requires a series of reactions that have been termed light and dark[13]. A closer examination of the structure of photosynthetic organisms reveals that all contain either one or two protein complexes known as reaction centres. It is here where the light reactions of photosynthesis take place. In oxygenic photosynthetic organisms there are two reaction centres which are referred to as Photosystem I and II. Anaerobic bacteria have only one reaction centre[2]. The reaction centres in these species of bacteria are either of the type I or type II variety, in analogy to Photosystem I and II in oxygenic systems[2].

Type I and Type II Reaction Centres

Type I reaction centres are also known as Iron-sulfur type reaction centres, and type II are also called Quinone-type reaction centres[47]. All photosynthetic organisms contain either a Type I reaction centre, a Type II reaction centre, or both. In higher plants and cyanobacteria the two types of reaction centres (Photosystem I and Photosystem II) are found embedded in the thylakoid membrane[3]. In eukaryotic photosynthetic organisms the thylakoid is located in the chloroplasts. Type I reaction centres are characterized by the 4Fe4S clusters that make up part of the electron transfer chain[47]. Type II reaction centres have a mobile quinone molecule that acts as an electron shuttle[4]. The two types of reaction centres are shown in the following cartoon.

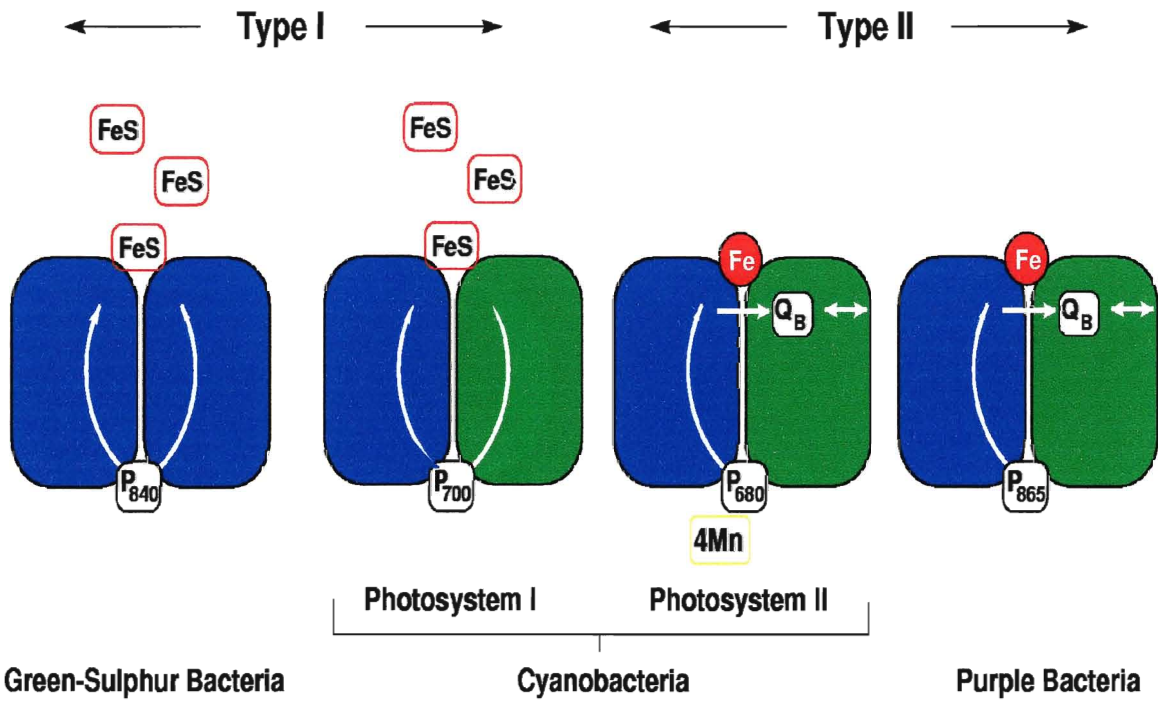

Figure 1-1: Comparison of Type I and Type II Reaction Centres (A. v d E)

This illustrates the overall structure type I and type II photosystems. The two ovals represent the main protein subunits of the reaction centres and the colors indicate

whether the reaction centre is a homodimer or a heterodimer. What all species have in common is the presence of the primary electron donor, which is a chlorophyll dimer that absorbs at wavelengths varying from 680 nm to 865 nm. Before its identification as a chlorophyll dimer, it was referred to as a Pigment (P) and its absorbance maximum. Thus we know them as P_{680}, P_{700}, P_{865} and so on. The difference in the absorbance maximum is an interesting point about the adaptability of these species of bacteria to use the available light. The arrows indicate the direction of electron transfer up one or both branches of the reaction centres. It can be seen in the figure that in Type II reaction centres the electron transfer is up only one of the branches and in Type I homodimers (such as Green-Sulphur bacteria) it is assumed that electrons are transferred up both branches. In PSI, it still under debate whether electron transfer occurs up one or both branches. FeS stands for the iron sulfur clusters that are the terminal electron acceptors in Type I reaction centres. Q_B is the mobile quinone molecule that acts as an electron shuttle in Type II reaction centres[4]. These reaction centres are what drive the light reactions of photosynthesis, which result in ATP synthesis, the reduction of $NADP^+$ to NADPH and the splitting of water molecules to release oxygen. The structures of PSII and PSI are known in detail, so we will begin by taking a closer look at these complexes.

Photosystem II

Photosystem II is a Type II reaction centre, also known as a quinone type. PSII has several important jobs, including the splitting of water molecules. This releases electrons and helps build the proton gradient needed for ATP synthesis[6]. The side product of water oxidation is the released oxygen molecules. As well, light energy is converted to electrical potential when a charge separation occurs across the thylakoid membrane[4].

PSII consists of 17 subunits and 13 cofactors and has a mass of about 300 kDa[6]. The following is a cartoon depicting the structure of PSII.

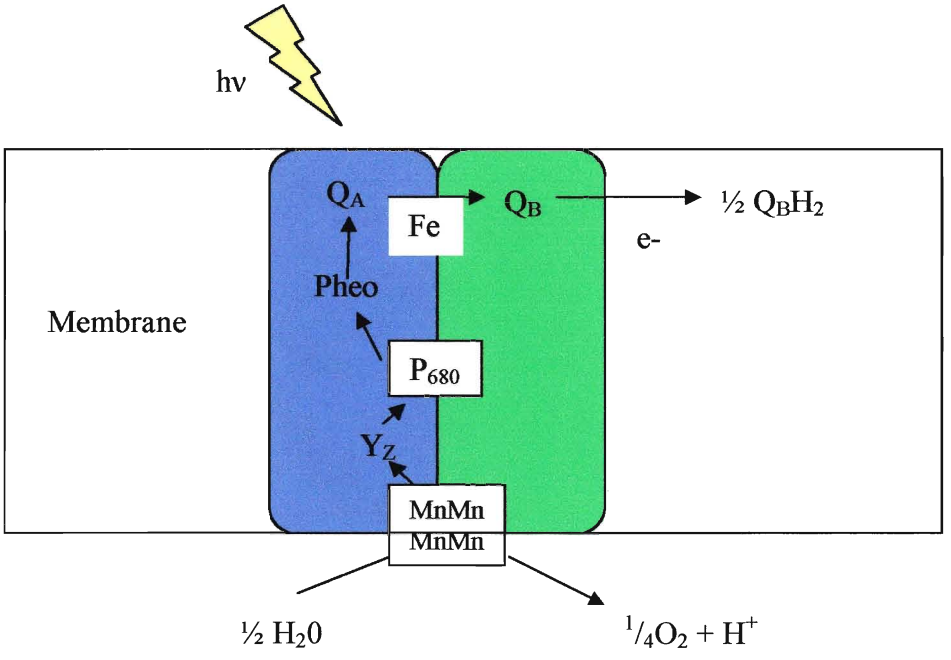

Figure 1-2: Schematic diagram of PSII (Based on a diagram from reference 7)

The important features of PSII include the water splitting complex and the chain of cofactors responsible for transferring electrons, including P_{680}, Pheophytin, Q_A and Q_B.

With the absorption of a photon P_{680} is excited to P_{680}^* and donates an electron to a pheophytin. This electron is then transferred to Q_A, a bound plastoquinone molecule. P_{680}^+ is reduced by an electron from a Tyrosine (Y_Z), which is reduced by the manganese cluster. After four turnovers of the reaction centre and the removal of four electrons from the manganese cluster, it is re-reduced by splitting two water molecules, releasing O_2 and 4 protons[4]. On the acceptor side, Q_A donates electrons to Q_B, a mobile plastoquinone which binds to PSII to receive electrons. Following two turnovers of the reaction centre, Q_B^{2-} picks up two protons and is released into the plastoquinone pool as a quinol and is replaced by a fresh plastoquinone[4].

The other type of reaction centre that is present in oxygenic photosynthetic organisms is Photosystem I. It is responsible for transferring electrons across the thylakoid membrane to reduce $NADP^+$ to NADPH

Photosystem I

Photosystem I, or PSI, is a multi-subunit protein that transfers electrons from the lumen to the stroma. This "light-driven plastocyanin-ferridoxin oxidoreductase"[3] is also found embedded in the thylakoid membrane. Cyanobacterial PSI contains 11 – 12 protein subunits, while plant PSI has 3 additional subunits[3]. The following is a schematic diagram of PSI.

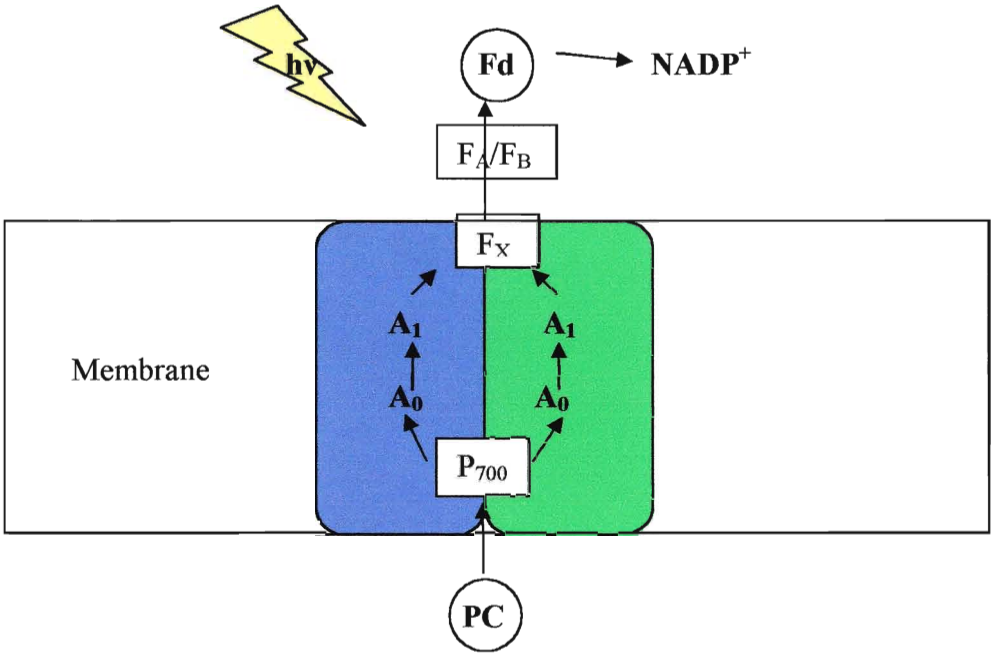

Figure 1-3: Schematic Diagram of PSI (Based on a figure from reference 8)

The two main subunits are PsaA and PsaB; it is to these proteins that the primary donor (P_{700}) and primary and secondary electron acceptors (A_0 and A_1) are bound on the stromal side of the protein[3]. PsaC, PsaD, PsaH and PsaE contain the ferredoxin (Fd)

docking site, and bind the two FeS clusters that function as terminal electron acceptors (F_A and F_B)[3]. PsaN and PsaF form the plastocyanin (PC) docking site[3]. Photosystem I contains 95 chlorophyll *a* molecules, 1 chlorophyll *a'* molecule, 22 beta-carotene molecules, 2 phylloquinones, 3 iron sulfur clusters, a Ca^{2+} ion, and 4 lipids and has a mass of 350 KDa[3, 12]. The chlorophyll molecules are used to collect photons and those at the core of the reaction centre are also involved in electron transfer[3]. The beta-carotenes are also light harvesters, and provide protection from light damage[3]. The phylloquinones and iron sulfur clusters are involved in electron transfer, while the roles of the Ca^{2+} ion and lipids are not yet known, but may be structural[3]. The role of phylloquinone as an electron acceptor was established in the 1980's and spectroscopic studies from the 1980's up to the present have revealed some aspects of the binding site[11, 32, 48, 49, 50, 51, 52 and references within]. In 1993, a low resolution (6 Å) X ray structure of PSI gave some insight into the structure of the binding site, however, the information was incomplete[21]. It showed the position of 45 chlorophyll *a* molecules and the three FeS clusters but the location of the primary electron donor, primary electron acceptor and secondary electron acceptor could not be determined without a doubt[21]. In 1997 the 4 Å structure revealed more detail about the structure, particularly about the locations of the antenna chlorophylls[3]. Recently the high resolution (2.5 Å) X ray structure was determined, and this provides a basis for studying the structure and function of phylloquinone in its binding site in more detail. It has resolved some features of PSI that, up to this point, had been unknown or ambiguous[10, 12]. The structure is shown in the following figure.

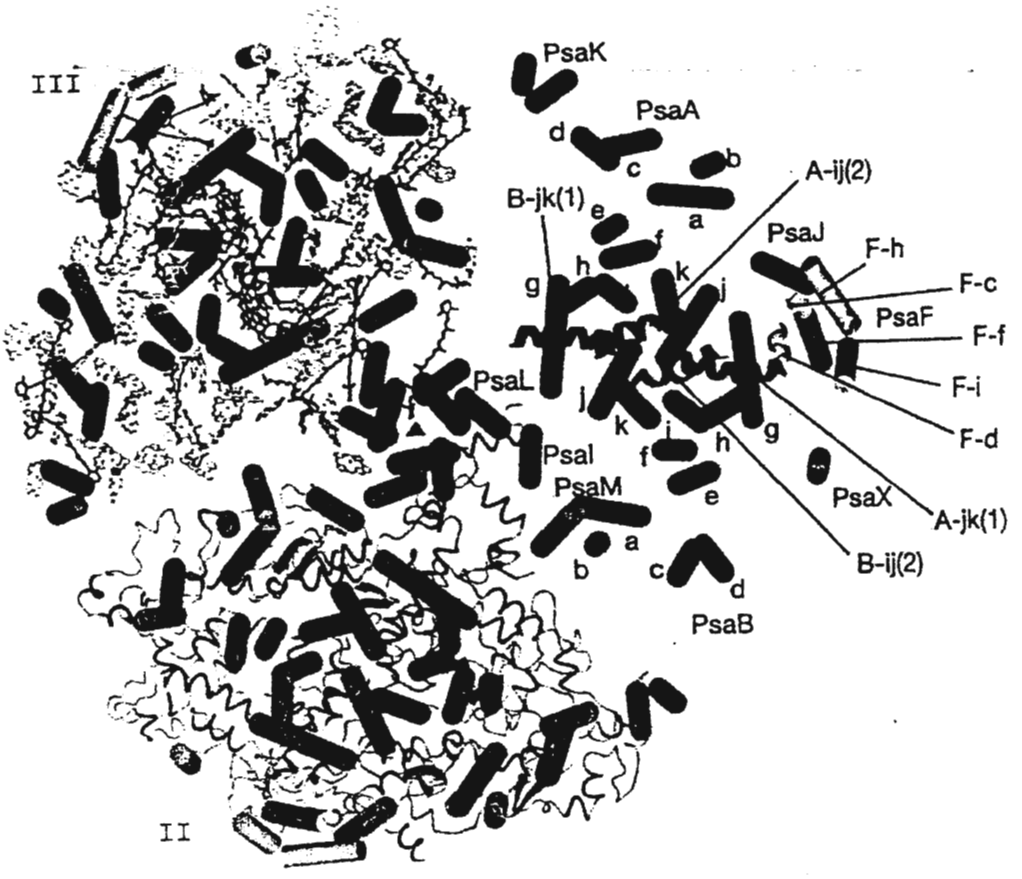

Figure 1-4: The X-ray structure of Photosystem I (From Jordan *et al.*, 2001)[12]

This figure illustrates that cyanobacterial PSI crystallizes as a trimer, that is, a group of three identical PSI units grouped together and it is also a trimer in the membrane[10, 12]. In this figure, the monomers are labeled I, II and III and each highlights a particular feature about the structure of PSI[12]. In one of the PSI units (labeled I) only the helices are shown to give a clearer picture of the subunits of PSI. Monomer II shows the "membrane-intrinsic subunits"[12] along with the α-helices[12]. The unit labeled III shows the helices, chlorophylls, carotenoids and quinone cofactors[12].

The cofactors involved in electron transfer are bound to the subunits PsaA and PsaB by helices g-j at the centre of the reaction centre (see monomer I)[12] and by PsaC

which is bound to the stromal surface and is not shown in Figure 1-4[3, 12]. The electron transfer cofactors are called P_{700}, A_0, A_1, F_X, F_A and F_B[3]. P_{700} is the primary electron donor, it is a chlorophyll dimer that when excited by a photon of light, donates an electron to A_0, the primary electron acceptor, which is a chlorophyll molecule. A_0 transfers an electron to the secondary electron acceptor, A_1, which is a phylloquinone molecule and A_1 transfers an electron to the terminal electron acceptors which are Iron-Sulfur clusters known as F_X, F_A and F_B that give PSI the classification as a type I reaction centre. Once F_B is reduced the electron is passed to a soluble ferredoxin which docks onto the reaction centre[3]. This all occurs on an extremely fast timescale which is shown in the following figure[18].

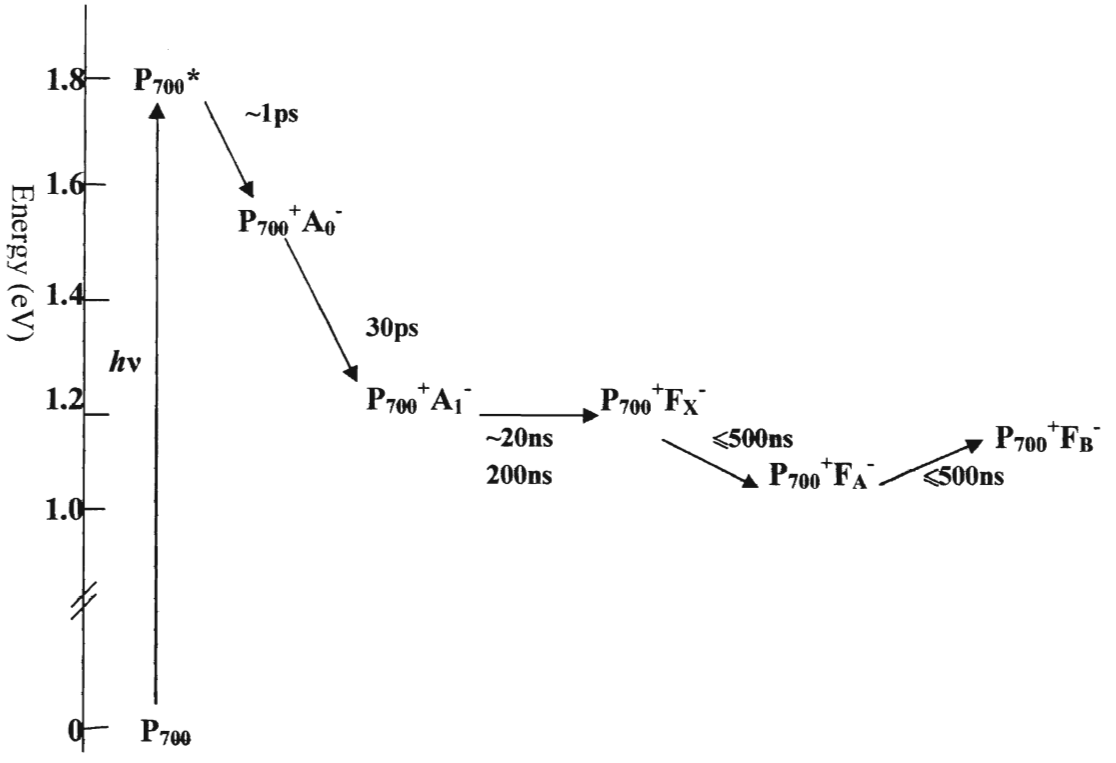

Figure 1-5: Rates of Electron Transfer in PSI (Based on figure from Brettel & Liebl, 2001)[18]

After the excitation of P_{700}, the electron is transferred to A_0 in about a picosecond[18]. Electron transfer from A_0 to A_1 occurs in about 30 picoseconds. Electron transfer from A_1 to F_X has a fast phase and a slow phase of about 20 ns and 200 ns. Studies have determined that electron transfer from $P_{700}^+F_X^-$ to F_A and F_B occurs on a timescale of about 500 ns or less[18], but the exact rates for these two steps are unknown[18,53]. The reason behind the two phases of electron transfer from A_1 to F_X is currently under debate. It has been proposed that the fast phase (20 ns) is due to an equilibrium being set up between $P_{700}^+A_1^-$ and $P_{700}^+F_X^-$. The slow phase (200 ns) results from the electron being transferred from F_X to F_A[18]. There are there are two branches of electron transfer cofactors, one branch is bound primarily by PsaA, the other by PsaB. It has been proposed that the two phases correspond to electron transfer up the two branches of PSI, with electron transfer occurring at different rates in each branch[18, 39, 50, 54, 55]. At this point, the experimental data supports both theories and the question is still under debate.

Another feature that has been revealed by the 2.5 Å structure of PSI is the distance between the cofactors in the electron transfer chain. Studies on electron transfer by Dutton *et al.*[56, 60] have shown that the rate is strongly distance dependent. An interesting question is whether or not the distances between cofactors in PSI have been optimized. The following figure shows the approximate positions of the cofactors in the A and B branches and the structures of the cofactors involved in electron transfer[10]. This is important, as it suggests that the A branch and B branch of PSI are not, in fact, identical.

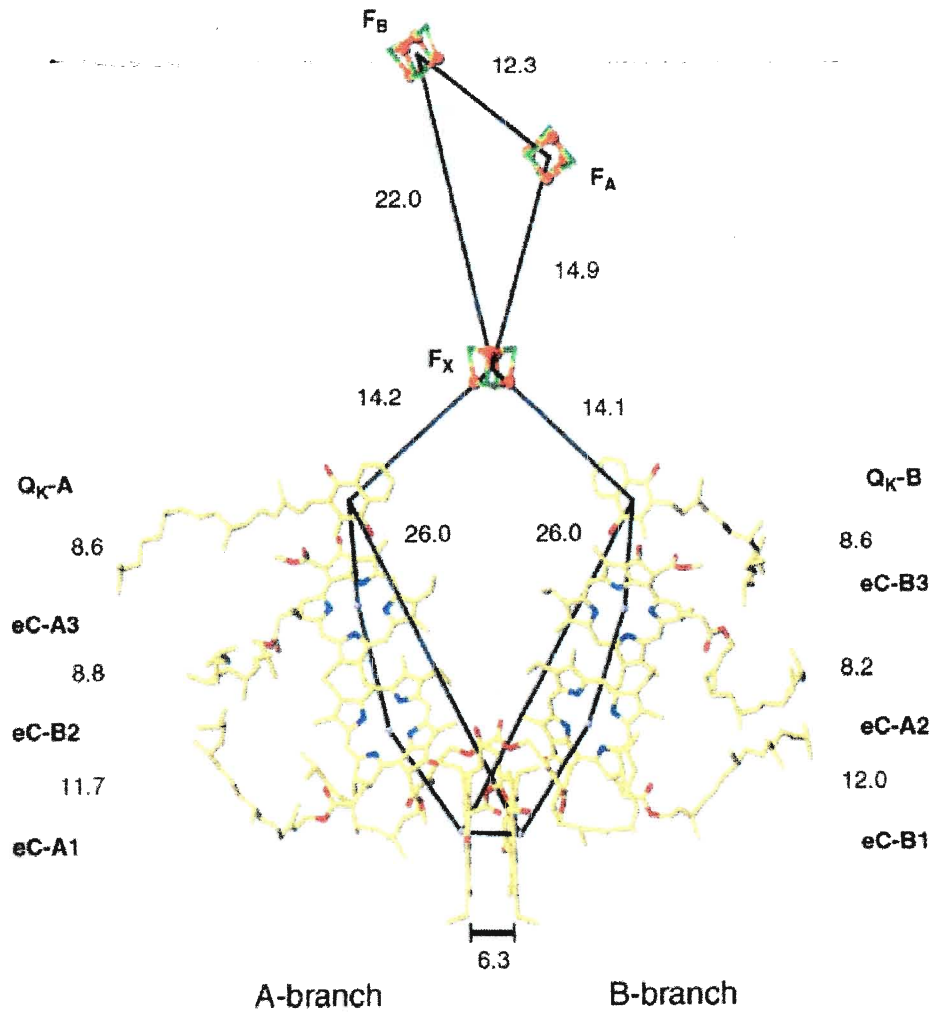

Figure 1-6: Distances between the Cofactors of PSI (from Fromme et al, 2001)[10]

Note that the distances between the cofactors in the A and B branches are slightly different. This could mean that electron transfer is favored up one branch. However, that raises a question: why go to the trouble and energy expense of creating two branches, if only one is going to be used? This is a convincing point for the two-branch theory. On the other hand, since both branches converge at F_X there is no advantage to having two branches either. It could be that one branch is used for electron transfer and the other retained for backup, in case of damage. To date, these questions are still under debate.

For oxygenic photosynthesis, these two reaction centres, PSI and PSII work in tandem. This process is shown most often in a diagram known as the Z Scheme.

The Z Scheme

The Z scheme is shown in the following figure and gets its name from the shape formed by the rapid increase and gradual decrease in energy of the cofactors as the photosynthetic species absorbs light and electrons are transferred through PSII and PSI.

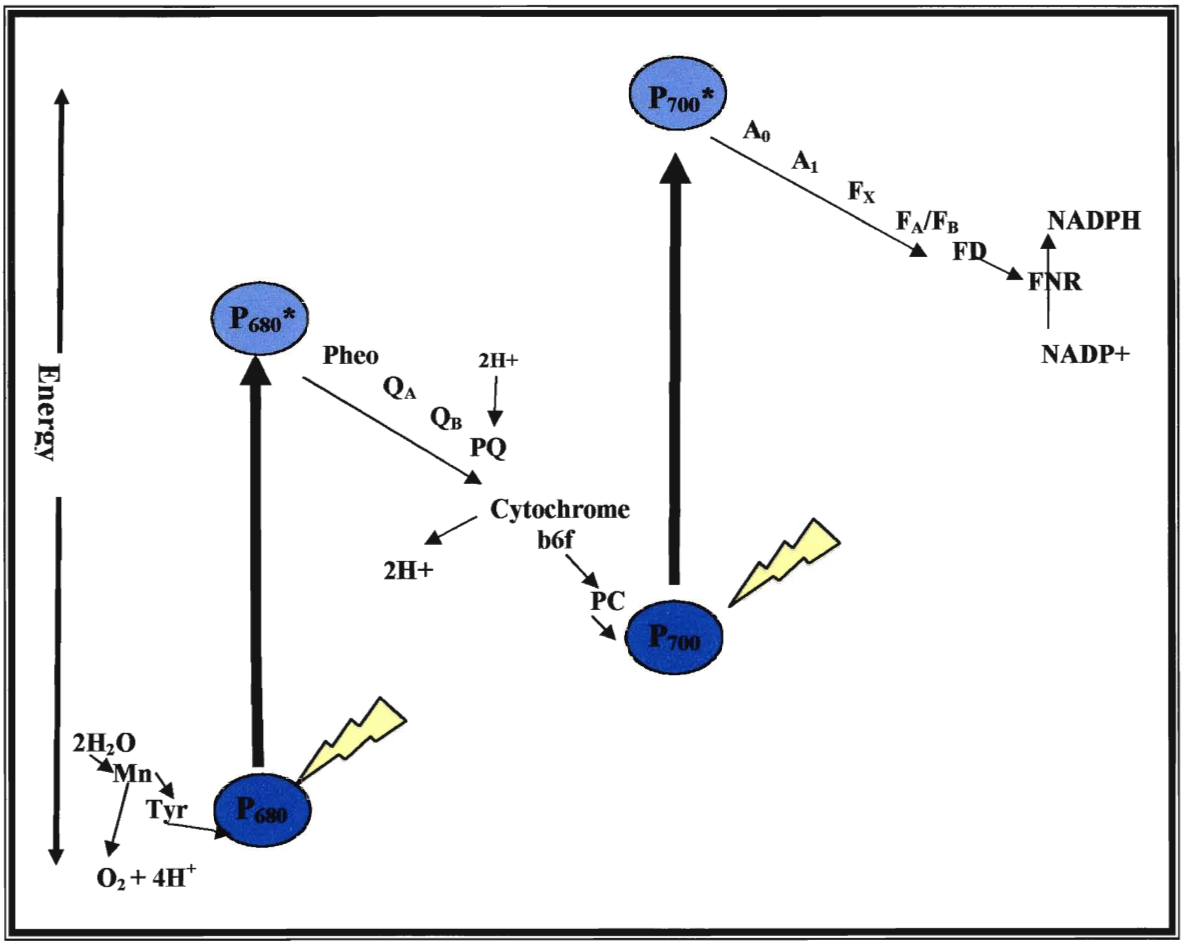

Figure 1-7: The Z-Scheme (Based on a figure from reference 5)

The Z scheme shows the transfer of electrons from PSII to Cytochrome b_6f, to Plastocyanin, to PSI, and finally, the reduction of NADP+ to NADPH. The scale labeled "Energy" in Figure 1-7 refers to the cofactor's ability to reduce the next cofactor[5]. Note

cofactor's ability to reduce the next cofactor[5]. Note that the Energy scale of the Z scheme goes from large negative values at the top of the scale to large positive values at the bottom[34].

There is another important feature to consider, this is the midpoint potential, E_M, of the cofactors. The midpoint potential is the point where the compound is half reduced, and half oxidized and the magnitude and sign of the midpoint potential tells us how likely a compound is to donate electrons to or accept electrons from other compounds[34]. If a compound has a midpoint potential that is large and negative (such as phylloquinone, with an E_M of approximately -0.7 V) it has a strong tendency to donate electrons (i.e., it is a good reducing agent)[34]. The excited donor has the most negative midpoint potential, each subsequent acceptor has a lower midpoint potential.

An interesting thing to note is that PSI, PSII and purple bacteria contain one or more quinone molecules. The type of quinone depends on the type of photosystem and species. This reveals the importance of quinones to photosynthesis in general and makes the study of quinones very valuable in the quest to unlock the secrets of photosynthesis.

Structure and Function of the Quinones in PSI and PSII

Quinones are widespread in nature -- in fact, ubiquinone gets its name from the fact that it is ubiquitous[45]. In the interest of brevity, our discussion here will be limited to those quinones which function as electron acceptors in photosynthetic reaction centres. The two quinones found in PSI and PSII are distinct from each other and appear to have been 'selected' to perform two rather different jobs. PSII contains two quinones called Q_A and Q_B; both are plastoquinone. The role of Q_A is to accept electrons from the pheophytin molecule and the role of Q_B is to accept two electrons from Q_A and diffuse

into the plastoquinone pool[4]. Q_A and Q_B are the same quinone, so the difference in their behavior must be due to the surrounding protein environment[3].

Plastoquinone is a benzoquinone with a long side chain, and two methyl groups attached to the benzyl head group. Its structure is shown in Figure 1-8.

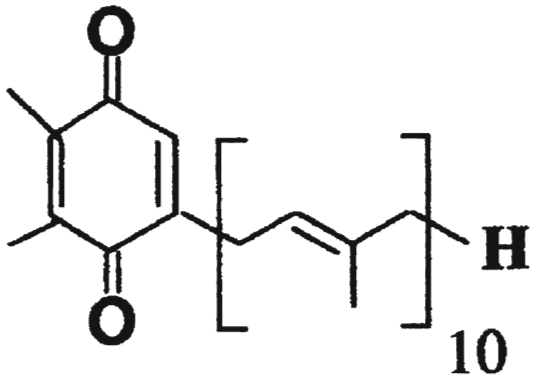

Figure 1-8: Structure of Plastoquinone

PSI, like PSII, contains two quinone molecules, but in PSI the quinones are phylloquinone. Phylloquinone is also known as Vitamin K_1, or more technically, 2-phytyl–3–methyl-1,4-naphthoquinone. Though there are several differences, plastoquinone and phylloquinone do share the features of a methyl group and a long tail. The following figure shows the structure of phylloquinone.

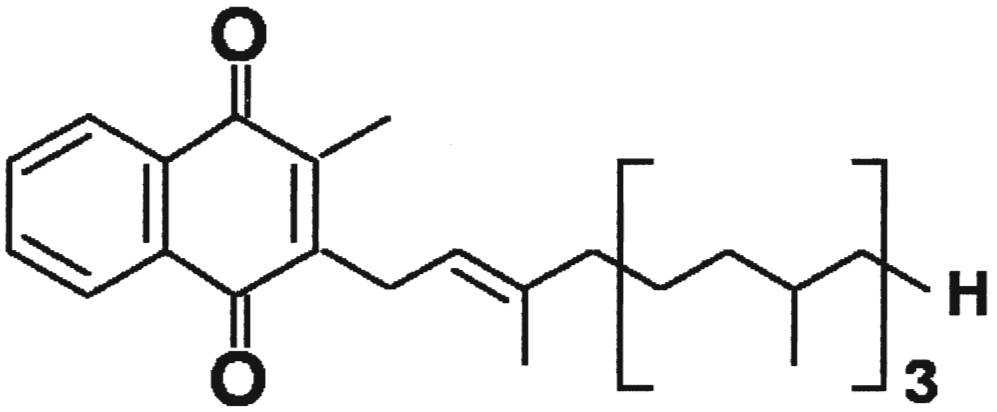

Figure 1-9: The structure of phylloquinone

There are three significant parts of phylloquinone, the naphthoquinone head group and the two side chains, methyl and phytyl. What are the characteristics that make it ideal for the secondary electron acceptor in PSI? Since there are a wide variety of quinones found in nature that could have been selected, it is well worth investigating what characteristics make phylloquinone so special. Is the A_1 binding site set up to accept only phylloquinone? The best way to answer this is to attempt to replace phylloquinone with structurally related quinones. The results will tell us what features of phylloquinone are responsible for its proper orientation in the A_1 site. For example, if a quinone with one side group is introduced, the position of the side group will tell us what feature of phylloquinone is responsible for ensuring proper binding in the A_1 site. What is the effect of introducing a disubstituted quinone, when only one of the side groups is structurally similar to those of phylloquinone? Are there size restrictions on the quinone that can be bound in the A_1 site? The use of quinones with a dramatically different size than phylloquinone will answer that question. In order to answer any of these questions, we must first solve the problem of getting phylloquinone out of the binding site, and getting non-native quinones in. This can be accomplished in two very different ways, through mutation experiments, or by extraction with organic solvents.

Incubation with Non-Native Quinones: Mutagenesis or Solvent Extraction?

There are two possible methods for replacing phylloquinone with non-native quinones in PSI. The first method is the very elegant one of mutagenesis[19]. Mutants of Synechocystis 6803 in *menA* and *menB* genes were created by interrupting the respective gene in the cyanobacteria[19]. These mutations prevent the biosynthesis of

phylloquinone[19]. The intention was that these mutations would create a species that did not have a secondary electron acceptor. Instead, studies on these mutants showed that plastoquinone was recruited from PSII and that these species are fully functional despite the structural differences between plastoquinone and phylloquinone[19]. In these mutants the orientation of the quinone is the same as in native PSI but the rate of forward electron transfer from Plastoquinone to F_X is slower than in wild type Synechocystis[19]. What makes *menA* and *menB* mutants ideal for incubation experiments with non-native quinones is that plastoquinone is not the native quinone and it can be very easily displaced by the non-native quinones.

Mutations in the *menG* gene were also created[28]. This mutation prevents the attachment of the methyl side group of phylloquinone, creating a species with 2-phytyl-1, 4-naphthoquinone in the A_1 site[28]. *men*G mutants are ideal for probing the role of the methyl group and the phytyl tail in the binding of phylloquinone[28]. In these experiments, the orientation of the quinone was the same as in native PSI, and the rate of electron transfer to F_X was slowed approximately twofold[27, 28]. These results indicate that the methyl group has little effect on the binding of phylloquinone in PSI, but even a small change in the structure of the secondary acceptor can have a dramatic effect on the rate of electron transfer[28].

For those who do not have the time or resources to perform mutagenesis, there is an alternate method. This is the 'sledgehammer' technique of extraction using organic solvents on PSI isolated from wild-type cyanobacteria[11]. In an early experiment by Biggins and Mathis (1988), it was demonstrated that one of the two phylloquinone molecules is readily removed by dry organic solvent, and the removal of the other

phylloquinone required the use of a less hydrophobic solvent[11]. It was suggested that the easily-removed phylloquinone was not involved in electron transfer[11]. Putting that interesting observation aside for the moment, this technique demonstrated that this treatment of PSI did not result in its destruction. Once phylloquinone has been removed, the PSI is unable to perform forward electron transfer and will, in theory, accept non-native quinones[11]. This is a very quick, easy and effective way of preparing PSI for incubation with non-native quinones. A disadvantage to this technique is the possibility of denaturing the protein. The extraction procedure also removes a significant portion of the carotenoid and accessory chlorophyll molecules, which is shown in the optical spectra of the extraction supernatant (Appendix I).

Electron transfer from A_0 to A_1 is significant, for this step stabilizes the charge separation and prevents the back reaction to P_{700}^+. Thus, the study of the secondary electron acceptor is crucial.

The Secondary Electron Acceptor, A_1

The secondary electron acceptor of PSI was an interesting puzzle for researchers. For many years, the identity of the cofactor called A_1, the secondary electron acceptor, was unknown. It was known that PSI contained phylloquinone, but it was not certain that it was A_1. Several groups obtained spectroscopic evidence that A_1 was phylloquinone. One study by Biggins & Mathis (1988) used flash absorption spectroscopy and compared the signal from PSI and extracted PSI, and extracted PSI incubated with phylloquinone[11]. HPLC analysis of the extraction supernatant confirmed that the full extraction procedure removed the two phylloquinones per P_{700} that were known to be present. It was found that removal of phylloquinone caused a signal characteristic of recombination of the

plastoquinone pool, meaning that phylloquinone binds in the A_1 site in the presence of an excess of plastoquinone. This reveals the selectivity of the A_1 binding site for phylloquinone. Experiments with non-native quinones will allow us to probe the characteristics of the surrounding environment, and may provide insight into the nature of the binding. The following figure shows the position of phylloquinone in the A_1 site of PSI.

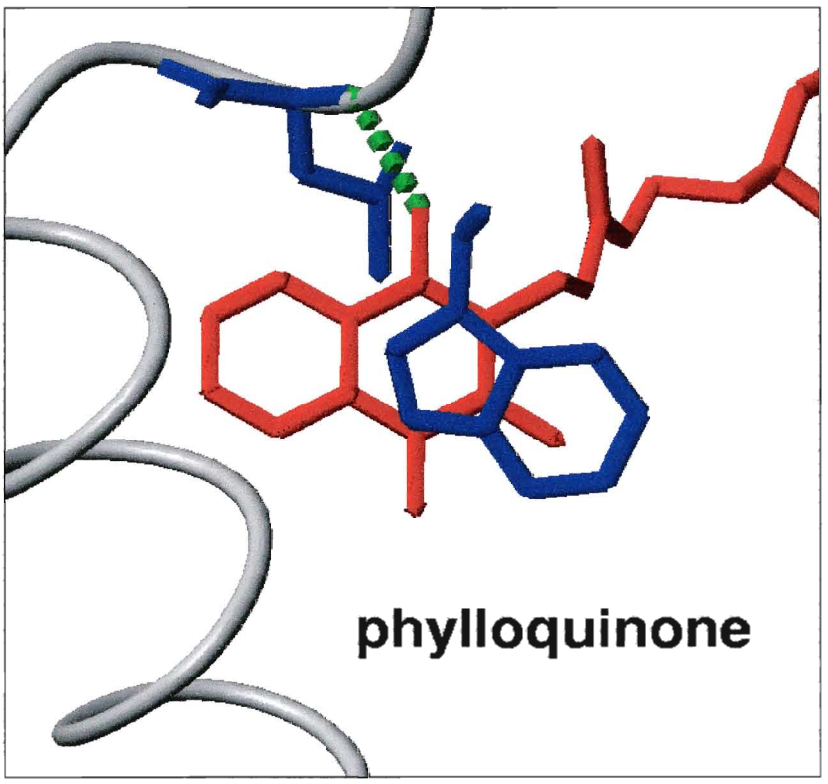

Figure 1-10: Bonding of phylloquinone in PSI (Credit: A van der Est & Y. Bukhman)

The asymmetric hydrogen bonding is very significant, because it provides a way of identifying the location of side chains on the quinones. The hydrogen bond acts as an electron withdrawing group, which in turn causes a decrease in electron density at the position *ortho* to the bond (the phytyl tail) and an increase in electron density at the position *meta* to the hydrogen bond (the methyl group). This has a pronounced effect on

the hyperfine coupling in the EPR spectrum, which will be discussed further in Chapter 2. By examining this effect when non-native quinones are incorporated into the A_1 site we can gain insight into the location of the side chain relative to the H-bonded carbonyl group.

The structure and function of PSI has been studied for decades. Techniques such as transient EPR and optical spectroscopy have provided a wealth of information about the cofactors involved in electron transfer. Therefore, a brief review of what has been done up to this point is essential.

Where are we now? Where are we going?

Quinone exchange experiments have been conducted since the 1980's. These experiments gave us valuable information about the identity of the secondary electron acceptor, its behavior in the binding site and the surrounding environment. A 1990 study by John Biggins studied a range of benzoquinones, naphthoquinones and anthraquinones to determine if they could function in the A_1 site[36]. It was first determined whether the foreign quinones would act as electron acceptors, then whether electron transfer to the iron-sulfur clusters was occurring. The method of analysis was flash absorbance spectroscopy. It was concluded that for a naphthoquinone to function in the A_1 site (restore electron transfer to the FeS clusters) it requires a long alkyl or phytyl tail[36]. This was revisited in 1992 through the use of EPR and explored the functionality of non-native quinones in the binding site based on the reduction potential[35]. These studies indicated that for forward electron transfer to the iron sulfur clusters, a long alkyl tail is required[35]. It was also revealed that a non-native quinone must have a reduction potential more positive than phylloquinone in order to restore electron transfer from A_0 to the quinone [35].

These results suggested that the binding site had stricter requirements for binding than had been previously reported by Iwaki and Itoh, who had found that neither the naphthoquinone headgroup nor the phytyl tail were needed for binding in the A_1 site [35, 36]. A 1991 study by Sieckmann, van der Est and Stehlik found the very interesting result that when phylloquinone is replaced with naphthoquinone, the orientation in the binding site is different[57]. They also found that the electron transfer past the foreign quinone (naphthoquinone and duroquinone) is slowed, which was attributed to the redox potential of the substituted quinones[57]. In addition, these studies demonstrated spectral narrowing and increased resolution of the hyperfine splitting in EPR spectra of PSI incubated with foreign quinones such as naphthoquinone[57]. This provided a starting point for selective deuteration experiments to determine what structural features are responsible for hyperfine splitting patterns[57]. 1994 gave us another set of quinone exchange experiments by Iwaki and Itoh[58]. The goal was to use the technique of flash photolysis to determine if a series of substituted anthraquinones and naphthoquinones would restore electron transfer to the iron sulfur clusters, or whether the foreign quinones would reduce P_{700}^{+}. It was found that the ability of the quinone to act an in the electron transfer chain had less to do with the structure than its redox potential[58]. This study was continued and a 1996 paper related to the free energy change ($\Delta G°$) of the electron transfer reaction between A_0 and the quinone acceptor A_1 (for both the native phylloquinone and a series of foreign quinones)[59]. Absorption spectroscopy was once again used for the analysis, and the $\Delta G°$ value for the electron transfer from A_0 to A_1 was estimated from the kinetics of the electron transfer[59]. This study found that the electron transfer from A_0 to A_1 appears to be optimized[59]. A 1997 study by Zech, van der Est and Bittl used pulsed EPR to study

$P_{700}^{+}A_1^{-}$ of intact PSI and PSI incubated with a series of foreign quinones[49]. In pulsed EPR experiments the radical pair causes an out of phase electron spin echo (ESE) exhibiting envelope modulation (ESEEM)[49]. The use of ESEEM (Electron Spin Echo Envelope Modulation) allows the distances between the cofactors to be determined. A 1998 study by Iwaki et al used the same technique on a different series of quinones[60]. Previous ESEEM studies had determined that there was a distance of 25.3 - 25.5 Å between P700 and A1[49, 60 and references within]. The distances obtained for P700 and the substituted naphthoquinones, benzoquinones and anthraquinone were similar to that of the native system, indicating that these quinones are capable of binding in the A_1 site[49, 60].

In addition, there is also a large body of work devoted to quinone exchange in purple bacteria reaction centres. The rates of electron transfer when bacterial reaction centres (bRC's) are incubated with many non-native quinones have been determined and the orientation of the non-native quinones has also been reported[30, 32, 48, 61]. Unfortunately, the extensive knowledge of the bRC did not assist in increasing our knowledge of the PSI reaction centre. A study by Füchsle *et al.* (1993) and one by van der Est *et al.* (1995) performed quinone exchange experiments on both PSI and the reaction centre of *R. sphaeroides* and found that the two types of reaction centres are quite different in their binding of non-native quinones[44, 32]. Specifically, the orientation of the quinone x axis (along the carbonyls) with respect to the dipolar axis is approximately 60°, and it is parallel in PSI[44, 32]. In addition, the appearance of the radical pair spectrum measured using EPR shows a different pattern of emission and absorption. Thus it is essential to perform more studies using PSI in order learn more about the binding of the quinone acceptor.

More recently, several mutant strains of Synechocystis 6803 were created. Of particular significance are the *menA*, *menB* and *menG* mutants, which were discussed earlier in Chapter 1. Experiments with these mutants that contain plastoquinone and phytyl naphthoquinone demonstrate the importance of the structural features of the quinones and the effect of redox potential and the protein environment on the rate of electron transfer[19, 28]. Solvent extraction and incubation (quinone exchange) experiments will complement these studies nicely.

This research project is concerned with several things. First, what features of phylloquinone are responsible for its binding affinity? Phylloquinone is a naphthoquinone with a methyl group and a phytyl tail; what features are responsible for its proper binding in the A_1 site? Previous studies of quinone exchange in PSI had reported conflicting results about what features were needed for proper binding in the A_1 site and had not focused on the orientation of the quinones. If we introduce a monosubstituted naphthoquinone, will the quinone orient itself with the side chain in the position normally occupied by the methyl group of phylloquinone, or that of the phytyl tail? What are the spatial restrictions of the binding site; will longer side chains be forced into the location reserved for the phytyl tail of phylloquinone? The series of non-native quinones was carefully selected in order to probe these questions. Selective deuteration of quinones will allow us to determine the source of hyperfine splitting in the EPR spectrum, thus allowing us to deduce the location of the side groups in the binding site. We can take advantage of the asymmetric hydrogen bond acting as an electron withdrawing group to determine the location of side chains, assuming that the same hydrogen bond is forming (as explained earlier in Chapter 1).

The other feature we are exploring is the high midpoint potential of phylloquinone. With foreign quinones present in the binding site, will we get electron transfer to the quinone and on to the iron-sulfur clusters? If we do get electron transfer to F_X, will the rate be faster or slower? Studies by Iwaki and Itoh[58, 59] used absorbance spectroscopy to determine the rate of electron transfer--will the rates of electron transfer obtained using room temperature EPR be the same? Since the rate of electron transfer from A_1 to F_X in PSI is not at a maximum, where does the rate lie (i.e., in the normal or inverted region on the Marcus Curve)?

Experiments involving PSI and non-native quinones will give us valuable information about the nature of the A_1 site in PSI, and its interaction with phylloquinone. With good planning, we may discover what it is about phylloquinone that makes it the quinone of choice for PSI.

Chapter 2

Methods and Materials

Transient Electron Paramagnetic Resonance (EPR)

Electron Paramagnetic Resonance spectroscopy has several names, it is also known by the aliases Electron Spin Resonance (ESR) or Electron Magnetic Resonance (EMR). These names arise from the properties of the substances that can be studied using the technique (paramagnetic species), the origin of the magnetic properties (electron spin) and how they are measured (resonant microwave absorbance). EPR is remarkably versatile and has been used in biology, physics, chemistry, medicine, and many other areas to study properties of solids, liquids and gases[25]. However, this technique is not as widely known as some others, so an introduction to why and how it works is in order. The related technique of Nuclear Magnetic Resonance (NMR), is more

familiar and shares many of the same principles[24]. While NMR measures the interaction of nuclear magnetic moments with radiofrequency radiation and a magnetic field, EPR spectroscopy measures the interaction between the magnetic moments associated with the electrons and an applied magnetic field using microwave absorption[23, 24]. Since our focus is EPR, we will primarily discuss the properties of electrons. The magnetic moment of an electron is due to contributions from both orbital and spin motions. The orbital contribution is:

$$\mu_{orbit} = \frac{-e}{2M_e}\vec{L} \qquad \textbf{Equation 2-1}$$

Where e is the charge of the electron, M_e is the mass of one electron and $\vec{L}$ is the orbital angular momentum, which is a vector. $-e / 2 M_e$ is defined as the Bohr magneton (β). The contribution from the spin is given:

$$\vec{\mu}_{spin} = \frac{-e}{2M_e} g_e \vec{s} \qquad \textbf{Equation 2-2}$$

Where $\vec{s}$ is the spin angular momentum. This equation introduces g, a constant known as the g value. The g value was introduced after early experiments obtained a value of μ_{spin} that was twice the expected value[24]. This is because the magnitude of $\vec{L}$ is 0, 1, 2, 3 while the magnitude of $\vec{s}$ is 0, ½, 1, $\frac{3}{2}$. For a free electron, the value of g is 2.0023, this value will be different for the unpaired electrons in a system. g_e is different from the expected value of 2 because of relativistic correction of the electron's velocity[24].

For molecules, it is difficult to calculate μ_{spin} and μ_{orbit} separately, so we introduce the "effective" g factor that relates the total magnetic moment to the spin angular momentum. It is given in the following equation.

$$\mu_{total} = \frac{-e}{2M_e} g_{eff} \vec{s} \qquad \textbf{Equation 2-3}$$

In a magnetic field $\vec{s}$ aligns parallel to the field because the total magnetic moment depends on the orientation of $\vec{L}$ and $\vec{s}$. The magnetic moment in a field depends on the orientation of the molecule and so does the effective g factor, so we write it as a tensor.

The g tensor is comparable to chemical shift in NMR. However, with the experimental setup used here, the g value cannot be determined accurately as the frequency is not known exactly. For our analysis we will instead focus on the shape of the spectra, which gives us important information about the radical pair, $P_{700}^{+}A_1^{-}$, the strength of hyperfine couplings of A_1^{-} and its orientation in the binding site.

Magnetic Resonance

In an EPR spectrum the signal is due to the transitions of the electron between spin states. These transitions occur when the microwave frequency is in resonance with the energy difference between the spin states, hence the term magnetic resonance[24]. The microwave radiation introduced has energy and a frequency. For EPR, energy can be related to the applied magnetic field, the g factor and the frequency.

$$E = h\nu = gB_o\beta \qquad \textbf{Equation 2-4}$$

The frequency at which transition of the electron between spin states occurs varies with the applied magnetic field[42]. Equation 2-4 can be rewritten in the following form.

$$\nu = g B_0 \frac{\beta}{h}$$ **Equation 2-5**

ν = the microwave frequency
g = the g value
B_0 = the applied magnetic field strength
β = the Bohr magneton (9.2740×10^{-24} J/T)
h = Planck's constant
$\beta/h = 1.3996 \times 10^{-10}$ Hz/T

The preceding equation shows that the resonance frequency depends on the applied field and the magnetic moment. X-band EPR is performed at a frequency of 9 GHz, with a magnetic field strength of 3.4 kG (this name comes from the fact that this frequency is in radar X band) corresponding to a wavelength of about 3 cm[17, 24]. X-band EPR spectroscopy is frequently used and can be performed at low or room temperatures[17]. Q-band EPR is performed at 35 GHz and 12.5 kG, and is normally used at very low temperatures[17, 24]. The spectra achieved at Q-Band have better resolution of signals with different g factors (see Equation 2-4) so the spectrum takes up a wider range of magnetic field and the contributions from the donor and acceptor ($P_{700}^{+}A_1^{-}$) are not overlapped to the degree that they are at X band. EPR experiments can also be done at much higher frequency and magnetic field strength, at the frequency known as W band. W-band EPR uses a frequency of 95 GHz and gives a wide spectrum. A drawback to W band spectroscopy is that the dimensions of the resonator are much smaller than with X or Q band and it is more difficult to transport the higher frequency microwaves. This makes it much more difficult to obtain a good quality spectrum with W band EPR spectroscopy.

The species that can be studied with EPR include free radicals, transition-metal complexes and triplet state molecules, to name a few[23]. EPR spectroscopy is an ideal

method for studying electron transfer in PSI as it can be used to observe both the triplet spectrum and radical pair spectrum.

The principles behind EPR spectroscopy and NMR are similar, but the spectrometer setup is quite different in appearance[24]. A schematic diagram of a typical Transient EPR spectrometer is shown in Figure 2-1.

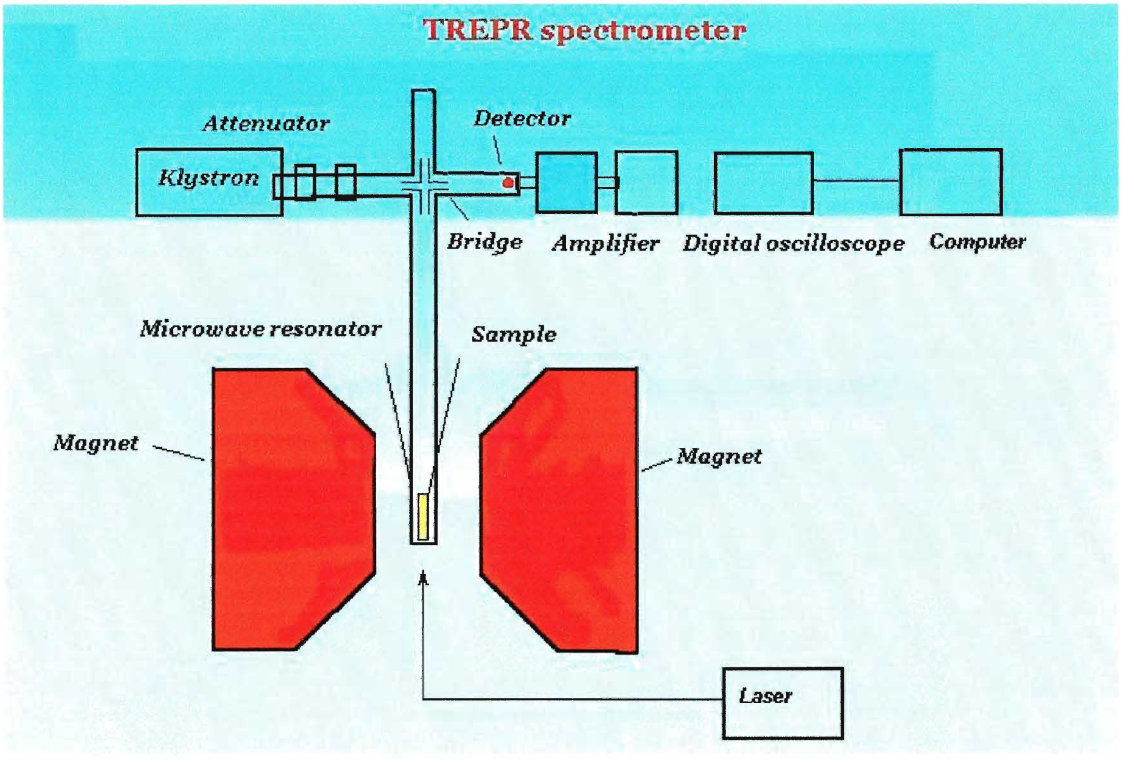

Figure 2-1: Equipment Setup for EPR Spectroscopy (Credit: Olena Bespalova)

. Microwave radiation is generated and sent from the klystron oscillator down the waveguide to the resonator[24]. Waveguides are hollow, rectangular gold-plated pipes whose dimensions match with the wavelength of the radiation used, and are ideal for the transportation of microwaves[24]. In a spectrometer that employs a "magic tee" (pictured), the energy is sent down the resonator to the sample. The resonator is critically coupled to the microwaves so that no power is reflected. If the sample absorbs the microwaves due to an EPR transition, the resonance is disturbed and the change in absorbance is detected

by the detector. The sample is held in place in the resonator in either a quartz tube or flat cell for proper signal acquisition[24]. The maximum electric and magnetic field are at different locations[24]. We use this to our advantage for samples in aqueous solution, at room temperature the use of a flat cell is essential in order to keep the cell in a position that will not result in interference with the signal from the water[24]. Flashes of laser light at a convenient wavelength and intensity (in our case, 532 nm, 1-10 mJ) are used to excite the sample, causing the formation of the radical pair or triplet state. The laser flash causes a transient change in absorbance. The signal is then sent to the amplifier and on to the Oscilloscope where the absorbance of microwaves is measured. This is all connected to a computer for analysis of the data.

PSI is a complex protein, so when selecting a method for observing the formation of the radical pair, we must make sure that the presence of the protein will not interfere with our signal. A distinct advantage to transient EPR spectroscopy is the fact that it will only detect light induced paramagnetic species, making it ideal for the study of PSI[42]. The presence of local fields can create a very complex spectrum. Local field refers to the fact that all of the electrons experience the applied external field and those induced by all the surrounding molecules. The local field is composed of the external field, the field due to surrounding nuclei and the field due to surrounding electrons. The field created by other electrons is sometimes referred to as Spin-Spin coupling; that due to the nuclei is Hyperfine coupling.

In a transient EPR experiment on PSI, a pulse of laser light is used to excite P_{700} and induces forward electron transfer through A_0 to A_1, forming the radical pair $P_{700}^{+}A_1^{-}$. By sweeping the magnetic field in a series of predetermined steps, we can determine

whether the radical pair is present, and based on the shape of the spectrum obtained, determine the orientation of the cofactors in the protein.

When the radical pair is formed, the two unpaired electrons originate from a pair of electrons on the donor with one of the electrons being transferred to the acceptor, separating them in space over a specific amount of time. The primary donor in ground state is a singlet state, i.e., all spins are paired. Formation of the radical pair $P_{700}^{+}A_1^{-}$ happens on such a fast timescale (~30 picoseconds[18]) we get a population in only those energy levels that have singlet character. The following figure shows the energy levels for two weakly coupled spins (i.e., the $P_{700}^{+}A_1^{-}$ radical pair)[29]. We can label the energy levels in Figure 2-2 according to their triplet or singlet character, or whether the electrons are spin up or spin down.

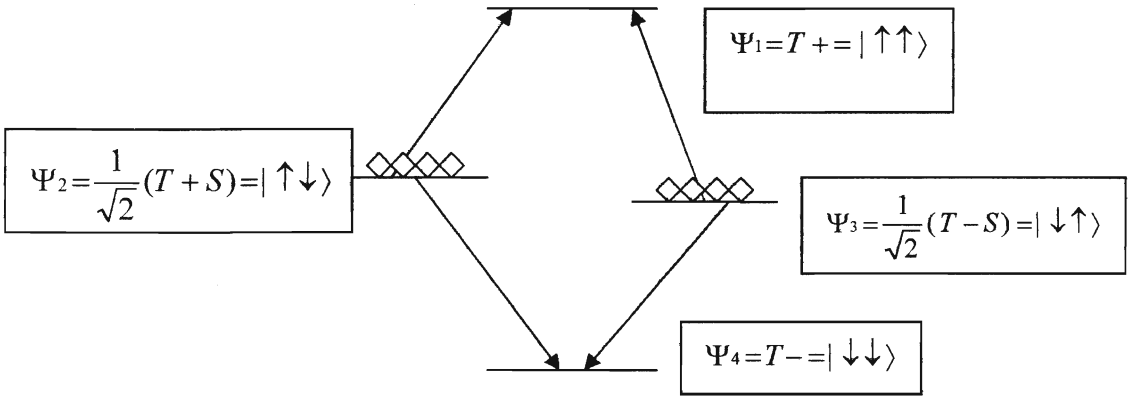

Figure 2-2: Populated Energy levels for a weakly coupled pair

Note that the diamonds occupying the energy levels in Figure 2-2 represent the probability of a radical pair being in a given state. In an EPR experiment one of the electrons can be promoted ($\psi_2 \rightarrow \psi_1$ or $\psi_3 \rightarrow \psi_1$) which causes absorption, or go to a lower energy level ($\psi_2 \rightarrow \psi_4$ or $\psi_3 \rightarrow \psi_4$) which causes emission.

Thus the appearance of the resulting EPR spectrum provides evidence that the radical pair has been formed. But what gives a transient EPR radical pair spectrum its distinctive shape? To answer that question, we will begin with a simple example.

Description of a Radical Pair EPR Spectrum

In the following section a brief description of why the EPR spectrum of a radical pair looks the way it does is given[29]. Consider a donor, D^+, and the acceptor, A^- in a magnetic field, B_o. We assume that due to the nature of the two molecules, the donor resonance is located at a higher magnetic field than that of the acceptor.

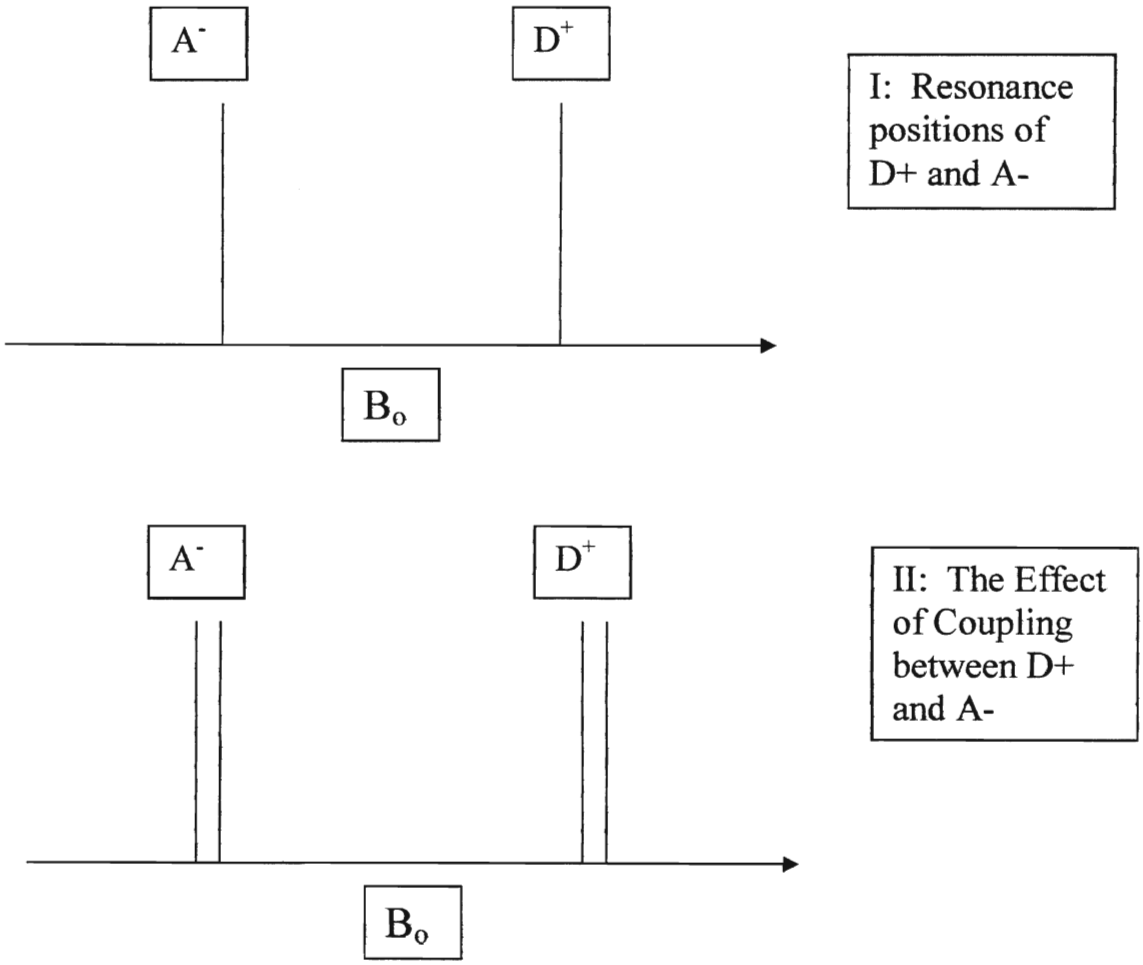

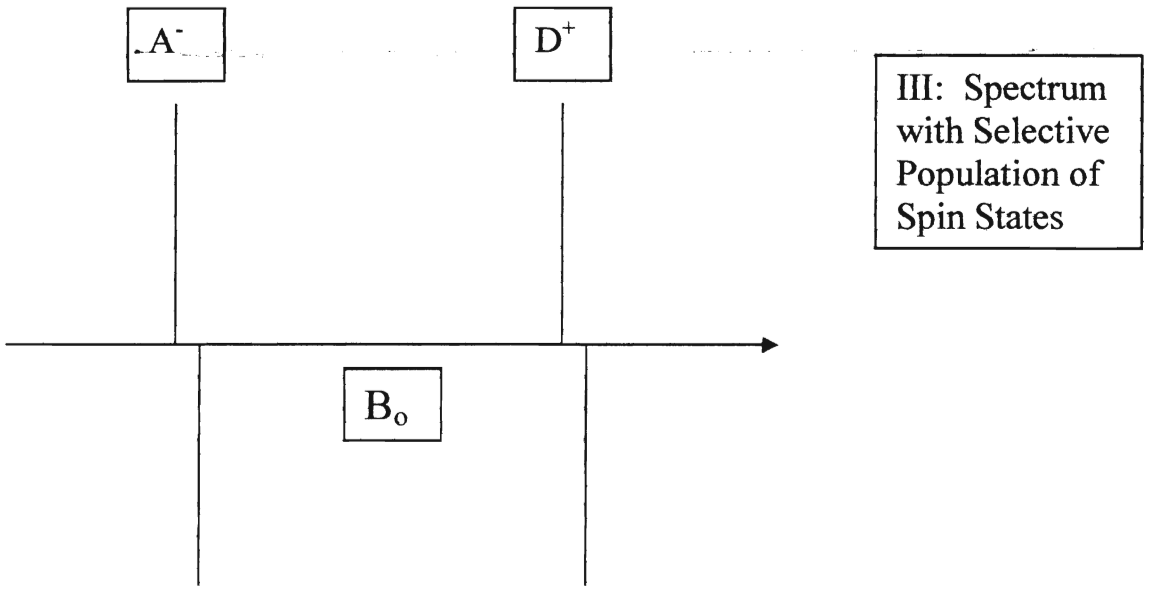

Figure 2-3: A Radical Pair EPR spectrum

In the absence of any local fields and ignoring the selective population, the donor, D and acceptor, A each give a single peak (as shown in Figure 2-3 section I). If the donor and acceptor are close enough to each other (for example, in PSI) the local fields created by the unpaired electrons causes a splitting of the signal. The separation of the two lines is the same for both the donor and acceptor and is defined as (2d + J). J is the exchange coupling and d is the dipolar coupling[42]. (Shown in Figure 2-3 II). The selective population of the spin states discussed above (in Figure 2-2) causes the phenomenon known as spin polarization and creates the pattern of emission and absorption illustrated in Figure 2-3 III.

We will now apply this to the specific case of the donor P_{700} and the acceptor phylloquinone, A_1 of PSI.

In this case, the hyperfine coupling due to magnetic coupling of the unpaired electron to the CH_3 group of phylloquinone is important. The following series of figures

illustrates the effect of this hyperfine coupling. We will rename our donor P_{700}^{+} and acceptor A_1^{-} to correspond to those of PSI.

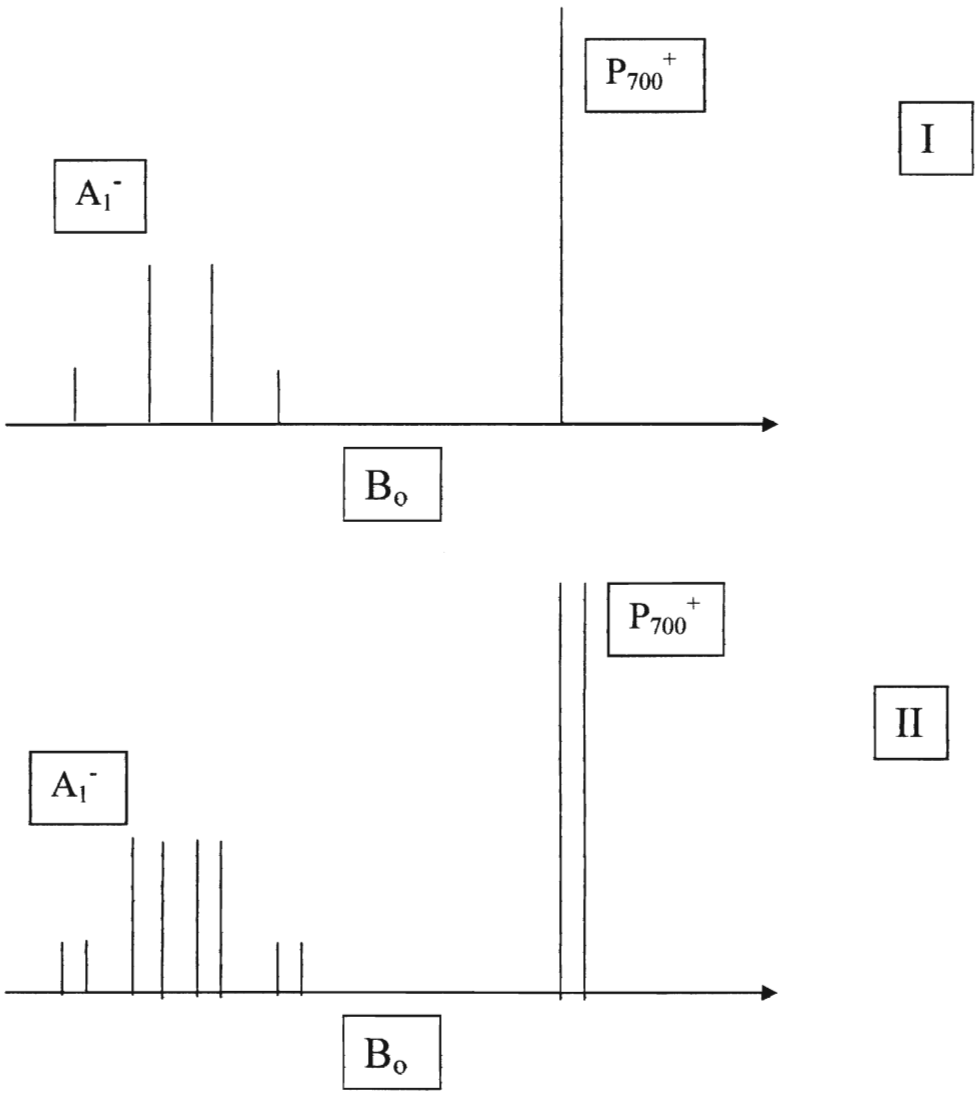

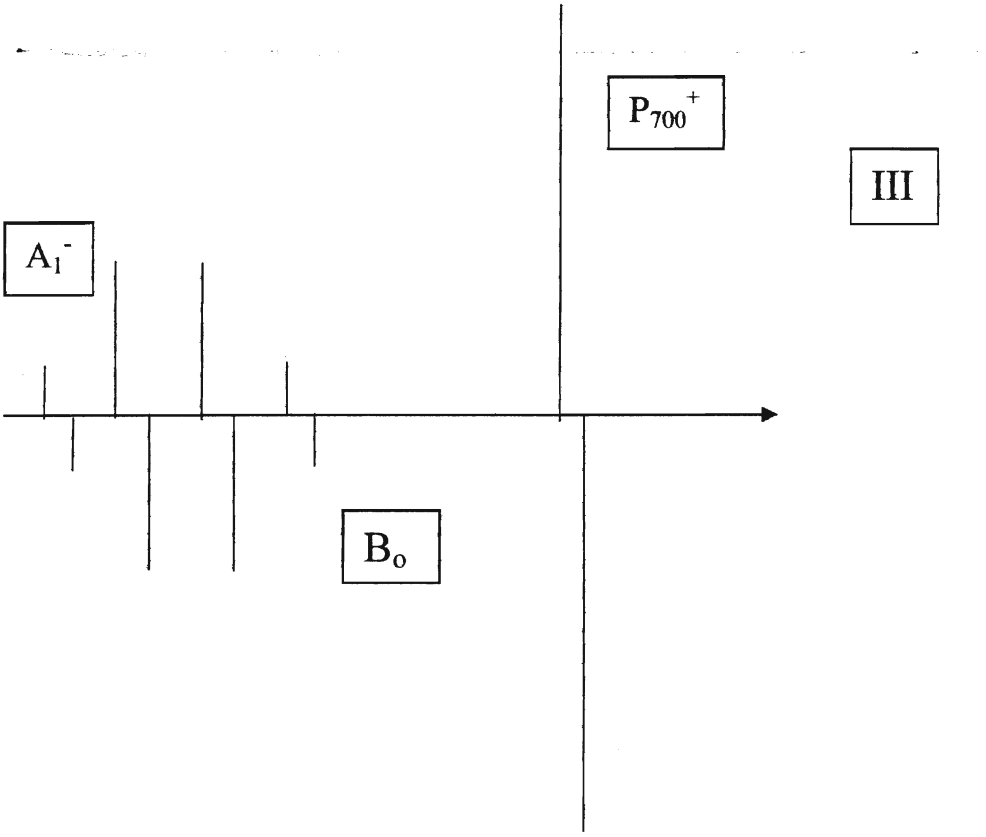

Figure 2-4: Stick spectrum for PSI

The hyperfine coupling to the CH_3 group of A_1 creates a 1:3:3:1 quartet pattern (Shown in Figure 2-4 I). There are n + 1 possible orientations of the protons spins, therefore because there are 3 protons on the methyl group of phylloquinone, we get a quartet. Each of these lines is then further split into a doublet because of the presence of the local field due to the unpaired electrons on the acceptor and donor (illustrated in Figure 2-4 II), and finally spin polarization causes the A/E (A=absorbance, E=emission) pattern shown in Figure 2-4 III.

In addition to CH_3 hyperfine coupling there are many other smaller couplings to other protons, giving a Gaussian lineshape[29]. This is illustrated in figures 2-5 and 2-6. Note that the magnetic field values in Figure 2-5 and 2-6 are arbitrarily assigned and

correspond roughly to the position of an EPR spectrum taken at X band. With the effect of line broadening added, the spectrum begins to more closely resemble the observed PSI EPR spectrum.

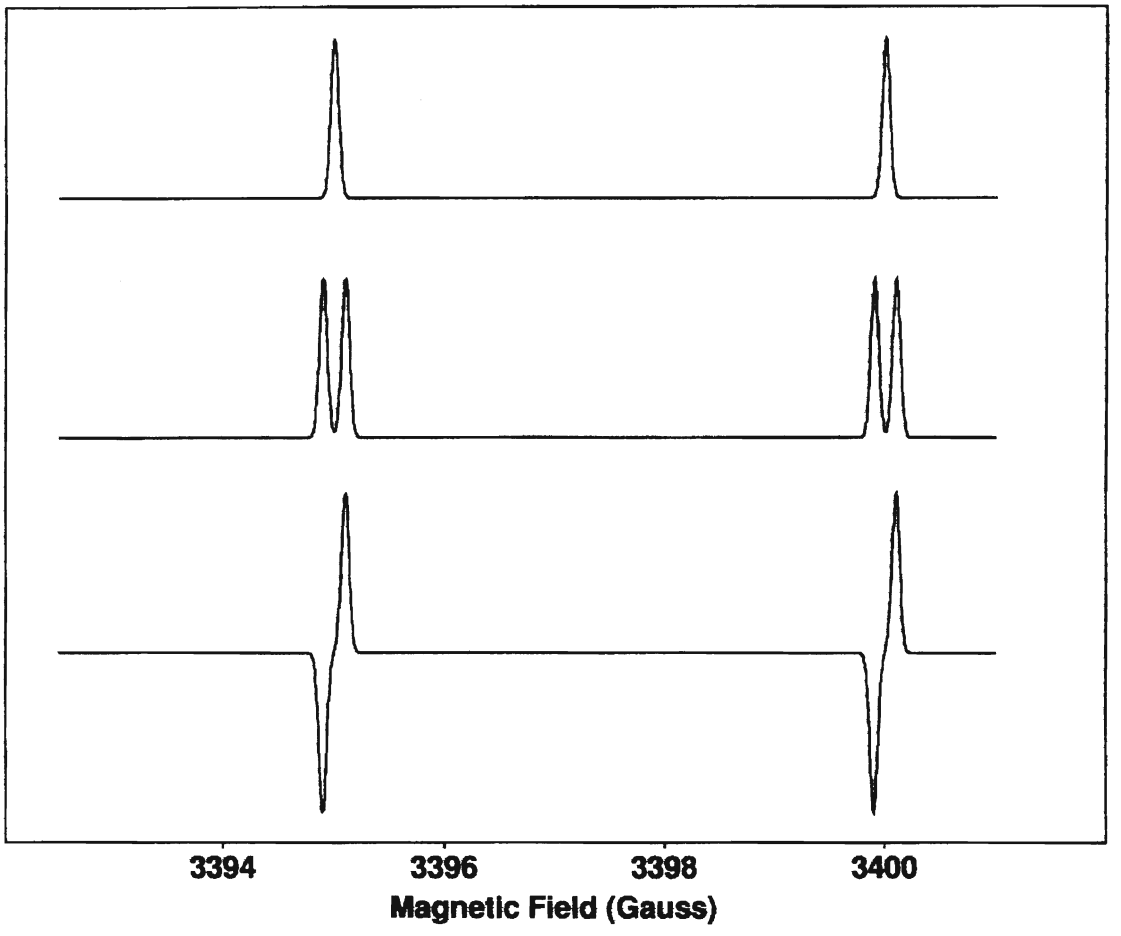

Figure 2-5: The effect of line broadening on a radical pair spectrum

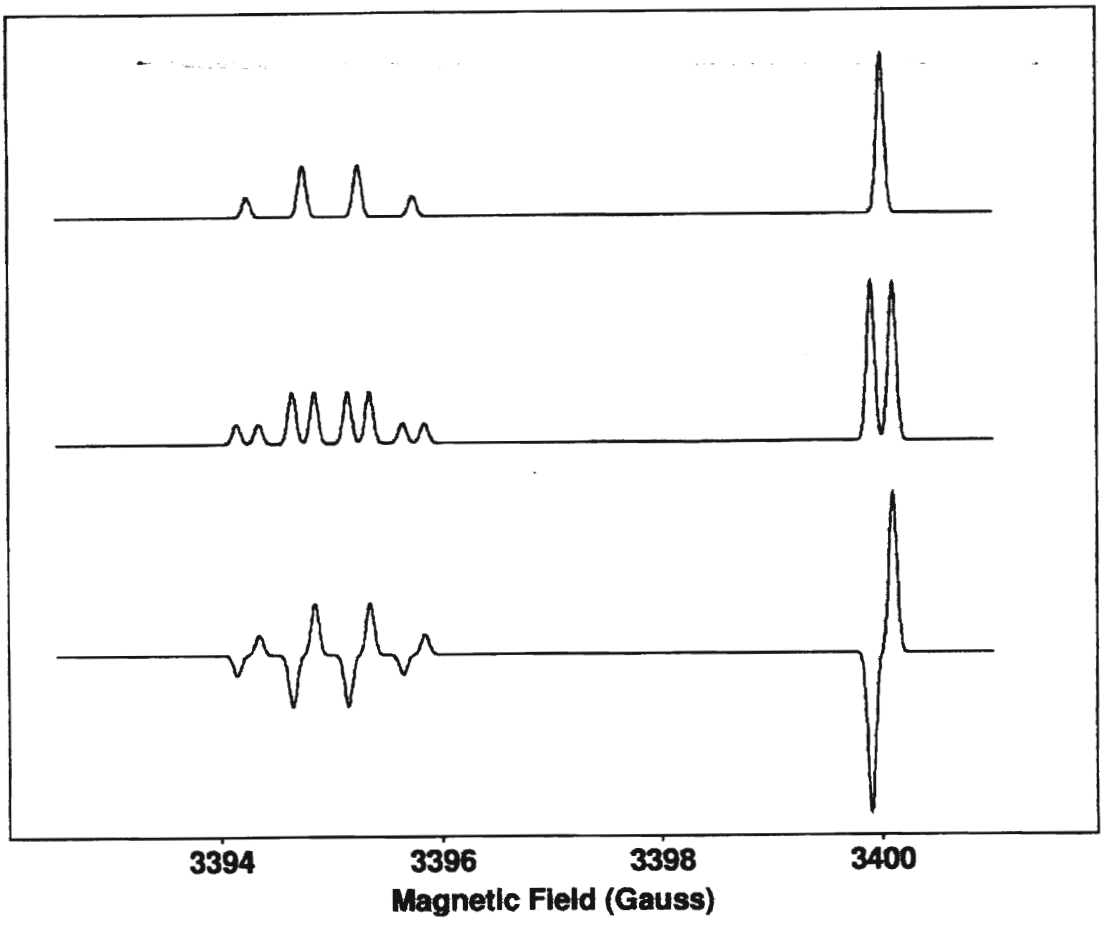

Figure 2-6: The effect of line broadening on the stick spectrum for PSI

However, there is one other effect that must be taken into account. Since we are dealing with a solution of PSI where the particles are randomly oriented, the pattern seen in Figure 2-6 (bottom spectrum) must be summed over all possible orientations, the end result being the typical EPR spectrum for $P_{700}^{+}A_1^{-}$. This sum is referred to as a powder spectrum and the following figure shows a calculated powder spectrum for a radical pair at 95 GHz (W band).

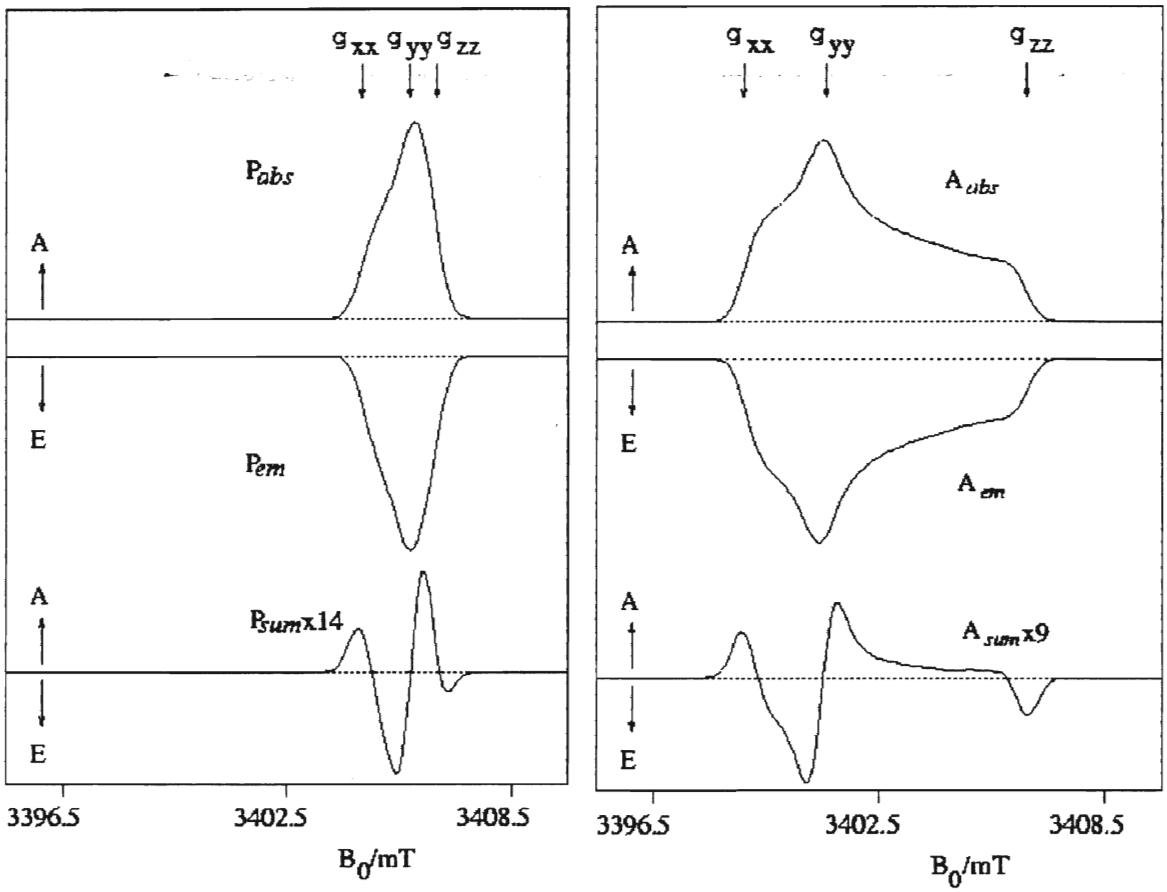

Figure 2-7: A Powder EPR Spectrum (Credit: Art van der Est)

The g tensor, which was mentioned at the beginning of Chapter 2, is not a single value. Instead, it consists of a matrix, with values of g_{XX}, g_{YY} and g_{ZZ} which are located at different fields (indicated in Figure 2-7). These values correspond to the x, y and z axes of the donor and acceptor[30]. The top two sets of spectra, labeled A_{abs} and P_{abs} and A_{em} and P_{em}, are the absorptive and emissive contributions from the acceptor and donor, respectively. The absorption and emission spectra of each radical are located at approximately the same field position and in this situation the absorptive spectrum of the acceptor (top spectrum of Figure 2-7, labeled A_{abs}) is shifted slightly downfield from the emissive spectrum. When the two spectra are added together, we obtain the spectra at the bottom of the figure, labeled P_{sum} and A_{sum}. Note the very low intensity of the spectrum,

this is because much of the signal is cancelled out when the emissive and absorptive spectra are summed. At lower frequency, (X band and Q band EPR) the separation between the signal for the donor and the acceptor is smaller than shown in Figure 2-7, but the contribution from the donor is always located at higher field and the acceptor is at a lower field position.

Now that we have learned why a radical pair EPR spectrum looks the way it does, we can move on to the other type of spectrum that we obtain from PSI after extraction of the quinone--the triplet spectrum. First we will clarify what the triplet state is, and how it comes into being.

Triplet vs. Singlet State

Neutral organic compounds usually have an even number of electrons and all are spin paired, hence the ground state is a singlet state (i.e., net spin S=0). This is illustrated in the following diagram.

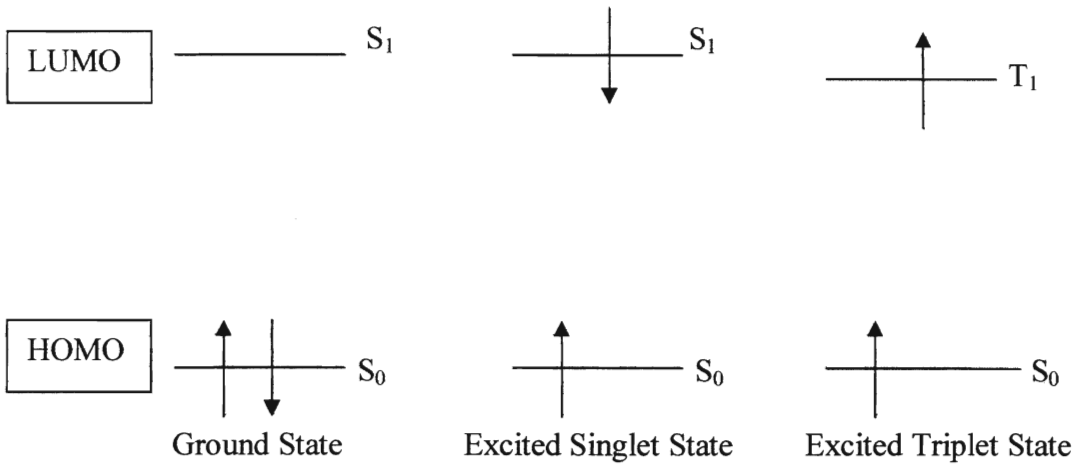

Figure 2-8: Arrangement of electrons in the Ground and Excited State

This diagram shows that ground state electrons in the Highest Occupied Molecular Orbital (HOMO) and promotion of an electron to the Lowest Unoccupied Molecular Orbital (LUMO). Absorption of visible light promotes electrons from the

ground state to an excited state. This is the first excited singlet state; because if higher excited states are populated they decay very rapidly to the first excited singlet state.

Because of the Pauli principle the ground state must be singlet state[26]. However, in the excited state the electrons may be spin paired, giving S=0 (i.e. a singlet state) or S=1 (a triplet state). Often, the triplet state is lower in energy than the excited singlet energy level. In order for the triplet state to return to ground state the excited electron must be flipped. Hence the lifetime of the triplet state is much longer than that of the singlet state. It can be as long as several microseconds.

How is the triplet state formed? There are two common situations that can occur. A molecule that is excited from S_0 to S_1 can go to the triplet energy level via Intersystem Crossing (ISC). When ISC occurs, the spin of the electron is reversed[43]. Despite the fact that triplet-singlet transitions are forbidden, intersystem crossing does occur. Since triplet-singlet transitions are forbidden, when a molecule is in the triplet state, it cannot easily return to the ground state. Thus the triplet states typically have a much longer lifetime than excited singlet states. The energy levels are shown in the following Jablonski diagram.

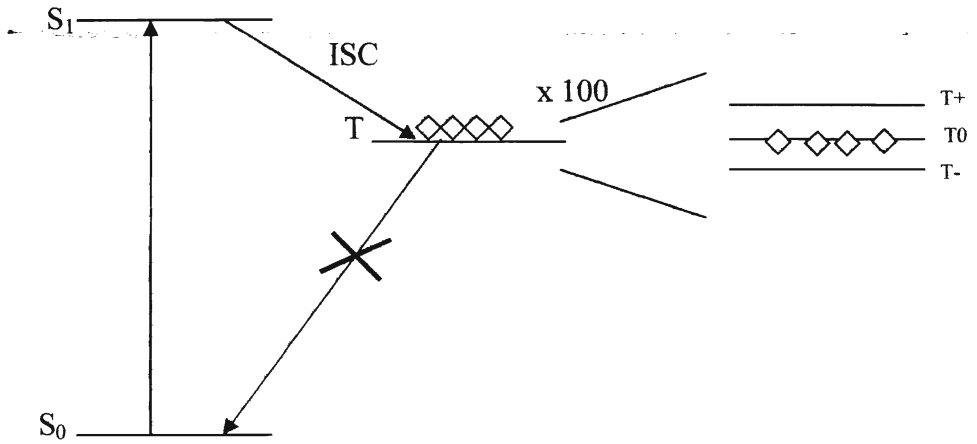

Figure 2-9: Jablonski Diagram showing energy levels of excited singlet and triplet states

The above figure shows intersystem crossing from the excited singlet state (S_1) to the triplet state (T). The diamonds indicate a population that has undergone intersystem crossing to the triplet state. The magnified portion of the above figure shows that the triplet energy level consists of three levels, called T_+, T_0 and T-. This splitting of the energy levels occurs because the electrons are not paired. So, the electron can both be spin up (+1, T_+), both spin down (-1, T-) or one up, one down (0, T_0)[42]. This figure shows that the population is at the T_0 level.

When phylloquinone is extracted from PSI we obtain the very distinctive transient EPR spectrum that is shown in the following figure.

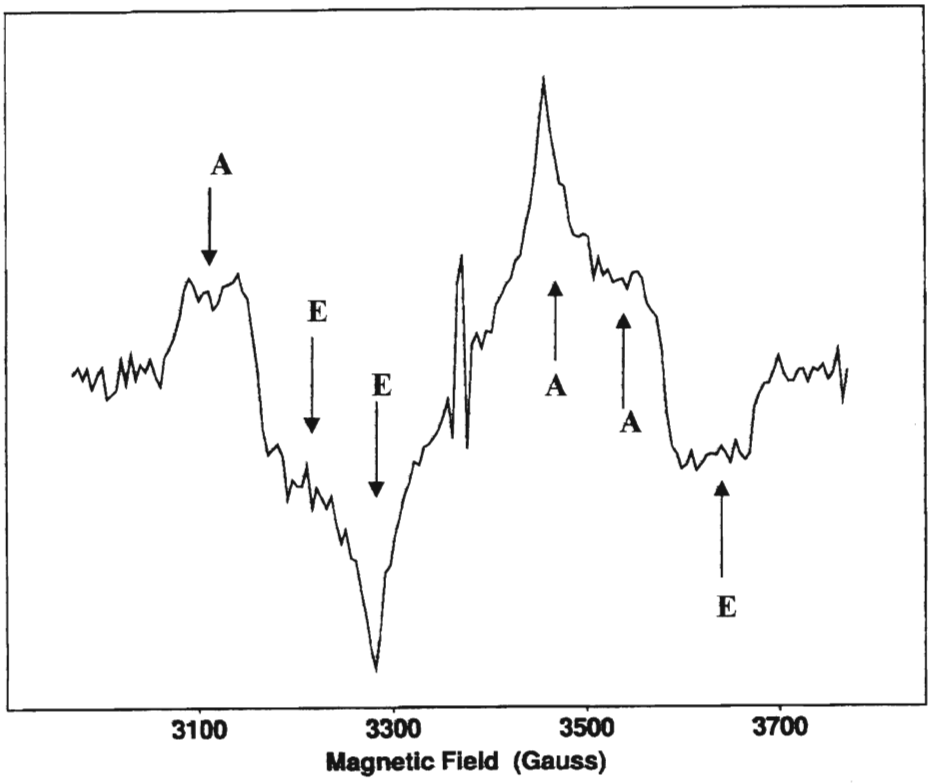

Figure 2-10: A Triplet Spectrum from Extracted PSI

This spectrum is the triplet state of chlorophyll. In a triplet spectrum, the properties we can observe are dominated by magnetic dipole-dipole interaction. This is the interaction of the magnetic moment of an electron in the field of another electron. This can be described in terms of parameters known as D and E. The value of D and E are given by the following equations.

$$D=\frac{3}{2}\left\langle\frac{r^2-3z^2}{r^5}\right\rangle \qquad E=\frac{3}{2}\left\langle\frac{y^2-x^2}{r^5}\right\rangle \qquad \textbf{Equation 2-6}$$

Where r = the distance between the two electrons
x, y, z = coordinates of electron 2 in an axis system fixed on electron 1.

What tells us that this is a spectrum of the triplet state of P_{700} and not due to another part of PSI is that the values of D and E parameters are the same as those obtained in experiments with a chlorophyll monomer[20 and references within]. The polarization pattern gives a population in T_0 for all 3 orientations. That is, this pattern shows that no matter how we orient the external magnetic field (i.e., parallel to x, y or z), T_0 is always populated. This is not possible by spin orbit coupling-driven Intersystem Crossing because it follows molecular symmetry and not the external field. So how is the $^3P_{700}$ being formed? The pattern shown in Figure 2-10 is indicative of the recombination of a radical pair. This process is illustrated in the following figure.

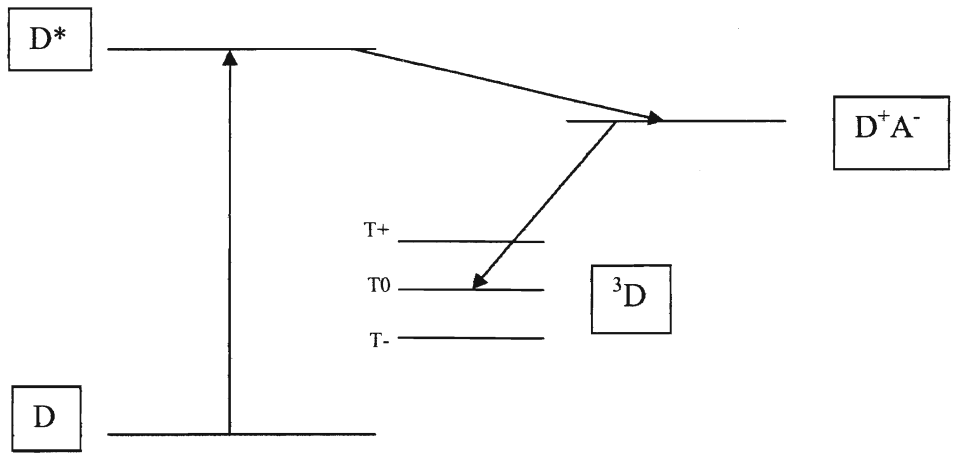

Figure 2-11: How a Triplet State is Formed by Recombination

It was shown in Figure 2-2 that the energy levels that get populated when a radical pair forms have both singlet and triplet character. Thus singlet/triplet mixing occurs between S and T_0 and recombination of the radical pair to the triplet state of P (^3P) populates only the T_0 level of ^3P. It is this population in the triplet level T_0 that causes the A/E/E/A/A/E pattern seen and this allows us to deduce that recombination and not intersystem crossing has occurred. The EPR triplet spectrum also looks dramatically

different from the radical pair spectrum, providing a simple assay for the effectiveness of the extraction. The fact that we see the triplet spectrum also indicates that there is electron transfer to A_0, indicating that the reaction centre has not been damaged by the extraction procedure. Furthermore, the incorporation of the non-native quinones can be monitored by the disappearance of the triplet spectrum and reappearance of the radical pair spectrum.

Our goal is to interpret the radical pair spectra in terms of orientation and interaction with the protein. Hyperfine coupling is important but its origin is not always clear and it can make the spectrum quite complicated. A helpful technique for resolving spectra is deuteration of the molecules involved. Here we have done several such experiments, so it is important to outline the influence of deuteration on hyperfine splitting.

Deuteration Experiments

Deuterium, also known as heavy hydrogen, is a useful tool for determining the source of the hyperfine coupling that causes splitting in the EPR spectrum. When we deuterate a quinone we replace either all or a specific number of protons with deuterium. Deuterium has a mass about double that of hydrogen due to the fact that it has a neutron, and has a magnetic moment about six times smaller than hydrogen, which produces a much weaker local field[26]. This means that the hyperfine coupling in a deuterated sample will be much smaller and will not be resolved in our EPR spectrum. Selective deuteration of a quinone will allow us to pinpoint the source of resolved hyperfine coupling by observing the disappearance of specific hyperfine splitting as protons are systematically replaced with deuterons.

Another feature of the transient EPR data is that they are sensitive to the rate of electron transfer. 1992 Nobel Prize winner Rudolph Marcus developed a theory to relate the rate of electron transfer to temperature, redox potential and the surrounding solvent molecules[37, 38]. We can use Marcus theory to analyze the electron transfer rates in our system.

Rates of Electron Transfer: Marcus Theory

An electron transfer reaction going from the initial state (D and A) to the final state (D^+A^-) can be represented by two parabolas.

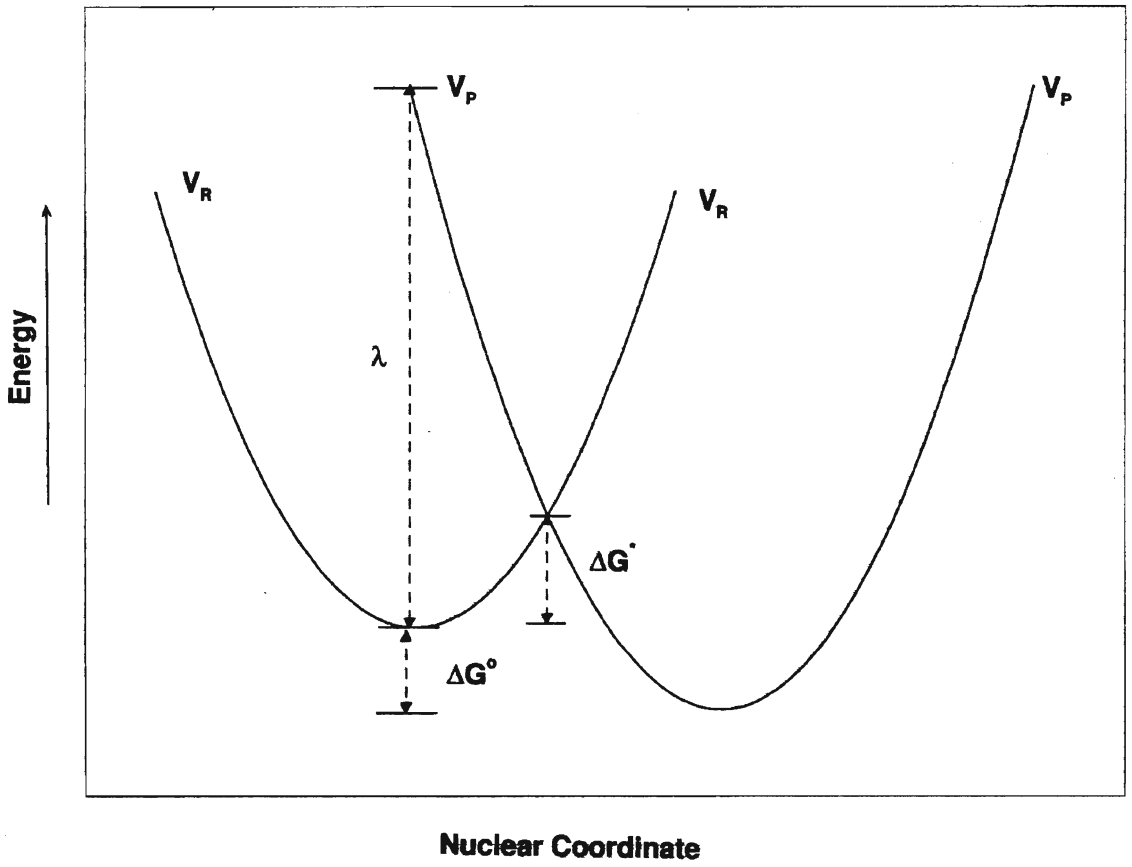

Figure 2-12: An electron transfer reaction

In this diagram the parabola labeled V_R represents the potential energy of the "reactants", i.e. the donor and acceptor before electron transfer, V_P represents the

potential of the "products" i.e., the radical pair generated by electron transfer. ΔG^* is the activation energy, the amount of energy needed for electron transfer to occur. $\Delta G°$ is the standard free energy change, the driving force behind the reaction. λ is defined as the reorganization energy of the reaction. The Franck-Condon principle states that electron transfer occurs faster than the nuclei can move[62]. As a result, the electron can only be transferred at the point where the two curves cross. The rate of electron transfer depends on the energy barrier, or at what point the two curves cross.

We can work out the value of the activation energy, ΔG^*, for the reaction by putting it in terms of $\Delta G°$ and λ; this gives us the Marcus equation.

$$\Delta G^* = \frac{\lambda}{4}\left(1 - \frac{\Delta G°}{\lambda}\right)^2 \qquad \textbf{Equation 2-7}$$

The Marcus equation can be rewritten to relate activation energy to the rate of electron transfer; this is shown in the following equation.

$$\ln k_{ET} = -\frac{\lambda}{4}\left(1 - \frac{\Delta G°}{\lambda}\right)^2 \left(\frac{1}{T}\right) + \ln k_{MAX} \qquad \textbf{Equation 2-8}$$

Where k_{ET} = the rate of electron transfer
k_{MAX} = the maximum rate of electron transfer

This shows that when the reaction is activationless, $\Delta G°$ is equal to λ and the reaction is at its maximum rate, thus the temperature has no effect on the rate of the reaction. Under these conditions the rate is k_{MAX}, so we can tell whether or not a reaction is proceeding at its maximum rate based on its temperature dependence.

A Marcus Curve is created by plotting ln k_{ET} vs. $\Delta G°$, shown in the following figure.

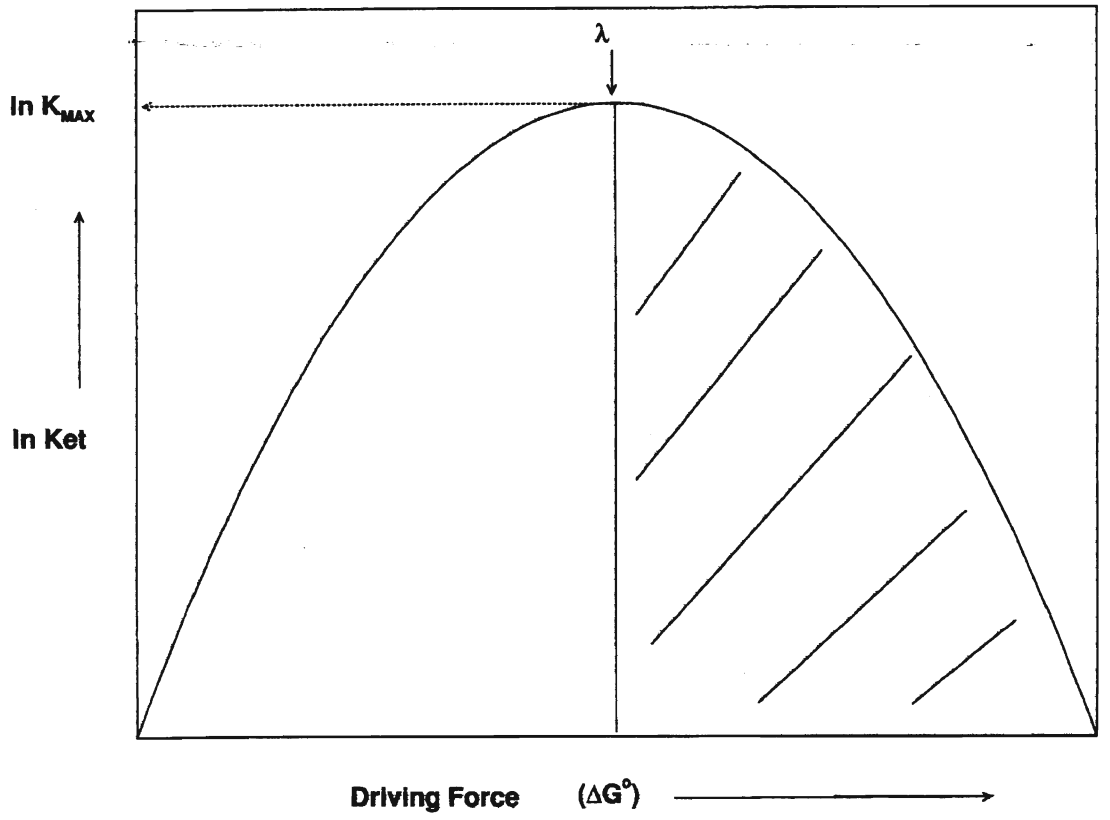

Figure 2-13: The Marcus Curve

The driving force is $\Delta G°$, and ln K_{ET} is the rate of the reaction. This figure shows that the maximum of the curve is located where $\Delta G° = \lambda$ and then the rate of electron transfer drops off with increased driving force (the shaded region in Figure 2-13). This is the Inverted Region of the Marcus curve, where we have a slow rate despite a large driving force[37, 38].

A 1998 study by Schlodder *et al.* measured the temperature dependence of electron transfer from $P_{700}^{+}A_1^{-}$ in PSI to F_X[41]. It was determined that the rate of electron transfer from A_1^{-} to F_X slows at lower temperatures (in the range of 300-200 K)[41]. The activation energy (ΔG^{*}) was approximately 0.22 eV and reorganization energy was about 1 eV[41]. Since the rate of electron transfer from A_1^{-} to F_X in PSI is not at a maximum,

experiments with non-native quinones that have midpoint potentials (and $\Delta G°$ values) that are both higher and lower than phylloquinone allows us to determine where on the Marcus curve the rate of electron transfer from A_1^- to F_X lies.

What Does an EPR Experiment Tell Us?

Unlike NMR, where usually the magnetic field is kept constant and the frequency is varied, in an EPR experiment frequency is kept constant and the magnetic field is varied over a specific range in which the spectrum is expected. In a time resolved EPR experiment, the data is displayed as a function of time and applied magnetic field. Figure 2-14 shows a Time Resolved EPR dataset.

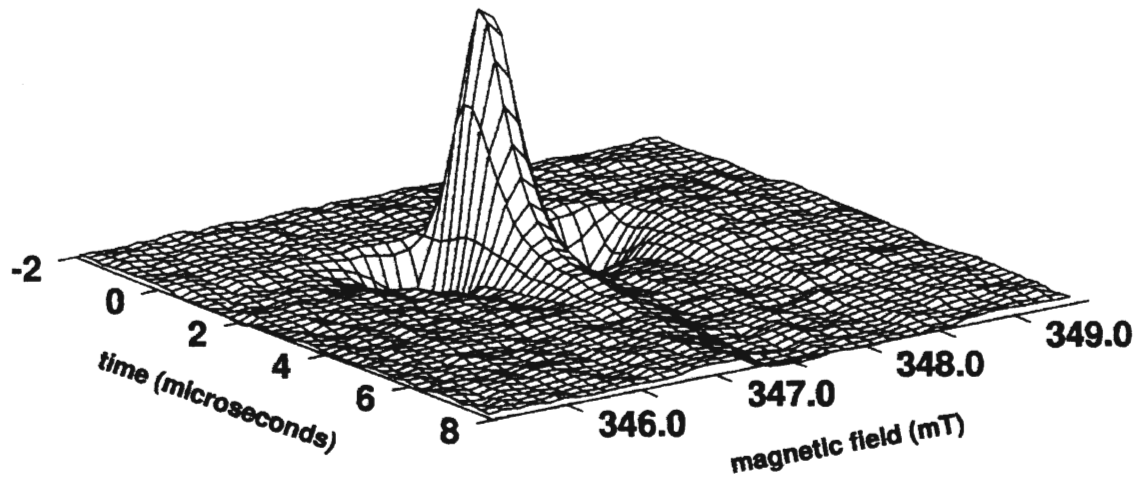

Figure 2-14: A typical Transient EPR Time-Field Dataset

Though very interesting to look at, if the EPR signal decays uniformly with respect to time, we do not obtain any additional information by plotting the time dependence. Normally, the spectrum is integrated with respect to time, and given as a function of applied magnetic field. For example, the following spectrum (Figure 2-15) is from the same data set shown in Figure 2-14, integrated from 0.4 μs - 0.8 μs.

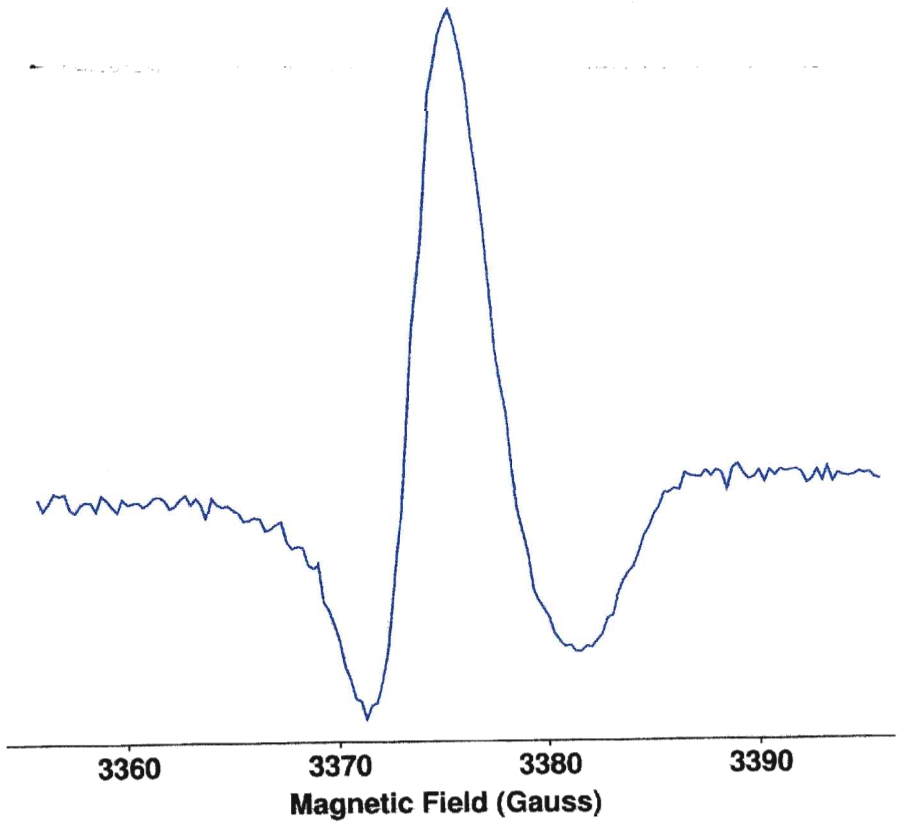

Figure 2-15: An EPR spectrum

Displaying a spectrum this way also makes comparison of spectra from different samples much easier. Analysis of the shape of an EPR spectrum can tell us about the strength and origin of the hyperfine coupling, and the orientation of the acceptor A_1 relative to the donor P_{700}^+. The fact that we see the radical pair spectrum means that the electron is in fact being transferred to the secondary acceptor, while the changes in the spectrum as a function of time at room temperature allows the kinetics of electron transfer from A_1 to F_X to be studied.

Though EPR provides a lot of information about our system, it is not without its drawbacks. It is important to acknowledge both the advantages and disadvantages to EPR spectroscopy.

EPR: Strengths and Weaknesses

A disadvantage to EPR is that it is not very sensitive. This means that to obtain a sufficiently strong signal, it is necessary to either use a lot of sample or perform a lot of averaging. Unfortunately, the organic solvents used in our extraction/incubation experiments destroy some of the reaction centres. Enough PSI survives the extraction procedure that the $P_{700}^{+}A_1^{-}$ radical pair still forms after incubation with non-native quinones, but there is a significant decrease in the signal strength, and as a result the signal to noise ratio is reduced.

An advantage to EPR, especially when dealing with extraction of phylloquinone and incubation with non-native quinones, is that it allows us to look at the formation of both the radical pair spectrum and the triplet spectrum using just one technique. What is most important is that the triplet spectrum is essentially zero in the region of the magnetic field where the radical pair appears. Thus any triplet spectrum that may be present after incubation is seen merely as a sloping baseline and will not interfere with our interpretation of the radical pair spectrum. Thus this technique is effectively blind to the damaged PSI.

Experimental

The cyanobacterium Synechocystis PCC 6803 was grown in 2 litre batch cultures using the methods of Biggins and Mathis (1988)[11]. Modifications to the growth procedure were the addition of 10mM $NaHCO_3$ and 10mM TES (pH 7.8) to maximize growth rate. Cells were harvested, washed and stored, and PSI was isolated from the cells according to the methods of Biggins and Mathis (1988)[11].

The native phylloquinone was extracted from lyophilized PSI using 99% pure hexane (Aldrich), and a mixture of 0.3% Methanol (Caledon) in Hexane. The extraction procedure was as described by Biggins and Mathis (1988); however, an extra extraction step using Methanol-Hexane was required to adequately extract phylloquinone in this case. After each extraction, the extracted PSI was tested using transient EPR to determine success or failure of the procedure.

The extracted PSI was resuspended in a buffer containing 50 mM Tricine, 0.2% Triton X-100 and 10% glycerol to prepare for incubation with non-native quinones. The quinones were dissolved in ethanol or n-propanol, depending on their solubility. It is important to note that control experiments were performed in a previous study that showed the alcohol used to dissolve the quinones did not have an effect on the EPR spectrum (Ragogna, unpublished data). From this we conclude that the solvent does not alter the protein.

A wide variety of quinones was selected for incubation in order to explore several questions about the significance of structural features of phylloquinone. Incubation times were 24 hours (AQ) and 2 hours (all other quinones). The structures of the non-native quinones used are shown in the following figure.

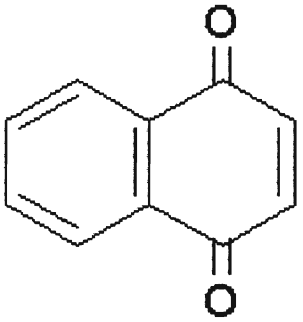

1, 4-Naphthoquinone[40]

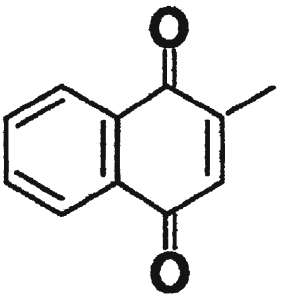

2-methyl-1, 4-naphthoquinone

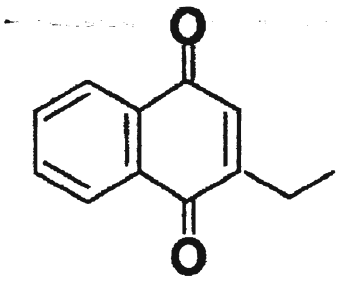

2-ethyl-1, 4-naphthoquinone

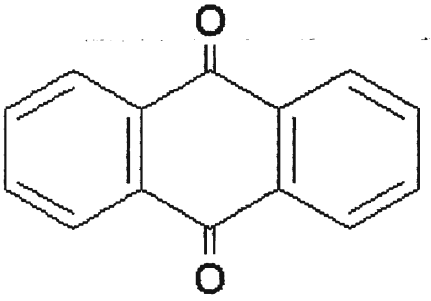

9, 10-Anthraquinone[40]

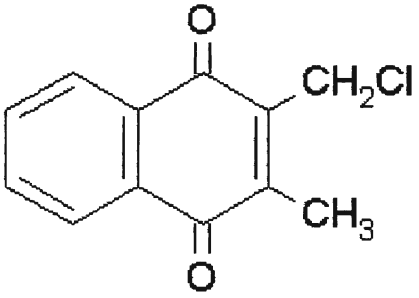

2-chloromethyl-3-methyl-1,4 naphthoquinone[40]

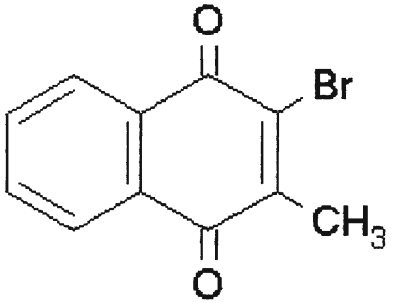

2-bromo-3-methyl-1, 4-naphthoquinone[40]

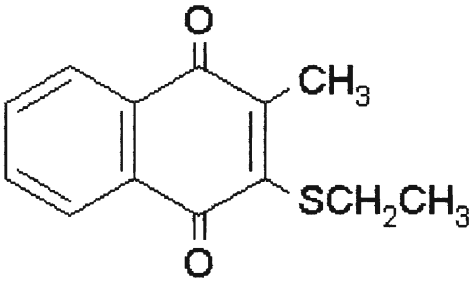

2-ethylthio-3-methyl-1, 4-naphthoquinone[40]

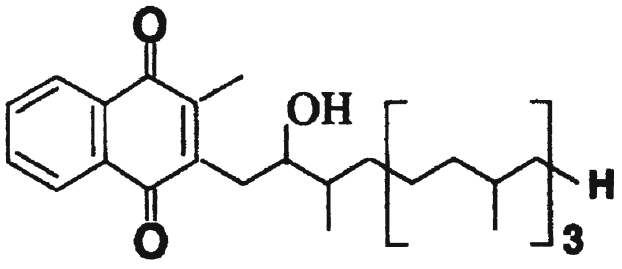

Hydroxy-phylloquinone

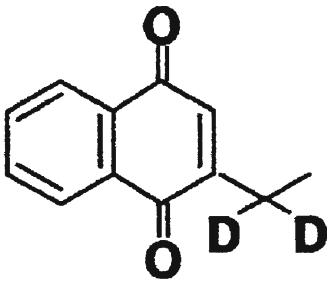

d2-2-ethyl-1, 4-napthoquinone

Figure 2-16: Structures of Non-Native Quinones Used

The importance of the methyl group and the phytyl tail was explored in the series of monosubstituted alkyl-naphthoquinones with an increasingly long side chain. 1, 4-Naphthoquinone, 2-Methyl-1, 4-Naphthoquinone, and 2-Ethyl-1, 4-Naphthoquinone were selected in order to determine if the length of (or absence of) a side group would affect the orientation of the quinone in the A_1 site. Another question that will be answered with this series of quinones is that if there is just one side group, will it assume the position of the methyl group or the phytyl tail? In other words, what feature in the native system is responsible for orienting the quinone properly? Hydroxy-phylloquinone was selected to determine what, if any, effect a change in the phytyl tail would have on the orientation in the binding site and on the rate of electron transfer. Spatial restrictions were tested through the use of Anthraquinone, which has an additional ring compared to the naphthoquinone head group. The series of disubstituted quinones was used to determine if they would bind with their side groups in a specific orientation and whether there is sufficient space in the A_1 binding site to accommodate a large, bulky group, such as a halogen.

EPR experiments were performed under several conditions. Low temperature EPR experiments were performed at both X-band (9 GHz) and Q-Band (35GHz). Temperatures were kept at 150K (X-band) using a liquid nitrogen cooling system, and at 80 K (Q-band) using a helium cryostat. Room temperature experiments were performed at X-band, using a flat cell. Two video amplifiers were used, one with a response time in the range of 1-2 μs and the other about 10 ns. The 'fast' amplifier was used for room temperature spectra; the 'slow' used for low temperature experiments and for qualitative determination of whether forward electron transfer from $A_1 \rightarrow F_X$ was occurring with

non-native quinones in the A_1 site at room temperature. Samples were illuminated using a Nd:YAG laser at 532 nm and 10Hz (X band) and a Nd:YAG/MOPO at 10 Hz and 532 nm (Q band).

Chapter 3

Results

Transient EPR gives a unique spectrum when the $P_{700}^{+}A_1^{-}$ radical pair of PSI is formed. In Chapter 2 it was discussed how the shape of this spectrum was due to spin polarization and hyperfine coupling to the CH_3 group of phylloquinone. When non-native quinones are incorporated into the binding site the intensity of emission or absorption and the overall shape of the spectrum will be altered. This may be due to changes in the hyperfine coupling of the protons of the non-native quinones compared to native PSI, or the result of the non-native quinone having a different orientation than phylloquinone. With a monosubstituted non-native quinone, it is possible that hydrogen bonding to the oxygen atom ortho or meta to the substituent will occur. It is also possible

that the side chain will be located in the position of the methyl group in intact PSI, or where the phytyl tail normally resides. When the native phylloquinone is removed by extraction with organic solvents, the distinctive triplet spectrum due to $^3P_{700}$ is apparent. It is valuable to use EPR to monitor the disappearance of the triplet spectrum and subsequent return of the radical pair spectrum after incubation with non-native quinones, which indicates successful replacement of phylloquinone. X band experiments, performed at 150K and 9 GHz give important information about the intensity of hyperfine coupling and can be used as a qualitative tool to determine whether successful replacement of the native quinone was achieved. Analysis of Q band (35 GHz) spectra obtained at low temperature (80K) will give key information about the orientation of the non-native quinones in the A_1 site. Room temperature X band experiments will show whether electron transfer is still occurring when a non-native quinone is present in the A_1 site.

X Band Transient EPR Experiments at 150K

In order to determine that the isolation and extraction procedures were not the cause of any change observed in the EPR spectrum, a series of control experiments were conducted. First the X band EPR spectrum of this cyanobacterium was measured using a sample of whole cells. In order to confirm that the isolation procedure was not affecting the radical pair spectrum, an experiment was performed on intact PSI that had been isolated from whole cells. The following figure shows the $P_{700}^+A_1^-$ spectrum of whole cells of Synechocystis 6803 compared with isolated PSI particles.

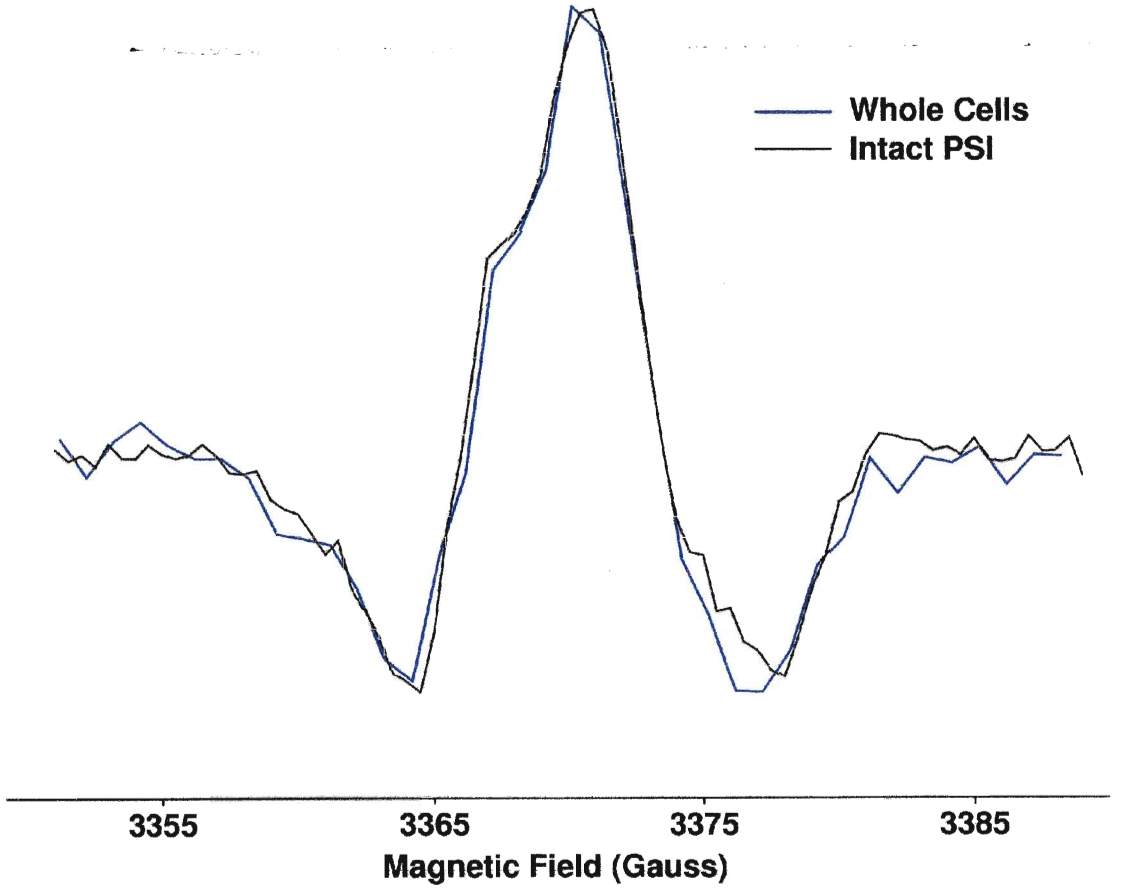

Figure 3-1: X Band Spectrum of Whole Cells of Synechocystis 6803 and Isolated PSI

A comparison to the EPR spectrum of whole cells shows that the two spectra are identical. The identical spectra confirm that the procedure for isolating PSI from the thylakoid membrane of Synechocystis 6803 does not damage PSI and will not prevent successful formation of the radical pair $P_{700}^{+}A_1^{-}$. Thus any change in the spectrum obtained from samples of extracted PSI incubated with foreign quinones will be due to the presence of the quinone and not an effect of the isolation procedure.

The spectra obtained in Figure 3-1 are due to the formation of the radical pair $P_{700}^{+}A_1^{-}$. At this point it is useful to point out the important features of the spectrum.

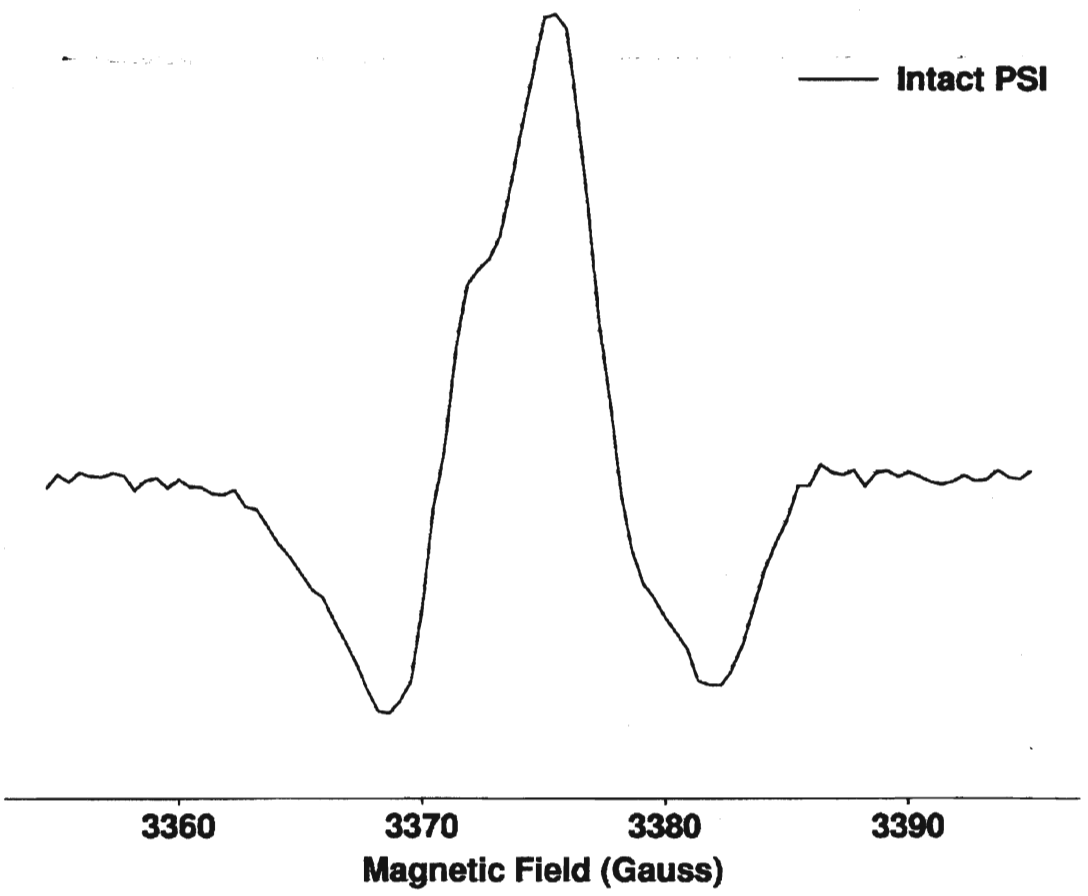

Figure 3-2: X Band EPR Spectrum of Intact PSI

This spectrum shows the contribution from the donor, P_{700} at the high-field end (~3382 Gauss) and the contribution from the quinone (A_1) at the low-field end (~3369-3379 Gauss) of the spectrum. The spectrum has the overall pattern of Emission/Absorption/Emission (E/A/E). The shoulder at around 3372 Gauss results from splitting of the signal due to hyperfine coupling to the protons of the 3-methyl side chain of phylloquinone. The splitting is not more resolved due to the presence of the 2-phytyl tail which also has hyperfine coupling to the unpaired electron. This 1:3:3:1 pattern is observed due to the asymmetric hydrogen bond to the carbonyl in the 1-position of the naphthoquinone head group which causes increased electron density to the group *meta* to the hydrogen bond.

The method used to remove phylloquinone from PSI was admittedly a harsh one. By definition, extraction of phylloquinone from the A_1 site with organic solvents requires denaturing the binding site. The question that must be addressed is whether PSI can withstand this treatment or whether it causes irreparable damage. Figure 3-3 answers that question.

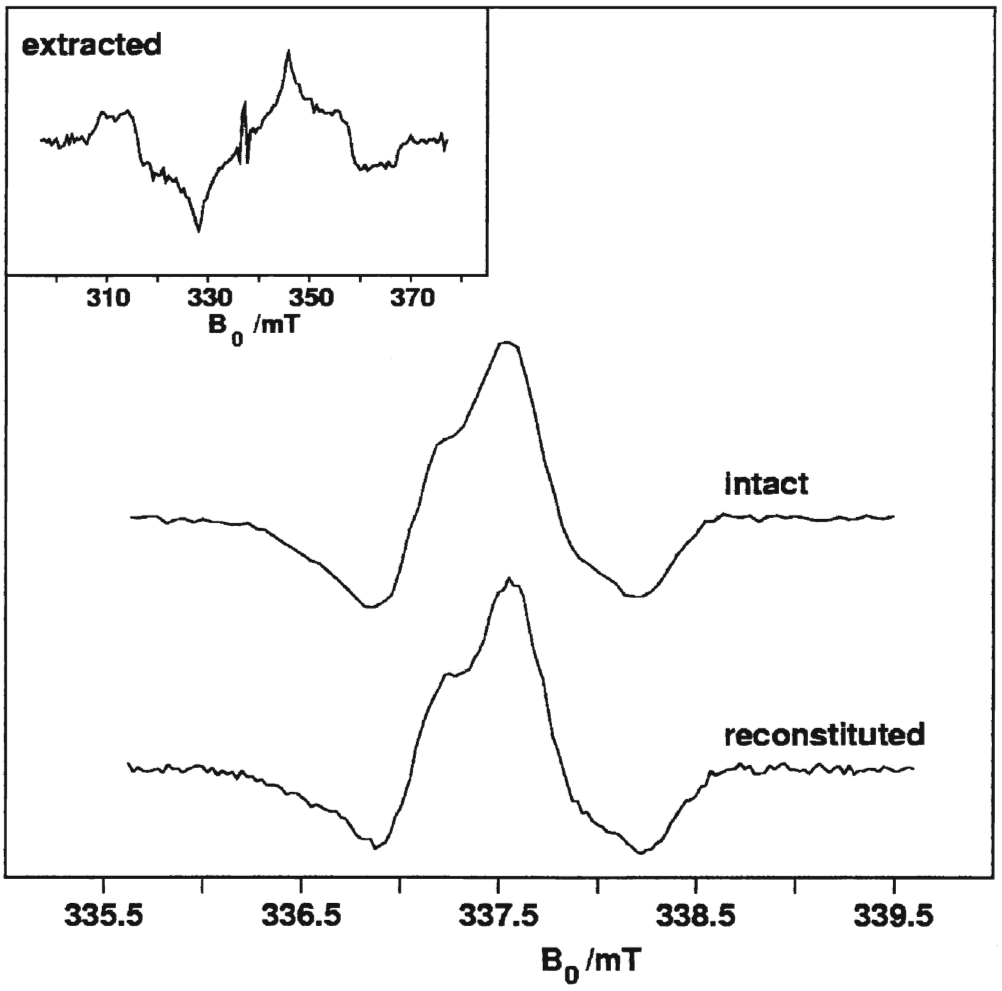

Figure 3-3: The Extraction and Reincubation of Phylloquinone in PSI[27]

The inset spectrum is the triplet spectrum of PSI after extraction with organic solvents. Note the scale of the spectrum is much wider than the radical pair spectra depicted in the main part of the figure. The triplet spectrum has the distinctive A/E/E/A/A/E pattern that indicates the formation of the $^3P_{700}$ state, because of

recombination of the radical pair (discussed in Chapter 2). The small spike in the triplet spectrum is a very weak radical pair spectrum that is due to the presence of a small amount of unextracted phylloquinone that remains in PSI. After incubation, the $P_{700}^{+}A_1^{-}$ spectrum is restored (labeled reconstituted in Figure 3-3) and is identical to the intact PSI radical pair spectrum. Thus we can conclude that there is no detectable damage to the binding site[27].

From this point on, for ease of reading, the transient EPR spectrum of extracted PSI incubated with a non-native quinone will be referred to as simply the spectrum of the non-native quinone. The abbreviations for the non native quinones that were used are listed on page 6.

Having demonstrated that any changes in the spectra would not be due to either the isolation or extraction procedure, the path was clear for a series of incubation experiments. First to be incubated was a quinone that was very similar in structure to phylloquinone, hydroxy-phylloquinone.

Replacement of the double bond of the phytyl tail of phylloquinone with a hydroxy group makes hydroxy-phylloquinone. This means that there is no longer π bonding from the C=C double bond, and also, the shape of the tail is changed. The effect on the X band spectrum is shown in the following figure.

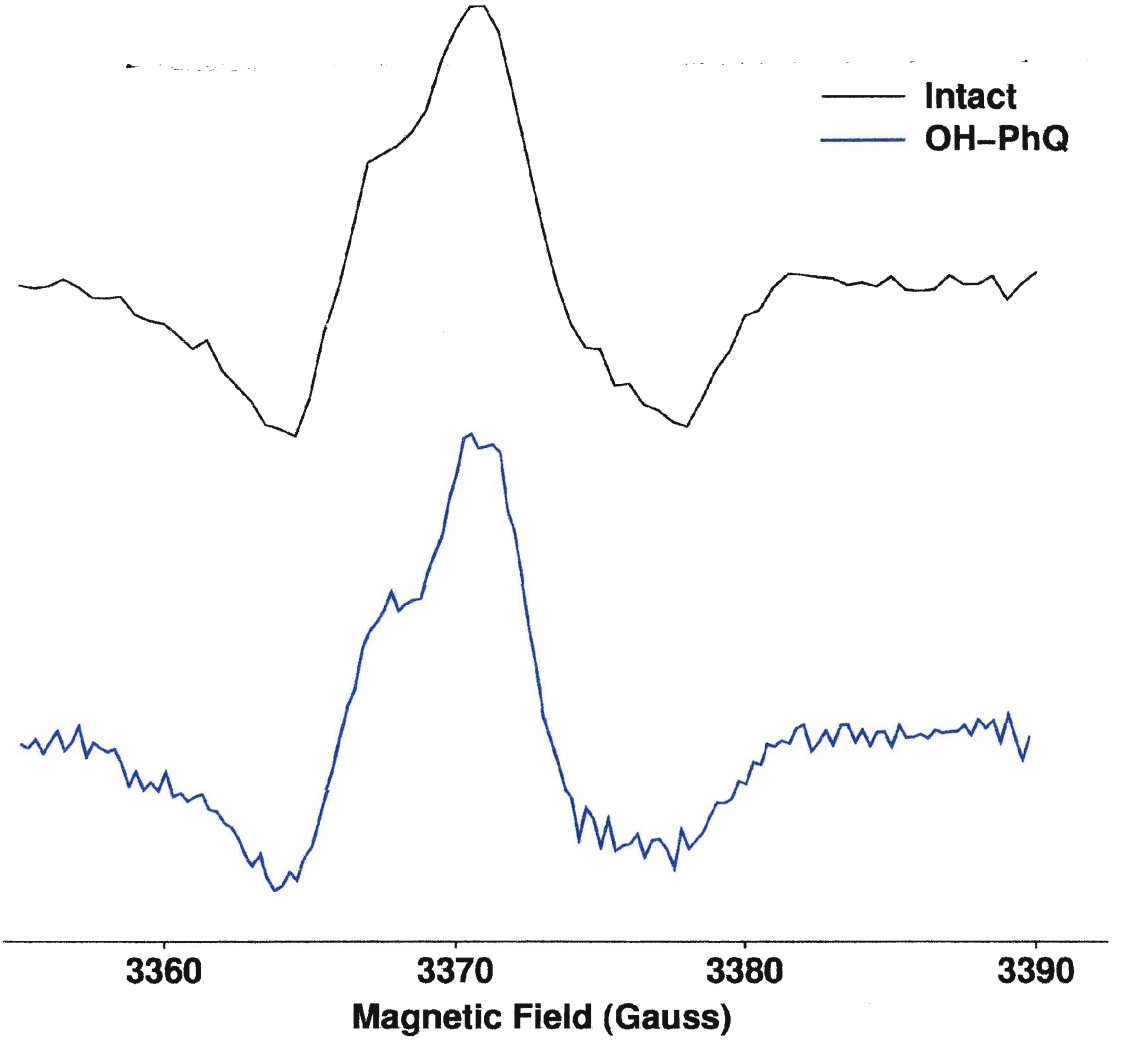

Figure 3-4: X band EPR spectrum of PhQ-OH at 150 K

The spectrum is very similar to the native spectrum, with the same 1:3:3:1 hyperfine splitting pattern seen in intact PSI. This indicates that the lack of the double bond in the phytyl tail has little effect on the formation of the radical pair or on the interaction of the quinone with the surrounding protein.

In order to determine whether the phytyl tail or the methyl group in phylloquinone is important for achieving the correct orientation in the A_1 site, a series of experiments using monosubstituted 1, 4-naphthoquinones was performed. The following series shows the effect of increasing the length of the side chain.

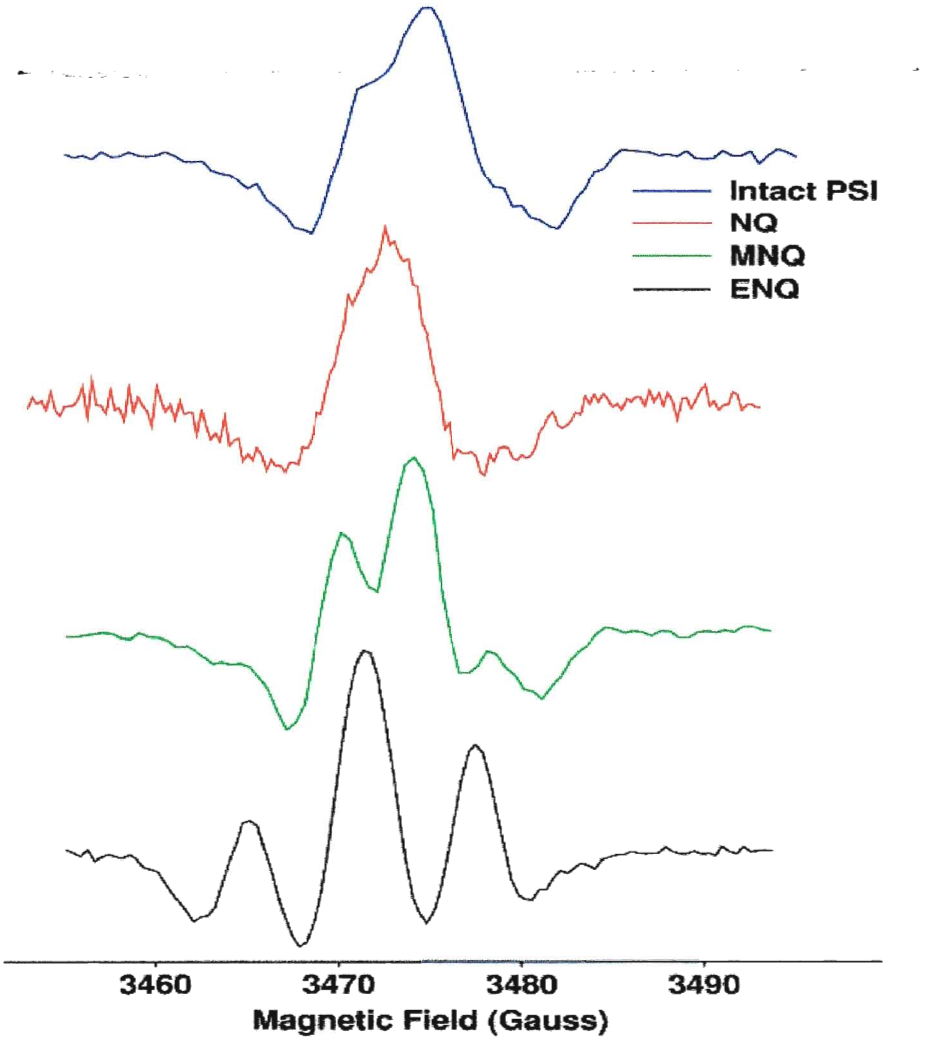

Figure 3-5: X band spectra of NQ, MNQ and ENQ at 150K

These spectra have been aligned using the position of the signal from P_{700} (at the high field end of the spectrum) as a reference point. This figure shows that when NQ is present in the binding site and the 'side chain' is merely a proton a clear hyperfine coupling pattern is not observed. It is possible that this quinone, which is essentially just the head group of phylloquinone, is being incorporated into the A_1 site with a distribution of orientations. This could be due to the absence of an asymmetric side chain[27].

The spectrum of MNQ is similar to that of native PSI, the hyperfine coupling is more pronounced but the splitting is nearly the same. The increased resolution of the

pattern in the MNQ sample is due to the fact that with phylloquinone there is hyperfine coupling to the CH_2 group of the phytyl tail which contributes to the hyperfine pattern, but this does not occur with MNQ. The fact that the splitting in MNQ is nearly the same as that of native PSI means that the spin density is the same thus the methyl group of MNQ has the same orientation as the methyl group of phylloquinone, *meta* to the hydrogen bonded oxygen.

It was expected that the phytyl tail would determine the orientation of phylloquinone in the binding site, thus it was uncertain how the monosubstituted quinones would be incorporated[27, 28]. The relatively small side groups selected could fit relatively easily into the site normally occupied by the methyl group or the phytyl tail. However, in the X band spectrum of ENQ it is apparent that a strong 1:2:1 hyperfine splitting pattern appears when ENQ is incubated with extracted PSI[27]. The pattern suggests that the side group is in the position *meta* to the hydrogen bond to the oxygen group of the quinone, and the coupling is to the CH_2 group of the ethyl side chain. Deuteration experiments will reveal the whether this is the source of the hyperfine splitting pattern.

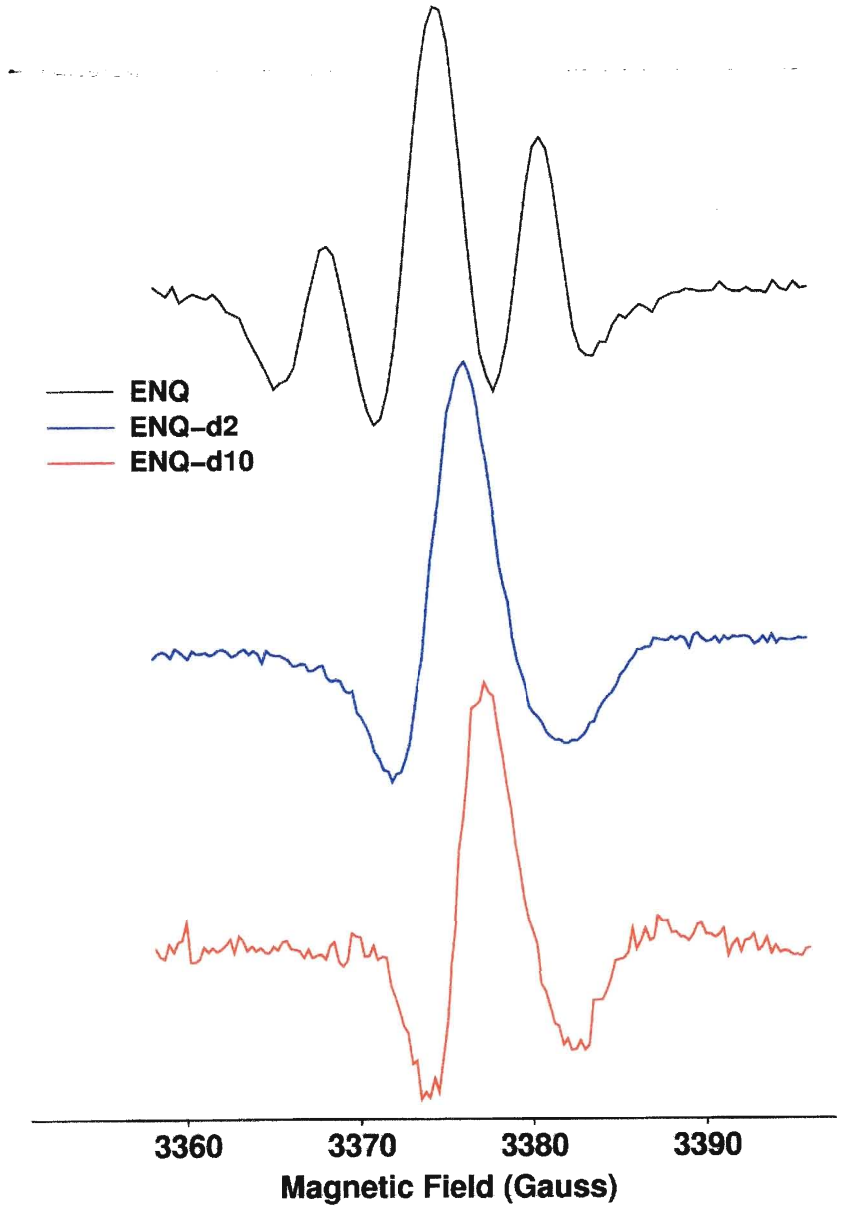

Figure 3-6: X band Spectra of a Series of Isotopically labeled Naphthoquinones

This series of spectra confirms that the splitting pattern is due to hyperfine coupling to the two equivalent protons on the methylene group. When the methylene protons are replaced with deuterium (the third spectrum down in Figure 3-6), the 1:2:1 splitting pattern vanishes. When the quinone is fully deuterated, we have the same E/A/E

pattern, but the lowfield feature of the spectrum is narrowed due to the presence of deuterium on the quinone.

Anthraquinone posed a unique challenge as it has a rigid bulky ring where the alkyl naphthoquinones have a single flexible chain, thus there was some question as to whether spatial restrictions would prevent its incorporation into the binding site. The results shown in the following figure, which compares intact PSI and extracted PSI incubated with AQ, indicate the remarkable versatility of the A_1 binding site.

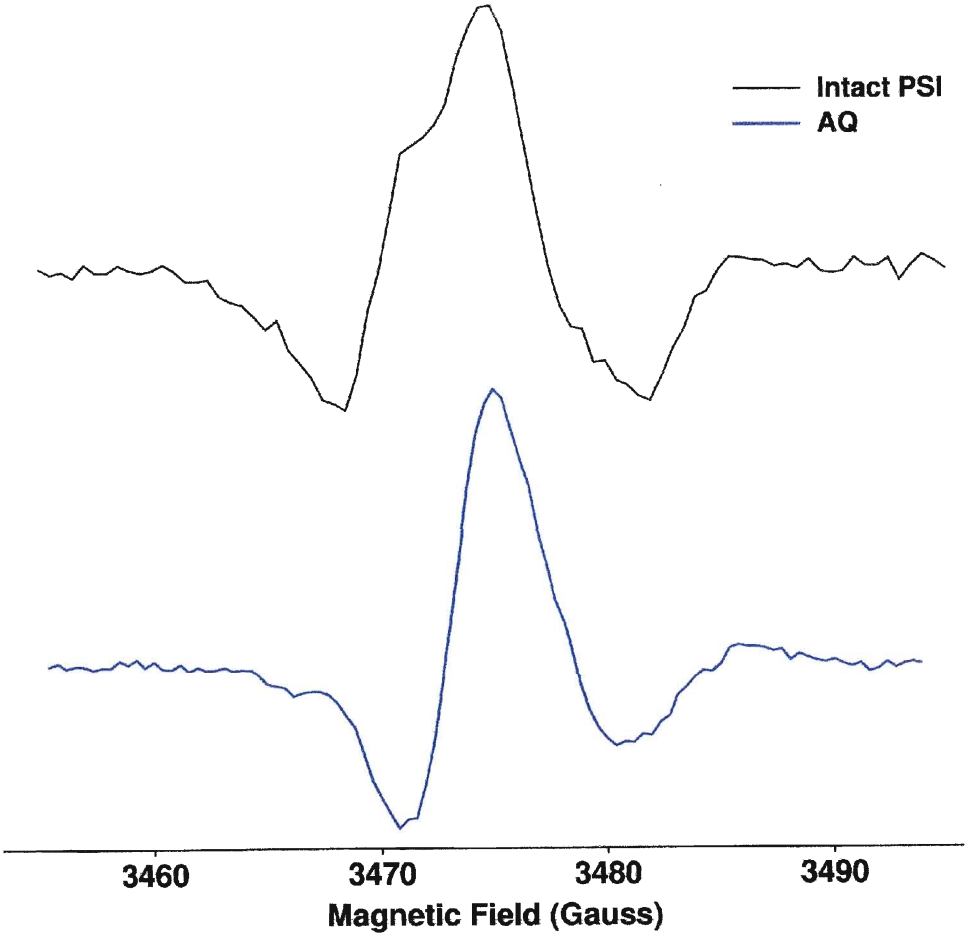

Figure 3-7: X band Spectrum of AQ compared to Intact PSI

The spectrum shows that when anthraquinone is incorporated into the binding site, the spectrum has an overall pattern of E/A/E. Because the 1:3:3:1 hyperfine splitting

pattern present in the spectrum of intact PSI is due to hyperfine coupling to the CH_3 group, it is absent in the AQ spectrum. Unlike with the monosubstituted naphthoquinones, we cannot deduce whether or not the hydrogen bond is intact when AQ is bound, because it lacks the strong hfs pattern such as that seen with ENQ.

After X band experiments were conducted to determine successful incorporation of non-native quinones in the A_1 site and the degree of hyperfine coupling, Q band EPR experiments were performed to determine the orientation of the quinone in the A_1 site.

Q Band Transient EPR Experiments at 80K

Q band EPR is conducted at a higher magnetic field than X band and the spectrum covers a wider range of magnetic field positions. As a result, the spectrum is not as compressed and the signal can be interpreted more easily, since there is less overlap between signal due to A_1 and P_{700}. As a result, a Q band spectrum can give us more information about the orientation of the quinones in the binding site.

It has been demonstrated using X band EPR that the isolation of PSI, extraction of the native quinone and subsequent reconstitution with phylloquinone does not affect the appearance of the spectrum. There is also no effect on the appearance of the spectrum at Q band, therefore any changes in the Q band spectrum of PSI incubated with foreign quinones will be due to the non-native quinone having a different orientation in the A_1 site. A typical Q band spectrum of intact PSI is shown in the following figure.

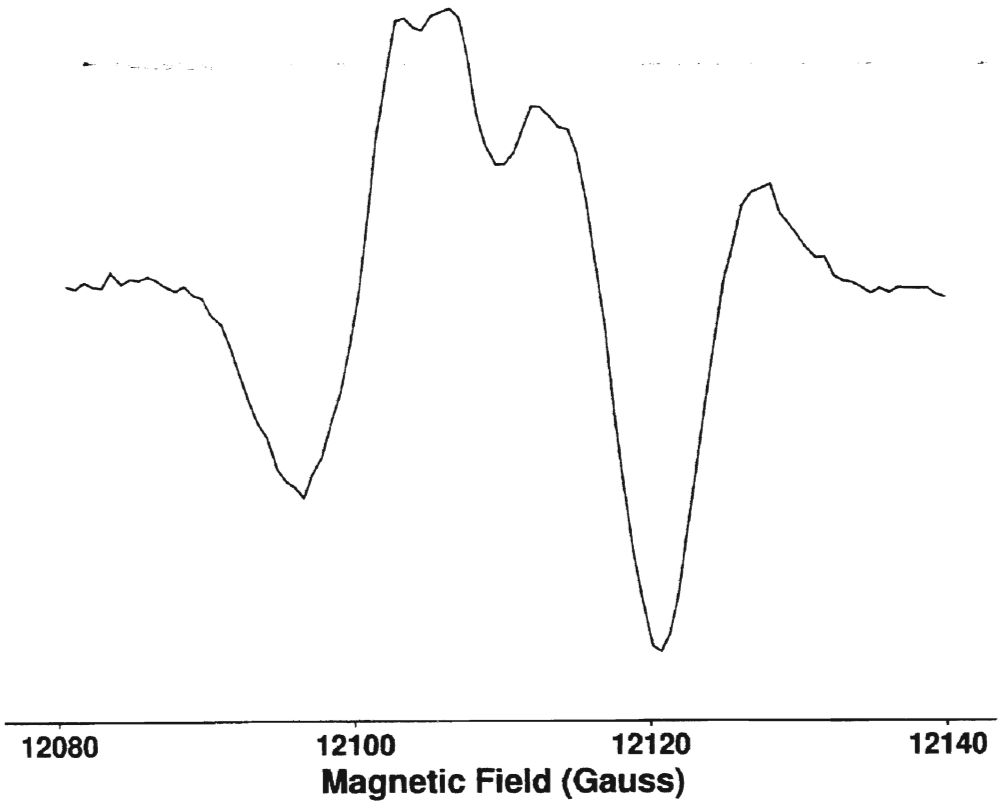

Figure 3-8: Q band spectrum of Intact PSI

In the native system, the spectrum has a pattern of E/A/A/E/A. The question of orientation of the naphthoquinone headgroup of non-native quinones will be addressed by looking at the pattern of emission and absorption that appears when the non-native quinones are incorporated into the A_1 site. We begin with the series of monosubstituted naphthoquinones that was first seen in figure 3-5 at X band.

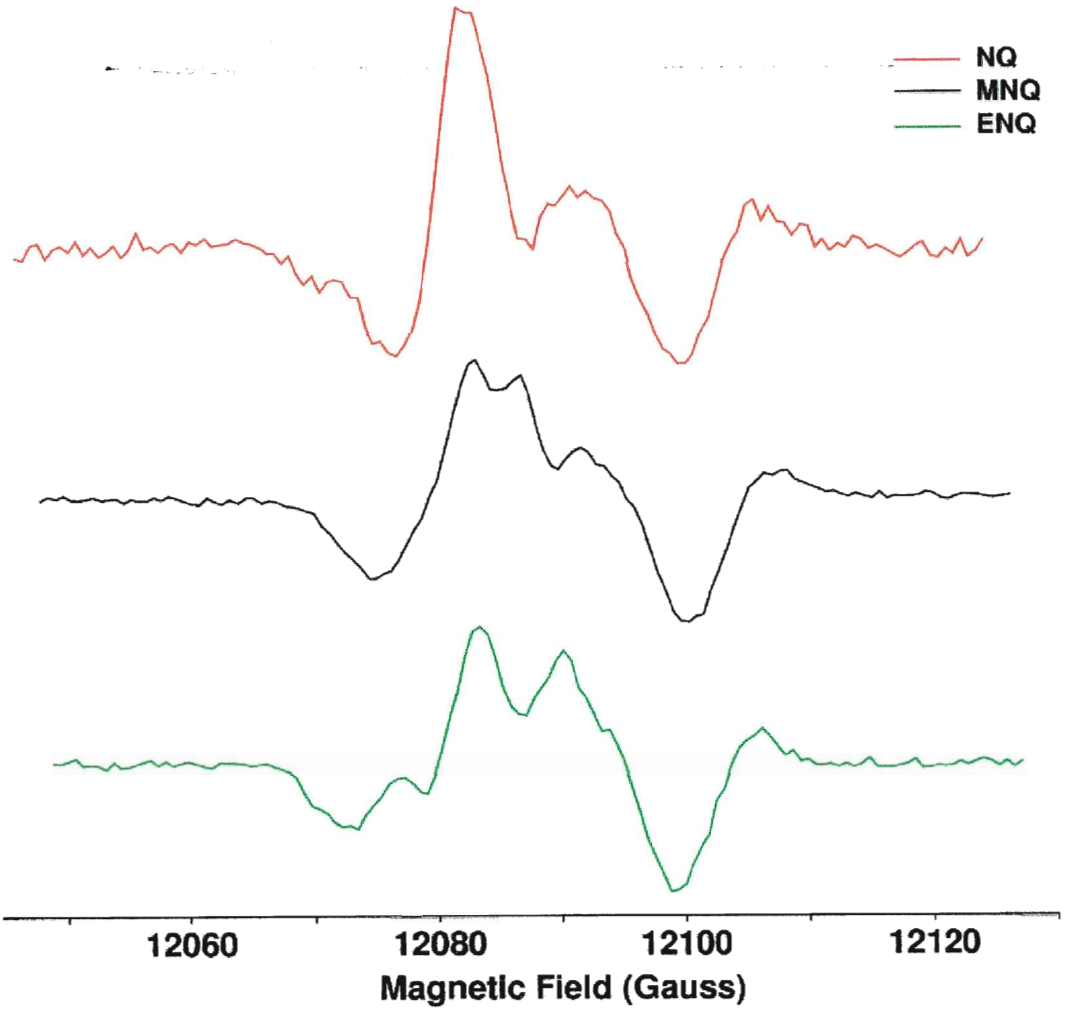

Figure 3-9: Q band spectra of PSI incubated with NQ, MNQ and ENQ

These spectra all have the same overall pattern of E/A/A/E/A as that of intact PSI, which means that the series of non-native quinones are all incorporated into the A_1 site with the same orientation as phylloquinone. Slight differences in the shape of the spectra can be attributed to differing hyperfine couplings with the series of non-native quinones, which primarily affects the absorptive features in the centre of the spectrum (~12080-12090 Gauss). The interpretation that the changes in the spectra are due to hyperfine coupling, and not some other factor, is corroborated by the series of spectra obtained with deuterated ethyl naphthoquinones.

As demonstrated at X band, the spectra of deuterated quinones do not have resolved hyperfine splitting. If we examine the overall pattern of the spectra of d2ENQ and d10ENQ we can determine whether the orientation changes with deuteration and ensure that differences in the features of the ENQ spectrum are due to hyperfine coupling.

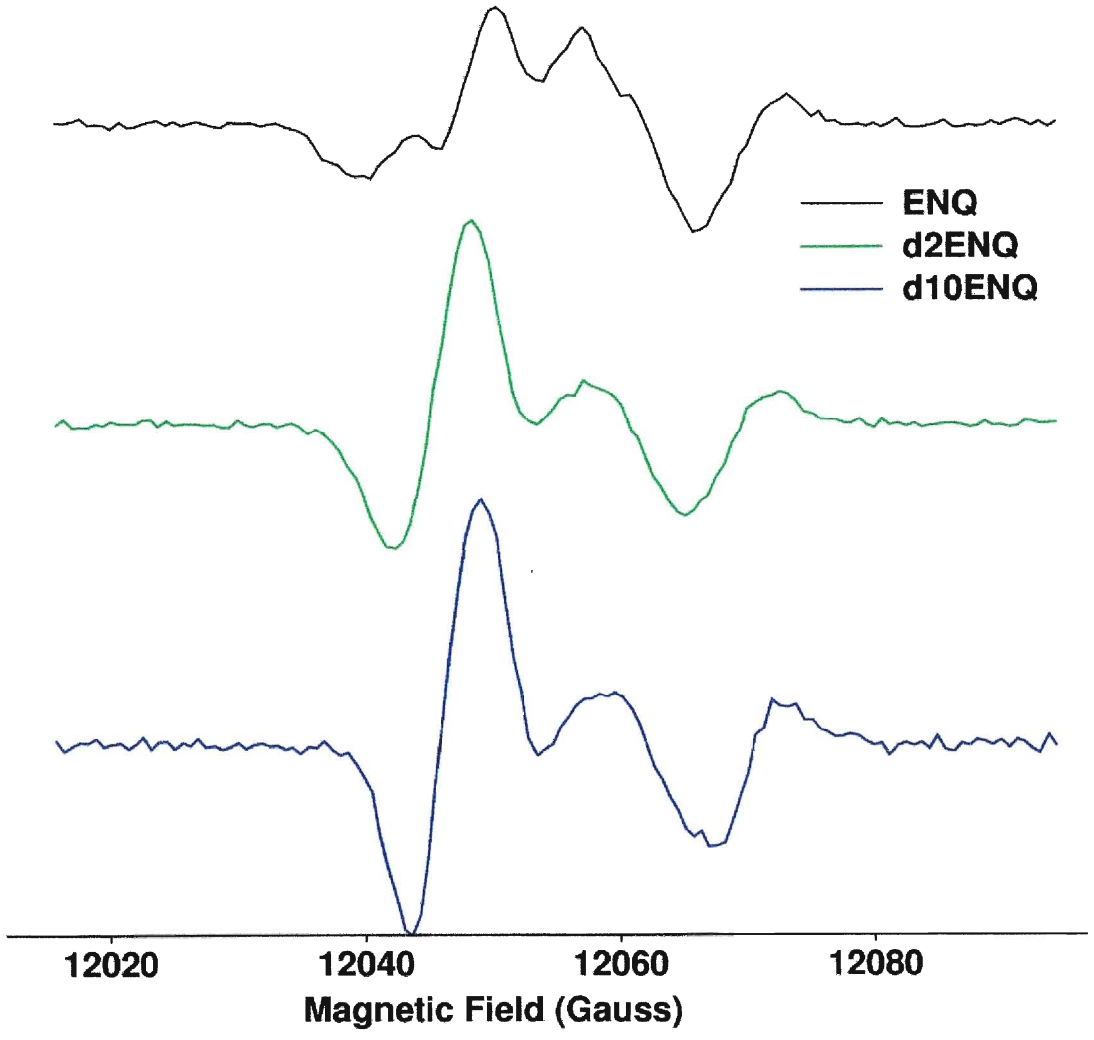

Figure 3-10: Q band spectra of PSI incubated with a series of isotopically labeled ethyl naphthoquinones

In Figure 3-10 we see that although the central features of the spectra are changing as the protons are replaced with deuterons, the spectrum still has an E/A/A/E/A

pattern, which indicates that the foreign quinones have the same orientation as phylloquinone. Replacement of the two methylene protons on the ethyl side chain (second spectrum) narrows the lowfield features of the spectrum, emphasizing the E/A/A/E/A pattern. Perdeuteration of the quinone narrows the spectrum further. The lowfield E/A feature of these spectra is very similar to that of the Q band spectrum of native PSI, indicating that the orientation of the quinones is the same[32].

A similar effect is seen when extracted PSI is incubated with perdeuterated NQ and MNQ, shown in Figure 3-11.

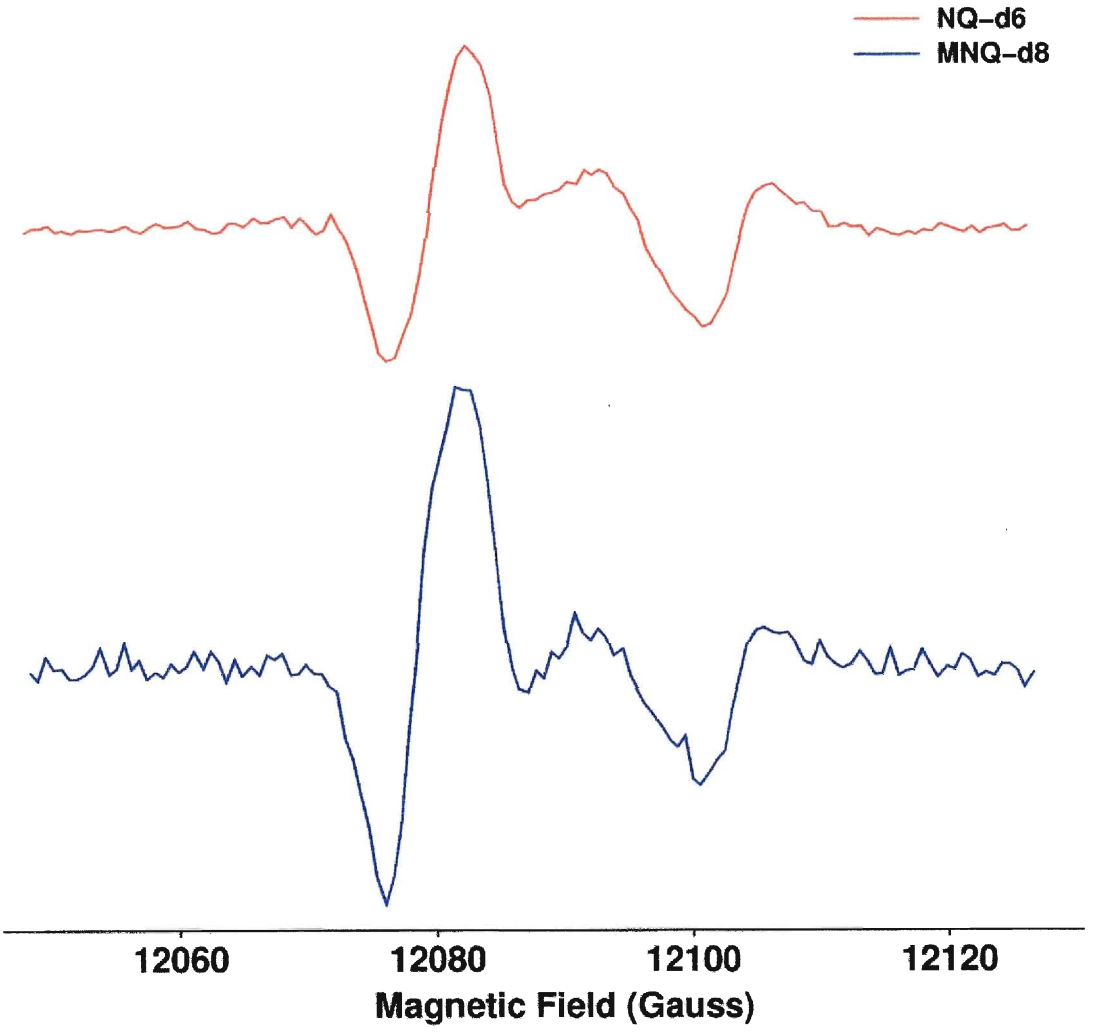

Figure 3-11: Q band Spectra of PSI incubated with d8-MNQ and d6-NQ

We see here that perdeuteration of MNQ and NQ emphasizes their similarity to the spectrum of intact PSI (Figure 3-8). The E/A at the low field end of the spectrum for d6NQ (~12075 - 12085 Gauss) is not as strong as that of d8MNQ. In the d8MNQ spectrum, the emissive portion is deeper, and the absorptive feature is higher, when the P_{700} (high field) signal is kept constant as a reference. This is probably due to a distribution of orientations of NQ.

A 1995 study by van der Est et al. simulated spectra to demonstrate the effect on the spectrum when the orientation of the quinone was changed[32]. In the calculations, the g tensor of the quinone was used as the "reference axis system"[32]. So a change in the orientation shows up as a change in the value of θ and φ, which describe the dipolar axis relative to the g tensor of the quinone[32]. The value of φ has a dramatic effect on the pattern observed in the Q (and K) band EPR spectrum[32]. The appearance of the spectrum changes, when the quinone is parallel to the dipole-dipole coupling vector, z_d, ($\varphi = 0$) there is a strong Emission/Absorption at the low field end of the spectrum. As the value of φ increases, the intensity of the E/A is lessened until we reach the "magic angle" of 54.7°, where the pattern changes to A/E/A at the low field end[32]. A common feature to all of our deuterated spectra is a strong Emission/Absorption at the low field end of the spectrum. This indicates that g_{XX} is parallel to z_d.[32]

The X band EPR spectrum of PSI incubated with anthraquinone did not allow us to determine whether the hydrogen bond is present when anthraquinone is incorporated into the binding site. However, the polarization pattern of the Q band spectrum of AQ will show whether the presence of the additional ring has an effect on the orientation of anthraquinone in the binding site.

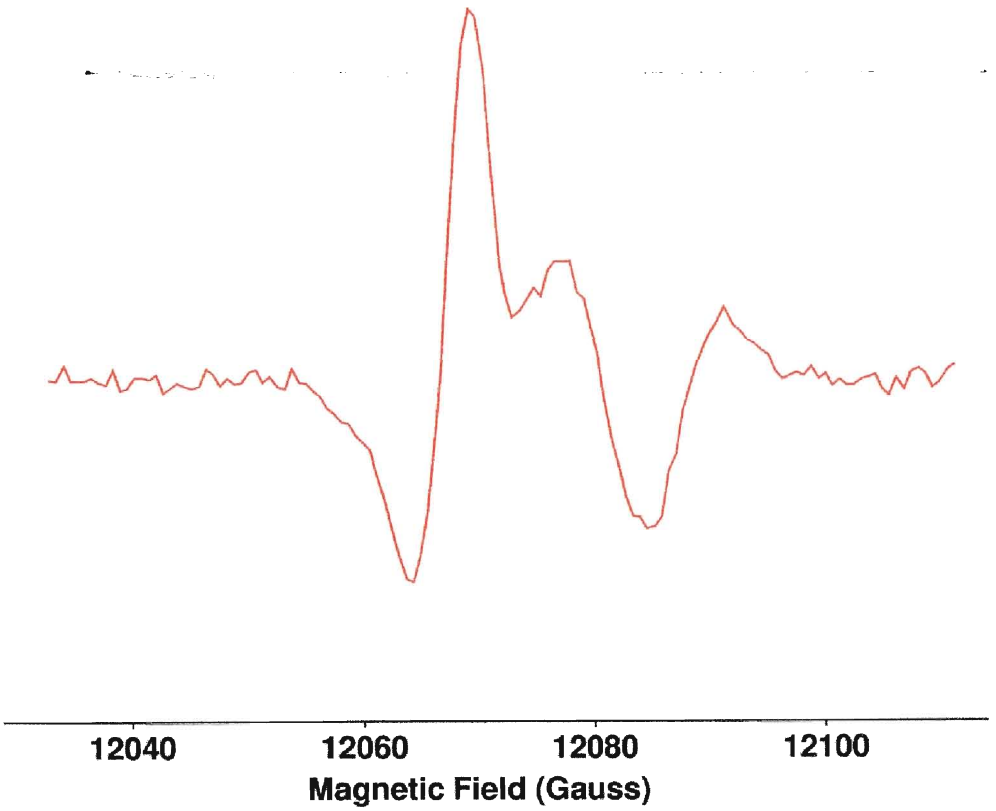

Figure 3-12: Q Band Spectrum of PSI incubated with AQ

Once again we see the now-familiar E/A/A/E/A shape of the spectrum, indicating that anthraquinone has the same orientation in the binding site as phylloquinone.

Previous studies with PSI incubated with 1, 4-Naphthoquinone had shown a very interesting result. It appeared that NQ was apparently incorporated in the A_1 site with an orientation in which the quinone was rotated by 90° with respect to the x-axis, compared to native phylloquinone[32, 57]. The features observed in the spectrum, namely an absorbance at low field and a narrow E/A pattern, correspond to a value of φ that is close to 90° and indicate that g_{YY} is parallel to z_d in contrast with PSI, which has g_{XX} parallel to z_d[32, 57]. However, when this experiment was repeated, using the same method of growth, isolation of PSI and extraction of phylloquinone, the results were quite different. The two spectra are compared in the following figure.

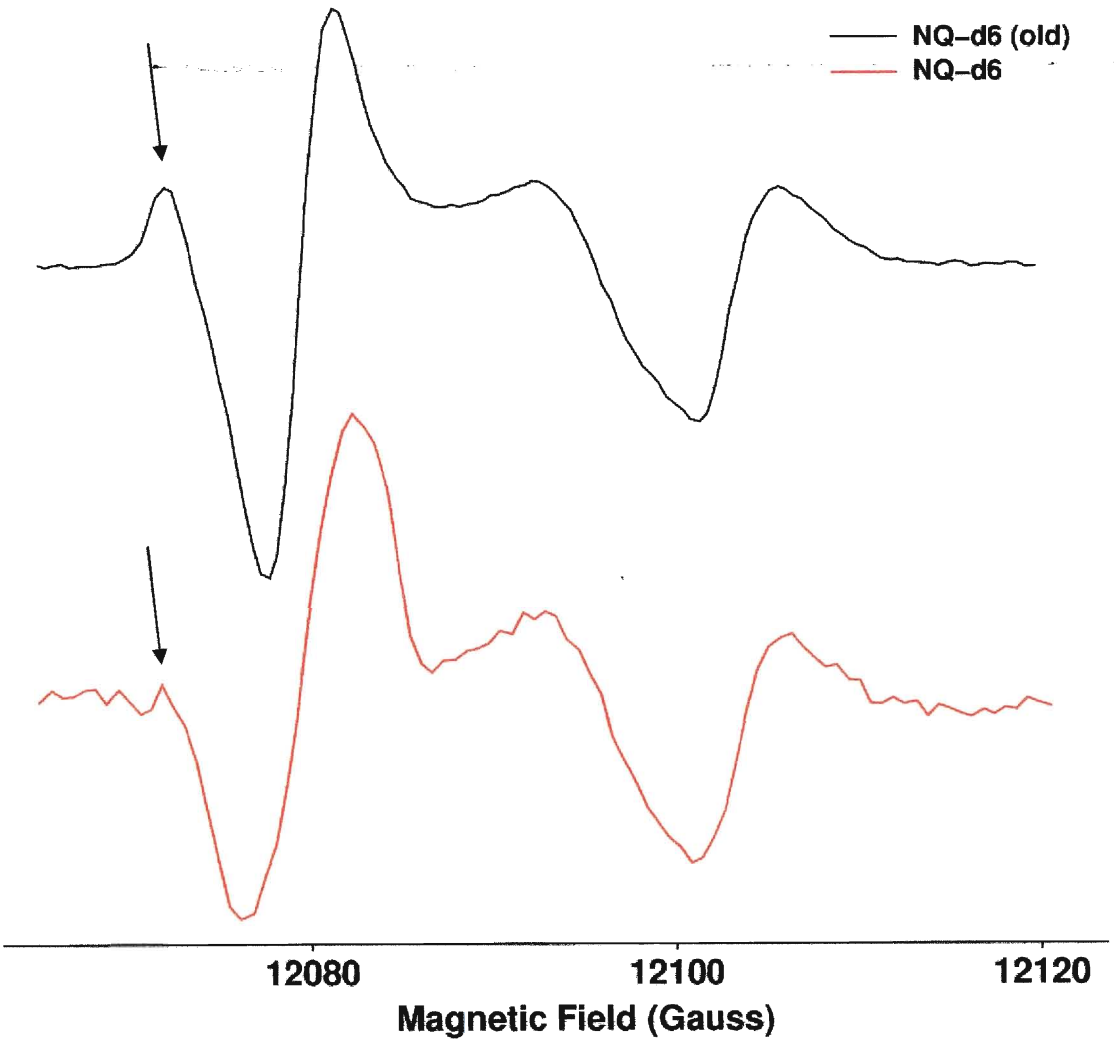

Figure 3-13: "The Naphthoquinone Dilemma"

Here we see that the pattern at the high field end, the contribution to the spectrum from P_{700}^{+}, is identical in both spectra. The difference is at the low field end of the spectra, where the contribution from the quinone appears. The spectrum labeled NQ-d6 (old), which has an A/E/A pattern at low field, indicates that g_{YY} is parallel to z_d[32, 57]. It was initially thought that NQ had weaker bonding to the protein, which prevented it from binding in the same orientation as phylloquinone[32]. However, the spectrum labeled NQ-d6 clearly shows the E/A pattern at low field, indicating that g_{XX} is parallel to z_d, that is,

the orientation is the same as phylloquinone. Recent experiments suggest that it was the method of sample preparation in the previous study that resulted in the different orientation, rather than the quinone used (van der Est, 2003, unpublished data). When D_2O is used during incubation with d6NQ, we obtain a spectrum similar to those observed in the previous studies[57]. When H_2O is used instead of D_2O, we see a spectrum similar to the X band spectrum of NQ-d6 obtained in this research project.

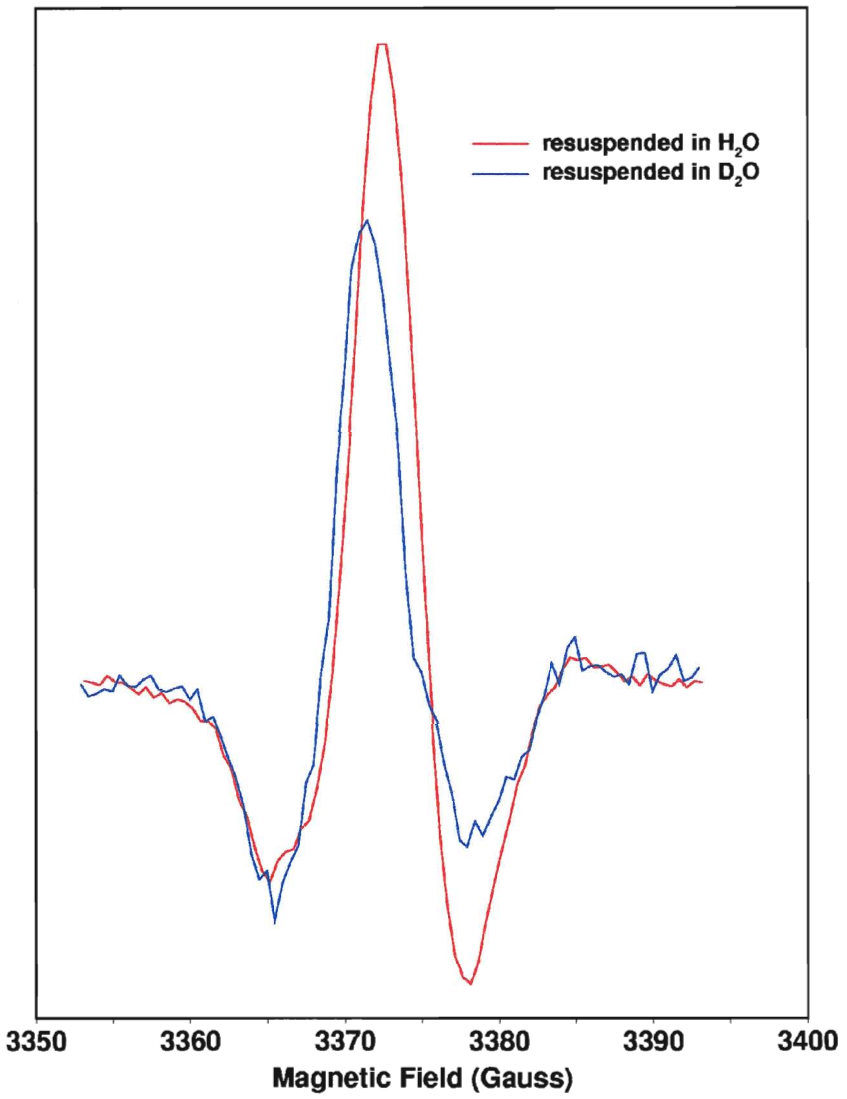

Figure 3-14: PSI incubated with NQ in D_2O and H_2O (Credit: Robyn Martin)

These results indicate that it is the presence of D_2O that affects the ability of the quinone to bind in the A_1 site, perhaps by affecting the hydrogen bond to the 1-carbonyl.

X Band EPR Spectra of 2, 3 disubstituted methyl naphthoquinones

We have now determined what orientation the quinone would have with a monosubstituted non-native quinone, or a quinone with a rigid ring. The next logical step was to use 2, 3-disubstituted methyl naphthoquinones to determine the orientation the quinone would have in the binding site. When a quinone with a single alkyl side chain was incorporated into the A_1 site, it is oriented so that the side chain is meta to the hydrogen bonded C=O. Will a quinone with both a methyl group and another side chain be incorporated with the methyl group meta or ortho to the hydrogen bond? Analysis of the hyperfine splitting pattern using transient EPR will allow us to determine the orientation of the disubstituted methyl naphthoquinones. The following figure shows the result of incubating with 2-chloromethyl- and 2-ethylthio- 3-methyl-1, 4-naphthoquinone.

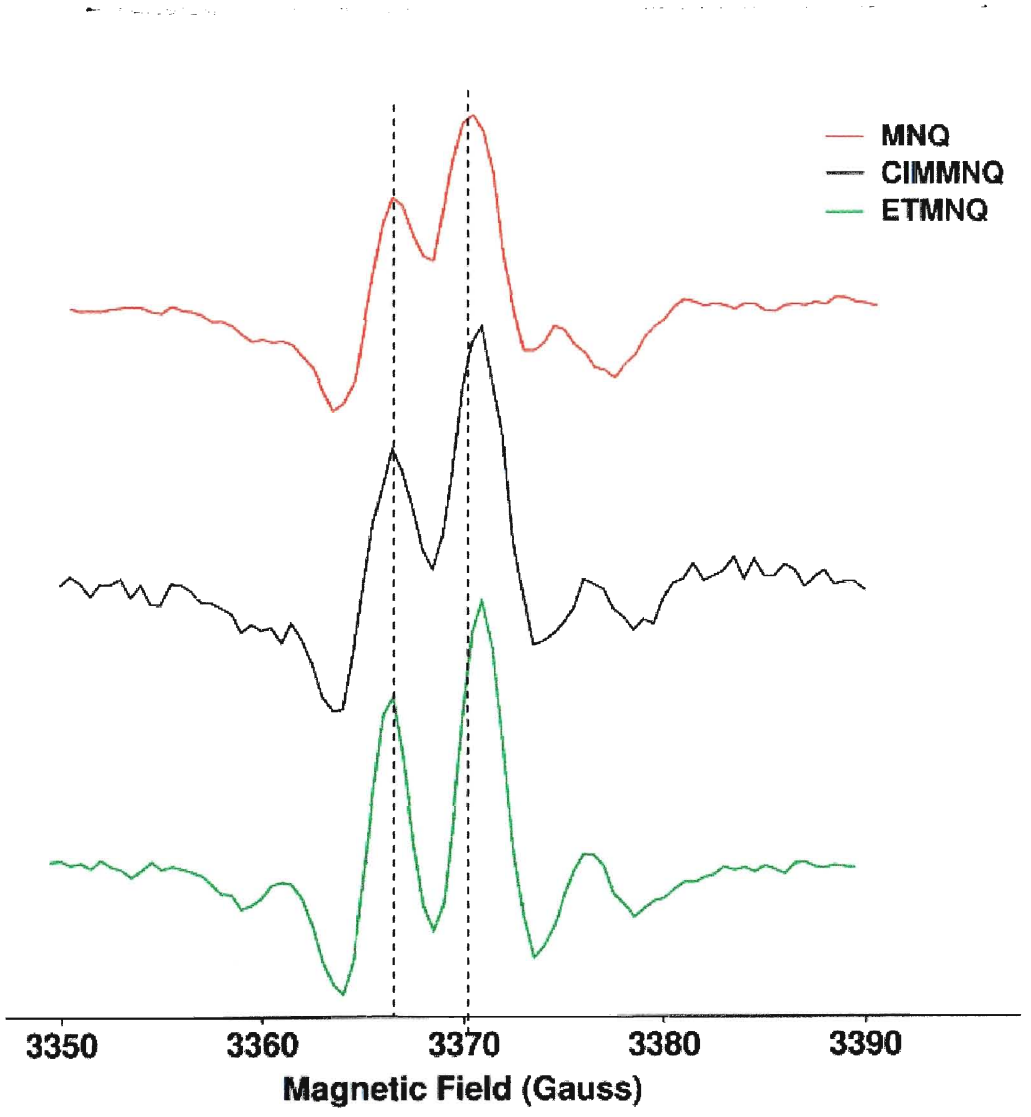

Figure 3-15: X band Spectra of 2, 3-disubstituted methyl naphthoquinones

The most striking feature of the spectra for these two disubstituted quinones is their similarity to the spectrum of MNQ. Q band spectra are needed to determine the orientation of these quinones properly, but the resemblance to the MNQ spectrum indicates that the orientation of the headgroup and the position of the methyl group are the same as for MNQ, and by extension, the same as in the native system. This means that the ethylthio- group and the chloromethyl- group are probably located in the position

normally occupied by the phytyl tail of phylloquinone. It appears that the presence of the ethylthio- or chloromethyl- side chain causes an increase in hyperfine coupling to the methyl group, which is revealed by the increase in the degree of splitting of the spectrum as the 1:3:3:1 pattern becomes clearer.

The limits to the size and type of quinone that can be successfully and reproducibly incorporated into a binding site that normally contains phylloquinone are revealed by incubation of extracted PSI with 2-bromo-3-methyl-1, 4-naphthoquinone. Bromine is a halogen, with an atomic radius of 1.14 Å, a mass of approximately 79.9 amu and an electronegativity of 2.8 [26]. This side group is quite different from the phytyl tail that it has replaced, which consists of basically non-polar C-H bonds and non-polar C-C bonds[64]. The effect is shown in the following spectrum.

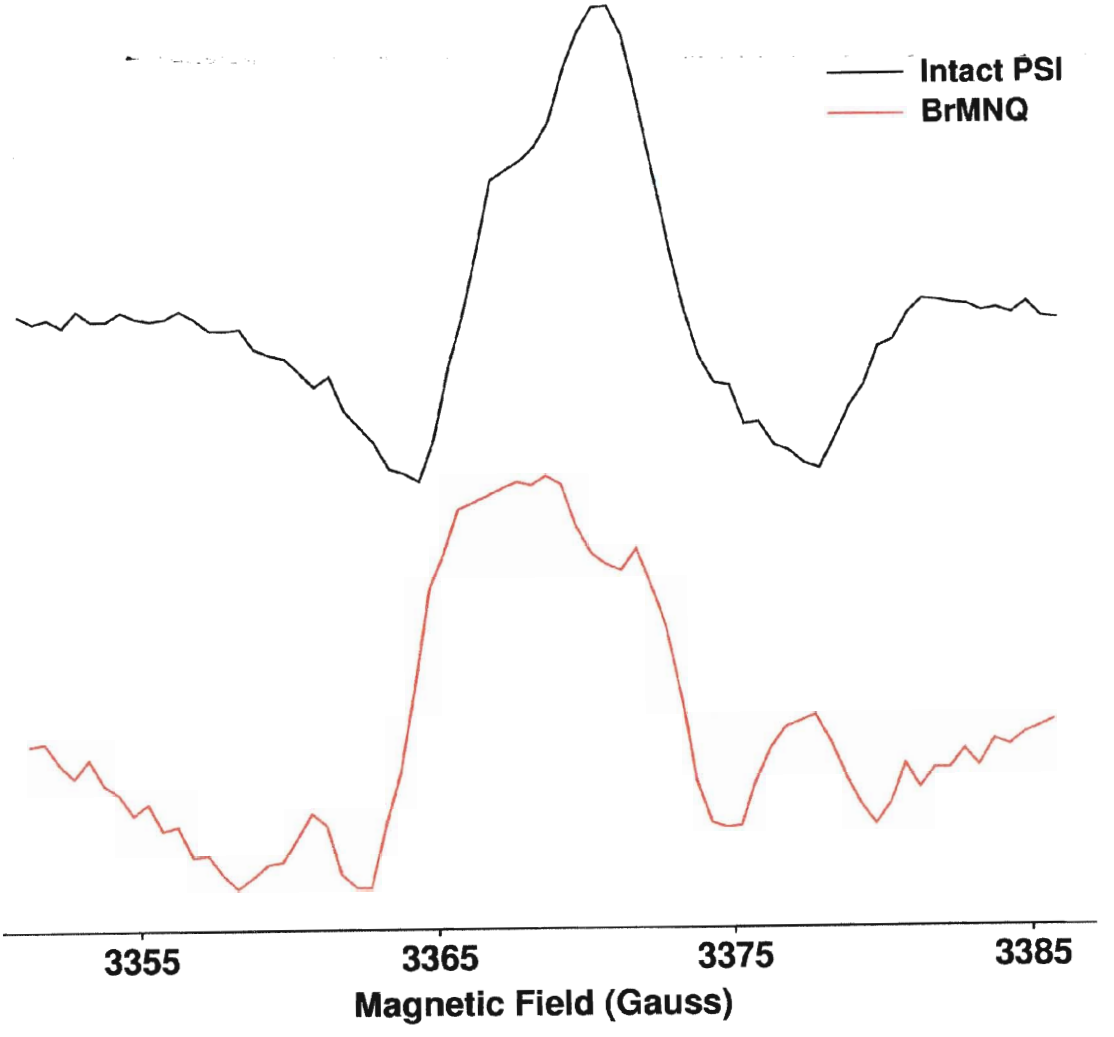

Figure 3-16: X band EPR spectrum of PSI incubated with BrMNQ

The poor resolution of the hyperfine structure is most likely due to presence of bromine atom directly next to the ring. We cannot detect the 1:3:3:1 pattern due to hyperfine coupling to the 3-methyl group that we could see so clearly in the case of 2-chloromethyl- and 2-ethylthio- 3-methyl naphthoquinone and thus cannot make any conclusions about the binding of the quinone.

The shape of the spectrum suggests that there is a distribution of orientations of the quinone. That is, the quinone is being accepted by the site, but it may not be incorporated in the same way in all cases.

X Band Transient EPR Experiments at 300K

EPR at room temperature is an excellent technique for determining the rate of electron transfer in PSI. This is especially important for experiments with incubation of non native quinones, in order to determine what effect the properties of the quinones have on the rate of forward electron transfer to the iron sulfur clusters.

By analyzing a room temperature EPR experiment, we can easily measure the lifetime of forward electron transfer to the iron-sulfur cluster F_X from A_1 provided it is greater than approximately 50 ns and less than the decay of spin polarization. To analyze a room temperature spectrum, one can use a fit program to extract the electron transfer lifetime, or merely compare the shape of the spectra to determine whether electron transfer is occurring. The following preliminary room temperature experiments do not allow an accurate determination of the electron transfer lifetimes and therefore will be discussed qualitatively.

Previous studies on intact PSI have demonstrated the temperature dependence of the rate of electron transfer from A_1 to F_X[41]. This implies that ΔG^* is not zero and therefore the rate of electron transfer is not at the maximum of the Marcus curve. The question posed with these non-native quinones is whether the rate of electron transfer will increase or decrease when they are present in the A_1 site.

It has been demonstrated that at X band, the EPR spectrum is unchanged when looking at whole cells and isolated PSI. It is important to ensure that this is also the case for the rate of forward electron transfer. That is, that the radical pair is forming and the PSI is still functional. The following figure provides that vital reassurance. Figure 3-16 shows transients extracted from the datasets of whole cells, intact isolated PSI and

extracted PSI incubated with phylloquinone (VK_1). The bottom set of transients shows electron transfer to A_1, and the formation of the radical pair $P_{700}^{+}A_1^{-}$, with the subsequent transfer to F_X, forming $P_{700}^{+}F_X^{-}$. The formation of $P_{700}^{+}A_1^{-}$ is indicated by the absorptive signal, and the signal decays with the transfer to F_X. The rate at which the electron is transferred can be extracted from the transients by measuring the time that it takes from the point of maximum absorbance to the point where the signal becomes emissive.

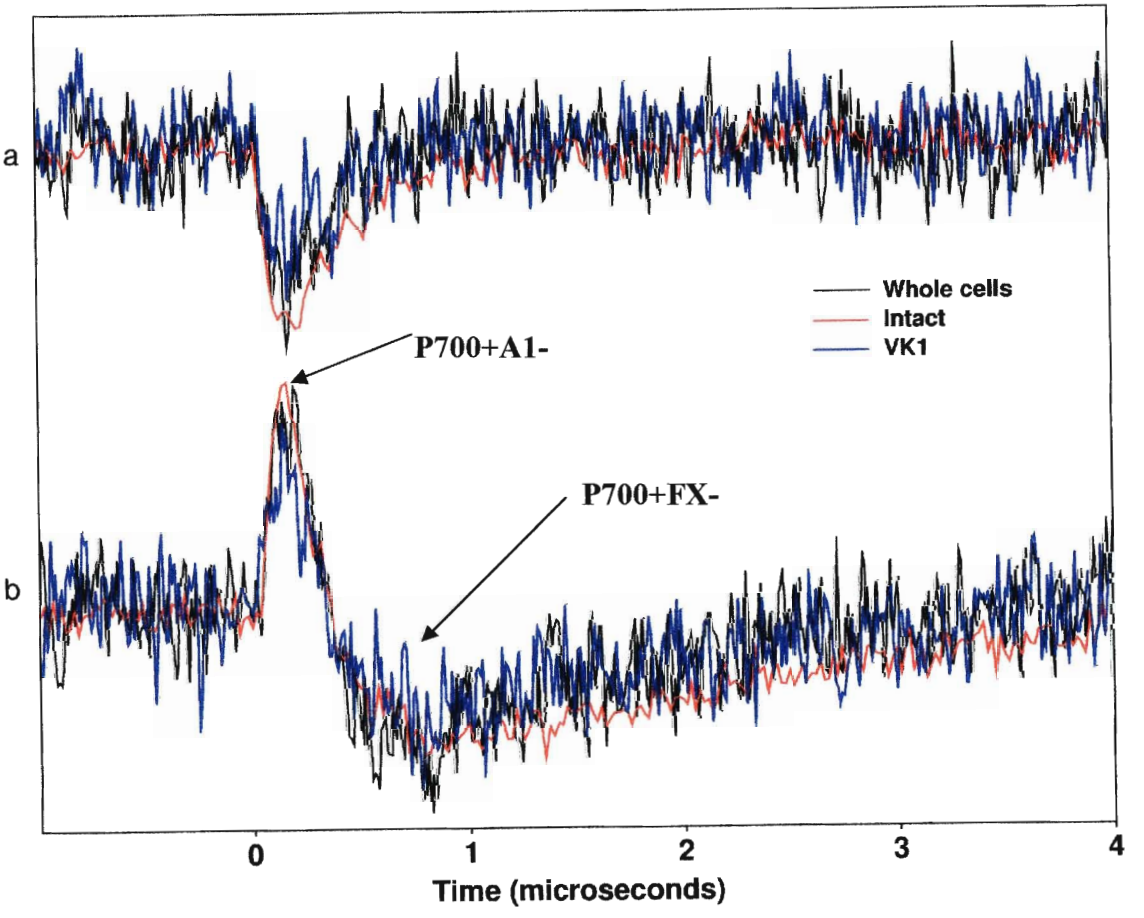

Figure 3-17: Whole Cells, Isolated PSI and extracted PSI incubated with Phylloquinone

The transients for whole cells, isolated intact PSI and extracted PSI incubated with phylloquinone are identical. This shows us that the isolation and extraction steps have no effect on the rate of forward electron transfer. It has previously been reported

that the rate of electron transfer from A_1 to F_X has two phases, 200 ns and 20 ns[18]. The fast phase cannot be detected with this method, but it is possible to see the 200 ns phase. For our purposes, the actual rate of electron transfer is not as important as the fact that all three preparations have the same rate.

Now that we know that the extraction procedure is not affecting forward electron transfer to F_X, we can move on to the PSI preparations incubated with non-native quinones. The following figure shows the transients extracted from room temperature EPR spectra of PSI incubated with NQ, MNQ, ENQ, OH-PhQ, ClMMNQ and BrMNQ. Room temperature experiments with the deuterated forms of naphthoquinone, methyl naphthoquinone and ethyl naphthoquinone were not conducted, since previous experiments indicated that deuteration did not affect the rate of electron transfer. Room temperature experiments with ethylthio-3-methyl naphthoquinone will be conducted at a later date.

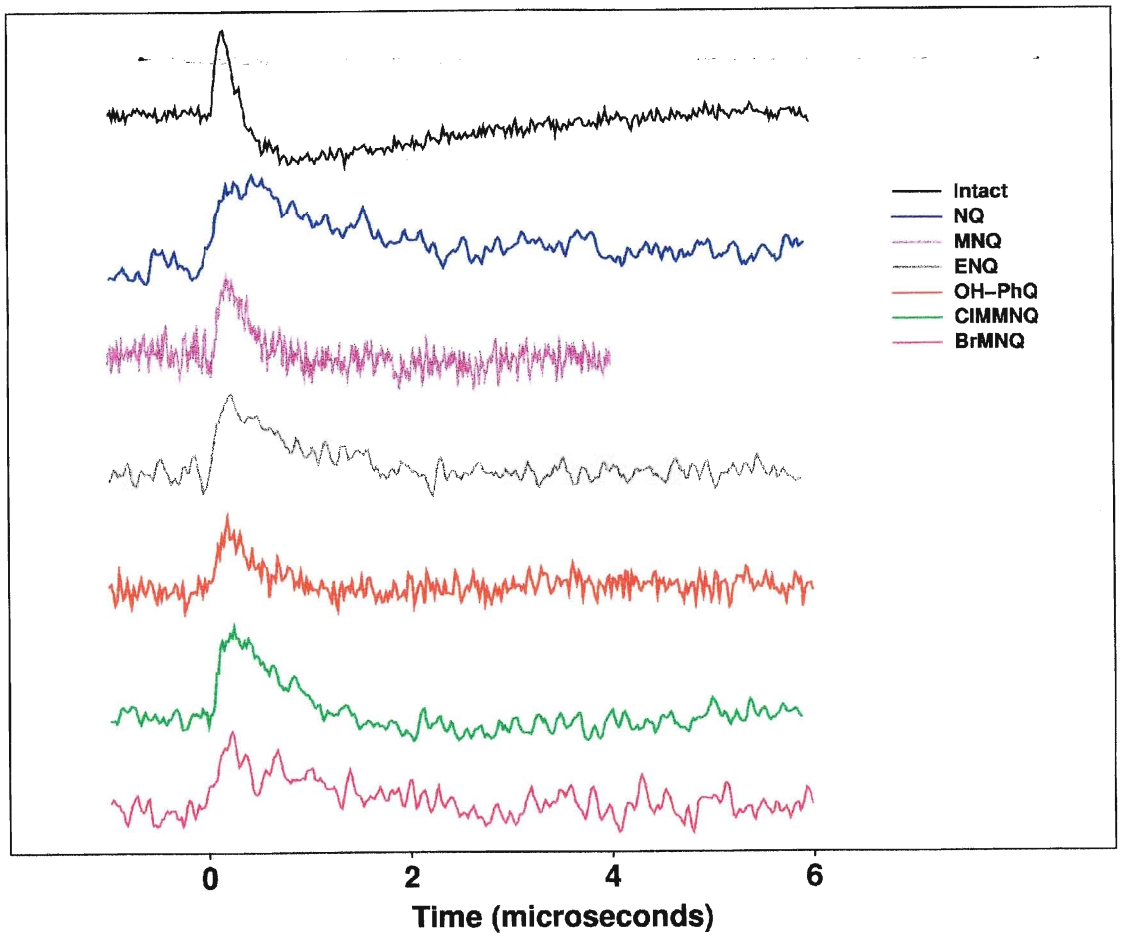

Figure 3-18: Transients from Room Temperature EPR Experiments of PSI incubated with a series of non-native quinones

What all of these transients have in common is the absence of the Absorbance/Emission pattern seen in that of native PSI. Instead, we get the absorptive peak that decays to zero, on approximately the same timescale as spin relaxation. This indicates that there has been electron transfer to the quinone from A_0, but the forward transfer from the quinone to F_X is either slowed past the point where we can detect it with this method, or it is not occurring at all. At this point it is unclear which of these two situations is occurring.

Room temperature spectra can tell us whether the radical pair is present, or the electron has already been transferred to the iron-sulfur clusters. The following figure is a room temperature spectrum of whole cells of Synechocystis 6803.

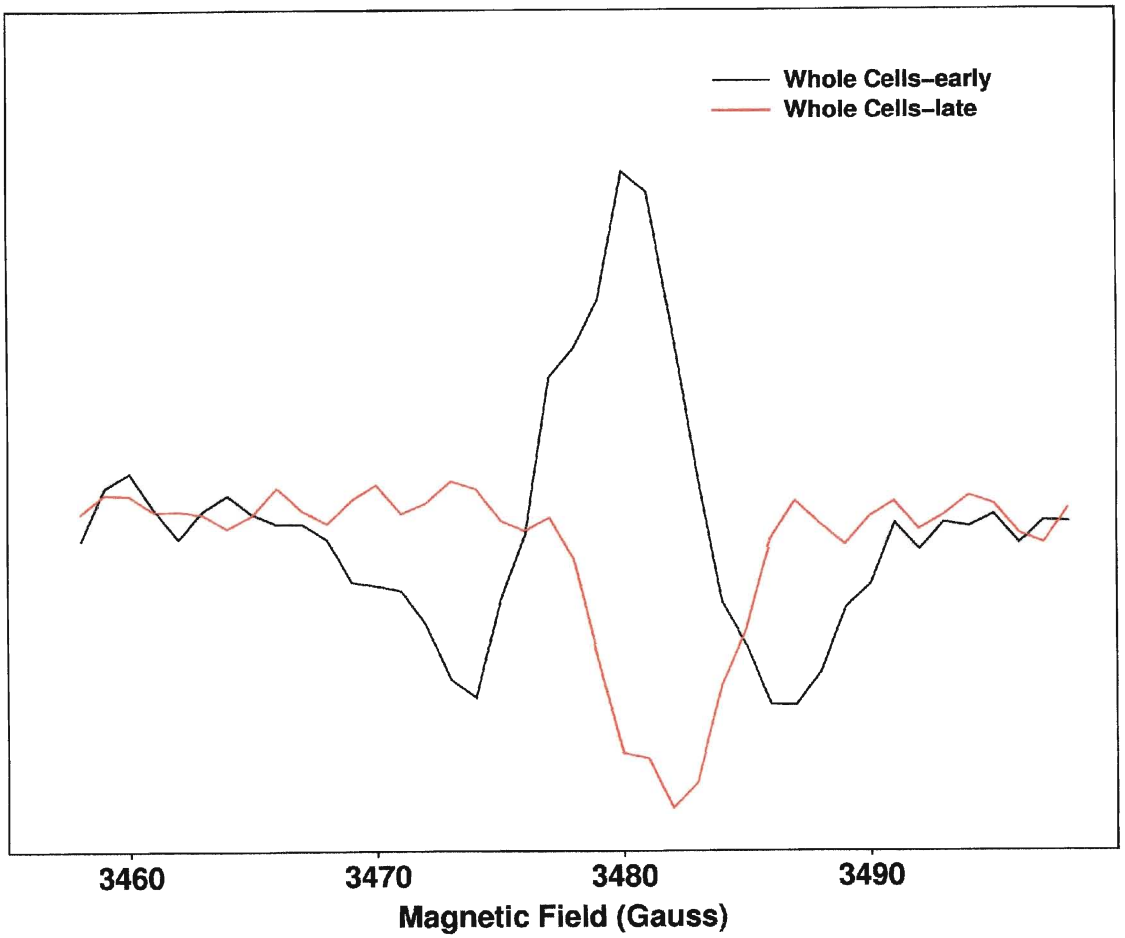

Figure 3-19: Room temperature Spectrum of Whole Cells

Here we can see that the spectrum changes dramatically, from the familiar Emission/Absorption/Emission pattern seen in the early spectrum (black line), to just Emission in the late spectrum (red line). The contribution from the quinone is located at the low field end, and with forward electron transfer to F_X the emissive signal disappears.

Anthraquinone is unique in our series of foreign quinones for several reasons. It lacks the flexible alkyl tail present in our alkyl naphthoquinones. Unlike the other

quinones studied (namely NQ, MNQ and ENQ) it has a midpoint potential that is more negative than phylloquinone. Its value of -830 mV in DMF is approximately 120 mV more negative than the potential of phylloquinone in DMF[35, 36]. This implies that anthraquinone has a higher $\Delta G°$ value than phylloquinone. The Marcus theory (discussed in Chapter 2) tells us that if the rate for electron transfer from $P_{700}^{+}A_1^{-}$ to F_X is in the normal region of the curve, incorporation of a quinone with a higher $\Delta G°$ value will result in an increased rate of electron transfer and if the rate is in the inverted region of the Marcus curve, the rate will decrease. The room temperature spectrum of AQ gives us our answer.

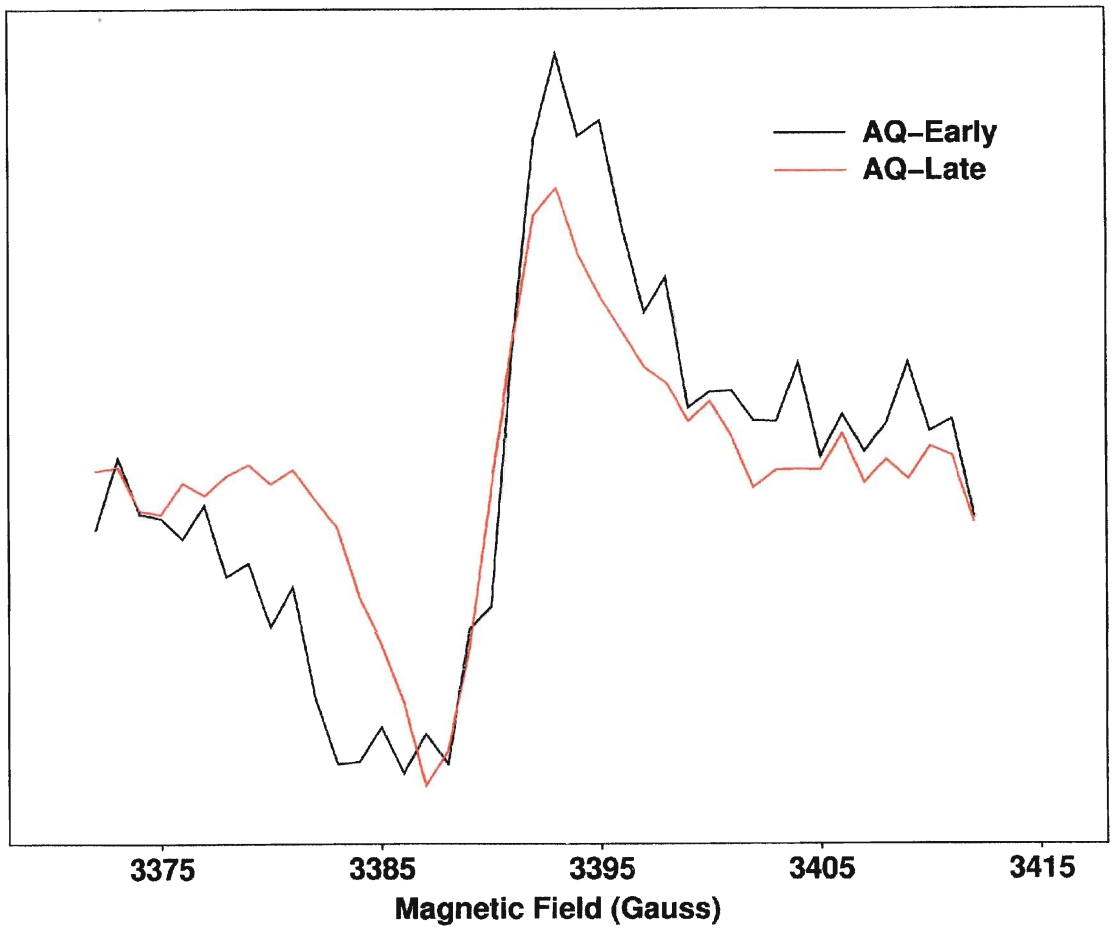

Figure 3-20: Room temperature EPR spectrum of PSI with AQ

In this figure, 'AQ-early' is a boxcar spectrum taken from 120-140. The spectrum labeled 'AQ-late' is a boxcar from 180-250. The early (black) and late (red) spectra both have an overall pattern of Emission/Absorption. The E/A/E pattern seen at low temperature has vanished. The contribution to the early spectrum from the quinone at the low field end (~3385 Gauss) is vanishing with time. This spectrum indicates that electron transfer from anthraquinone to F_X is occurring and it seems to be occurring on a faster timescale than that in native PSI. This suggests that the rate of electron transfer from A_1 to F_X is in the normal region of the Marcus Curve.

Summary of Results

Table 3-2: Location of side chains, orientation of head group and effect on the rate of electron transfer

Quinone	Location of side chains(X-band Spectrum)	Hyperfine Splitting	Headgroup Orientation (Q-Band Spectrum)	Rate of Electron Transfer
NQ	Symmetric molecule	Not visible	Same as wt	Slower than wt
MNQ	Meta to H-bond	1:3:3:1	Same as wt	Slower than wt
ENQ	Meta to H-bond	1:2:1	Same as wt	Slower than wt
OH-PhQ	CH_3 meta to H bond	1:3:3:1	n/a	Slower than wt
AQ	Symmetric molecule	Not visible	Same as wt	Faster than wt
ClMMNQ	CH_3 meta to H bond	1:3:3:1	n/a	Slower than wt
ETMNQ	CH_3 meta to H bond	1:3:3:1	n/a	n/a
BrMNQ	Cannot determine from spectrum	Cannot determine from spectrum	n/a	Slower than wt

Chapter 4

Discussion

The resilience of PSI is truly amazing, which is illustrated by the fact that it can stand up to incredibly harsh treatment with organic solvents and still have successful forward electron transfer. Even when mutations are introduced that prevent the synthesis of the secondary electron acceptor, PSI is capable of functioning by using the other available quinone, found in the plastoquinone pool of the thylakoid membrane[19]. In fact, when phylloquinone is reintroduced to extracted PSI, the hyperfine coupling, spin polarization and even the rate of electron transfer remains the same. As well, with just one exception (2-Bromo-3-Methyl naphthoquinone), PSI seems to be able to reproducibly bind a wide variety of naphthoquinone derivatives.

The extraction of phylloquinone from PSI using organic solvents is a harsh but effective method. Although this procedure does remove a significant number of chlorophyll and carotenoid molecules along with phylloquinone (See Appendix 1 for optical spectra) this has no detectable effect on the electron transfer to A_1 after phylloquinone is reintroduced to the extracted PSI. This is demonstrated both by the low temperature X band EPR spectrum that shows the hyperfine coupling is identical to intact PSI and by the room temperature data that shows the rate of forward electron transfer is identical for whole cells, isolated PSI and extracted PSI incubated with phylloquinone. One side effect of the extraction procedure is that a portion of the reaction centres do stop working. The result is a reduction in the signal to noise ratio of the spectrum following extraction and incubation; however, the presence of the nonfunctional PSI doesn't interfere with the spectra obtained.

There is some question about the structural features of phylloquinone that are responsible for its binding affinity for the A_1 site. It is known that there is a hydrogen bond to the backbone of leucine residue A722 (in the A branch) and B706 (in the B branch) to the carbonyl oxygen in position 1 of phylloquinone, but not to the carbonyl oxygen in position 4. This bond acts as an electron withdrawing group and increases the electron density at the 3 position of the ring, *meta* to the hydrogen bond. By examining the hyperfine coupling pattern of non-native quinones we can determine the position of the side chain. Previous studies had shown that when a mutation was introduced (*men*G) that prevented the methyl group from being attached during the biosynthesis of phylloquinone (making 2-phytyl-1, 4-naphthoquinone, PNQ) the quinone was still oriented in the same way as phylloquinone[28]. This was demonstrated by the

Emission/Absorption pattern that indicates g_{XX} is parallel to z_d and strong hyperfine coupling to the proton on the ring in the 3-position of PNQ[27, 28]. This result suggested that it was the phytyl tail and hydrogen bond that were responsible for the orientation of phylloquinone in the A_1 site. We selected a series of 2-alkyl 1, 4-naphthoquinones in order to determine if all monosubstituted naphthoquinones would be positioned with their side group in the position normally occupied by the phytyl tail. In contrast to the experiment with *men*G mutants, the series of experiments we performed with ethyl- and methyl- naphthoquinone revealed the importance of the methyl group for proper orientation in the A_1 site. 2-methyl-1, 4-naphthoquinone (MNQ) exhibited a methyl hyperfine coupling pattern, indicating that the methyl group was in the same position as the methyl group of phylloquinone in the A_1 site. The hfs seem with ethyl naphthoquinone indicated that the ethyl group is incorporated in the location normally occupied by the methyl group. Surprisingly, even when naphthoquinones with a single alkyl side chain of up to 6 carbons are incorporated into PSI, the orientation remains the same as that of intact Photosystem I, but with the single side chain in the position of the 3-methyl group of phylloquinone (Pushkar *et al.*, unpublished data, 2002). One might expect that methyl-naphthoquinone would have the methyl group in the same position as phylloquinone, but size restrictions would mean that naphthoquinones with longer side chains would have the side chain forced into the position of the phytyl tail in native PSI[27]. In the case of 2-ethyl-1, 4-naphthoquinone our results show strong hyperfine coupling to the CH_2 group of the ethyl side chain. This indicates that the side chain is located in the position *meta* to the hydrogen bond to the protein backbone. Though we cannot state without a doubt that there is a hydrogen bond from the carbonyl group of the quinone to

Leucine A722 and B706, it is most likely the case. If the hydrogen bond is present, the position of the ethyl side chain must be in the same location as the methyl group of phylloquinone in native PSI in order to exhibit the strong hyperfine splitting. At this point it is not clear why the non-native quinones would all be incorporated in the binding site with their side chain in the position of the methyl group.

The shape of the low temperature X band spectrum of ethyl naphthoquinone indicates that there is strong hyperfine coupling to the ethyl side chain. Deuteration experiments demonstrated that this coupling is to the methylene group of the ethyl side chain. The pattern with intensities of 1:2:1 shows that these two protons are equivalent for if they were not equivalent we would see a pair of doublets rather than the 1:2:1 pattern. To determine the position of the side chain protons, we must find the situation where the two protons are equivalent. The value of the isotropic coupling constant is proportional to the spin density of the ring carbon, (ρ_c^{π}) and to $\cos^2\theta$, given by the following equation[27].

$$a_{iso}(H_\beta) = \rho_c^{\pi}\,(B_0 + B_2 \cos^2\theta) \qquad \textbf{Equation 4-1}$$

Where θ is the angle between the C-C bonds and the C-H bonds and the p_z orbital[27]. The values for B_0 and B_2 are constants with values of 9 MHz and 122 MHz, respectively[27]. For ENQ, where we see two equivalent protons, the angle θ must be the same[27]. There are two points where this can occur, shown in the following figure.

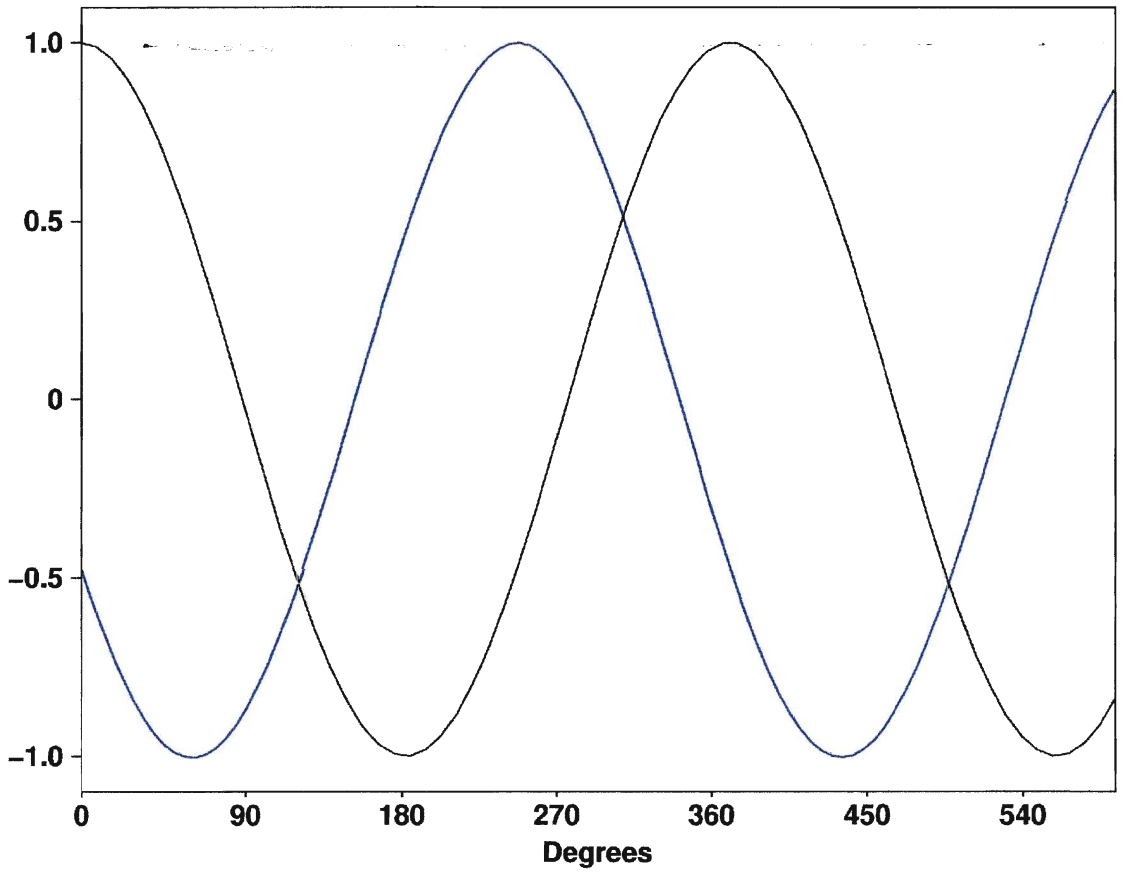

Figure 4-1: Cosine curves for equivalent protons

This shows that there are two possible positions where the protons are equivalent (i.e., where the curves cross). This corresponds to the C-C bonds being in the same plane as the naphthoquinone ring, where the C-H bonds have a value of $\theta = 30°$ or one of the C-H bonds is outside the plane and the C-H bonds have a value of $\theta = 60°$ [27]. The question to be answered is what position is more likely? If we assume that the spin density at the carbon *meta* to the hydrogen bond (where the ethyl group is bonded) is the same as in native PSI, only the case where the C-C bond is in the plane of the ring makes sense[27]. In order for the out of plane configuration to occur, the spin density would have to be three times larger than in native PSI[27]. Since we are merely replacing a methyl group with an ethyl group it is not likely that the spin density would be that much larger. Therefore,

although the out of plane conformation cannot be ruled out, the most probable orientation is in the plane, with the protons are straddling the ring[27].

These results suggest that the methyl group of phylloquinone plays a significant role in determining the proper orientation of the quinone in the A_1 site. The next logical question is, if the absence of the phytyl tail does not affect the orientation of the quinone, why does nature go to the trouble of synthesizing it? Our findings suggest that the methyl group is significant, but what should we make of recent experiments with 2-phytyl-1, 4-naphthoquinone showed that it also has the correct orientation[27, 28]? The answer may be related to the midpoint potential of the quinone and its effect on the rate of forward electron transfer.

Hydroxy-phylloquinone is made by replacing the double bond in the phytyl tail of phylloquinone with a hydroxy group. These experiments allow some insight into the effect of the double bond of the phytyl tail, by examining the effect on the EPR spectrum when it is absent. The low temperature X band EPR spectrum looks identical to that of native PSI, revealing that the presence or absence of the double bond, being further down the chain, has very little effect on the hyperfine coupling. However, the rate of forward electron transfer is slowed, to the point where we cannot determine if there is electron transfer to F_X. This is not due to the extraction procedure, since the control experiments indicated that the reconstituted sample containing phylloquinone had the same rate of electron transfer as intact PSI. The shape of the low temperature spectrum is consistent with the spectrum of intact PSI, where the hyperfine coupling pattern is due to the methyl group, and the contribution to the coupling by the phytyl tail is seen only in a blurring of the 1:3:3:1 quartet pattern.

When 1, 4-naphthoquinone is incorporated into PSI, the results are variable. Experiments have been performed where the same technique was used on the same species of cyanobacteria, and a different orientation was obtained in each case. One possible explanation is because of the small size of this quinone. 1, 4-naphthoquinone is the head group of phylloquinone, where the methyl group and phytyl tail have been replaced with protons. This could give the quinone some flexibility in the binding site, allowing for a distribution of orientations. Or, the quinone could have weaker binding to the protein[32]. However, recent findings have shown something very interesting: it appears that the orientation of napthoquinone in the A_1 site depends on the method of incubating the quinone (van der Est, unpublished results). This is a reminder of the importance of ensuring that the method of sample preparation is not affecting experimental results.

Incorporation of anthraquinone into the A_1 site gives some remarkable results. Despite the presence of a ring on the naphthoquinone head group, the orientation in the binding site remains the same as in native PSI. Room temperature EPR experiments showed that forward electron transfer is still occurring, and in fact, the rate of electron transfer to the iron sulfur cluster has increased. Recent temperature dependence experiments using PSI incubated with AQ suggest that the rate of electron transfer from A0 to A1 has slowed (Pushkar, unpublished results). This is most likely related to the more negative midpoint potential of AQ compared to phylloquinone.

Results from low temperature X band EPR experiments using disubstituted quinones that are similar in size to those of phylloquinone resulted in similar spectra as those of the monosubstituted quinones studied. This indicates that when these non-native

quinones are bound, the methyl group is in the same position as the methyl group in phylloquinone. When compared to the spectrum of 2-methyl-1, 4-naphthoquinone, the spectra are essentially the same, but the hyperfine splitting pattern appears to be more pronounced. This is an interesting observation, since in native PSI the presence of a side group at the 2 position causes a decrease in the resolution of the spectrum. It appears that 2-chloromethyl-3-methyl-1, 4-naphthoquinone (ClMMNQ) contributes less to the hyperfine coupling than the phytyl tail, and 2-ethylthio-3-methyl-1, 4-naphthoquinone (ETMNQ) contributes even less than ClMMNQ. The presence of the chlorine and sulfur molecules must be responsible for this effect. This could be related to the fact that alkyl groups are inductively electron donating and halogens are inductively electron withdrawing[31].

When a disubstituted quinone with a halogen attached directly to the ring is introduced into extracted PSI, it creates a very messy situation. The results indicate that the quinone is not being incorporated into the binding site in a predictable fashion. This could lead to our spectrum where the hyperfine coupling cannot be resolved, and in fact, very little can be said about the orientation. Room temperature experiments on PSI incubated with 2-bromo-3-methyl-1, 4-naphthoquinone show that there is electron transfer to the quinone despite the lack of clarity in determining the incorporation into the binding site.

Though not all of the rates of forward electron transfer have been determined, it can be stated without a doubt that forward electron transfer is occurring to the acceptor when a non-native quinone is present in the A_1 site. It has also been demonstrated using extracted PSI incubated with phylloquinone that the isolation, extraction or incubation

steps are not responsible for any change in the rate of forward electron transfer to the quinone or the iron sulfur clusters. Thus any change we see in the rate is due to the incorporation of a non-native quinone into the A_1 site. Though electron transfer is occurring, it is consistently slower than in native PSI, except in the case of anthraquinone, where it is faster.

Since anthraquinone results in faster electron transfer to the iron sulfur clusters, it might be tempting to think that it would make a better secondary electron acceptor than phylloquinone. However, the higher midpoint potential of anthraquinone also makes it harder for it to accept the electron from A_0. This appears to cause a reduction in the rate of electron transfer from A_0 to anthraquinone (Pushkar *et al.*, unpublished data). In addition, the solubility of anthraquinone is quite low, and getting it incorporated into the A_1 site is a challenge all its own.

The rate of electron transfer in PSI is not at its maximum on the Marcus curve, this was demonstrated by studies that show the temperature dependence of the rate[41]. Room temperature EPR experiments with quinones having a less negative midpoint potential have rates of electron transfer slower than that of native PSI, and the quinone with a more negative midpoint potential has a faster rate. These observations suggest that the rate of electron transfer from $P_{700}^{+}A_1^{-}$ to F_X in PSI lies in the normal region of the Marcus Curve.

Chapter 5

Conclusions and Future Work

First and foremost these experiments show the remarkable resilience of Photosystem I. Even after treatment with harsh organic solvents, removal of a vital cofactor involved in electron transfer, and introduction of a non-native replacement for A_1, PSI still exhibits forward electron transfer.

X band experiments with the series of monosubstituted naphthoquinones showed the importance of the 3-methyl side group of phylloquinone in achieving proper orientation in the A_1 site. The non-native quinones were incorporated with the single side chain in the position normally occupied by the 3-methyl group of phylloquinone, even when the length of the side chain was increased. This also appears to occur with the series of disubstituted naphthoquinones that all contained a 3-methyl group. However, it

also appears that incubation of a quinone that contains a halogen such as bromine cannot be incorporated reproducibly in the A_1 site. This was indicated both by the poor resolution of the EPR spectrum and by the difficulty in obtaining a sample that would give an adequate signal to obtain an EPR spectrum.

Q band experiments on PSI with non-native quinones revealed that all of the monosubstituted naphthoquinones were incorporated into the A_1 site with the same headgroup orientation as the native quinone. As well, an interesting result was obtained with naphthoquinone, where it appears that the technique used for incubating the non-native quinone determines whether the orientation in the binding site will be the 'correct' orientation or not. This is presumably due a loss of hydrogen bonding.

These experiments have confirmed that the rate of electron transfer is reduced with the replacement of the native phylloquinone with the series of non-native mono- and di-substituted naphthoquinones. The exception to this is that incubation with 9, 10-Anthraquinone results in an increase in the rate of electron transfer to F_X.

Future work to expand on these results includes determining the orientation of the di-substituted 3-methyl-1, 4-naphthoquinones in the A_1 site using Q Band EPR. W band EPR will give us even more information about the orientation of non-native quinones in the A_1 site. In addition, field modulation experiments at room temperature will allow the determination of the rate of back electron transfer with extracted PSI incubated with non-native quinones.

The question of whether we can improve on nature will remain unanswered until a non-native quinone that is easily incorporated into the A_1 site and will increase the rate of forward electron transfer is found. The search continues.

References

1) R. E. Blankenship. Origin and early evolution of photosynthesis. Photosynthesis Research 33: 91-111, 1992.

2) R. E. Blankenship & H. Hartman. The origin and evolution of oxygenic photosynthesis. Trends in Biochemical Sciences 23 March 1998.

3) P. Chitnis. Photosystem I: Function and Physiology. Annu. Rev. Plant Physiol. Plant Mol. Biol. 2001. 52:593-626.

4) A. Zouni, H. Witt, J. Kern, P. Fromme, N. Krauss, W. Saenger & P. Orth. Crystal Structure of photosystem II from Synechococcus elongatus at 3.8Å resolution. Nature 409, 739-743 (2001).

5) www.molecadv.com, Z scheme diagram. Govindgee, 2000.

6) W. Rutherford & P. Faller. The heart of photosynthesis in glorious 3D. Trends in Biochemical Sciences 26 6 June 2001.

7) www.jonneild.com/imagesPSII/ColourPDII/coreSml.jpg PSII structure diagram

8) www.jonneild.com/images/PSII/PSI.jpg PSI structure diagram

9) J. Hanley, Y. Deligiannakis, A. Pascal, P. Faller, A.W. Rutherford. Carotenoid oxidation in Photosystem II. Biochemistry 38 26 1999, pp 8189-8195.

10) P. Fromme, P. Jordan, N. Krauβ. Review: Structure of Photosystem I. Biochimica et Biophysica Acta 1507 (2001) 5-31.

11) J. Biggins & P. Mathis. Functional Role of Vitamin K1 in Photosystem I of the Cyanobacterium Synechocystis 6803. Biochemistry 1988, 27, 1494-1500.

12) P. Jordan, P. Fromme, H. Witt, O. Klukas, W. Saenger & N. Krauβ. Three Dimensional structure of cyanobacterial photosystem I at 2.5 Å resolution. Nature 411 21 June 2001.

13) D. Voet & J. Voet. Biochemistry 2nd Edition. John Wiley and Sons New York 1995.

17) A. Carrington & A. McLauchlan. Introduction to Magnetic Resonance with applications to chemistry and chemical physics. Harper & Row and John Weatherhill Inc. New York and Tokyo, 1967.

18) K. Brettel & W. Leibl. Review: Electron Transfer in Photosystem I. Biochimica et Biophysica Acta 1507 (2001) 100-114.

19) A. Semenov, I. Vassiliev, A. van der Est, M. Mamedov, B. Zybailov, G. Shen, D. Stehlik, B. Diner, P. Chitnis, J. Golbeck. Recruitment of a Foreign Quinone into the A1 site of Photosystem I. Altered Kinetics of electron transfer in phylloquinone biosynthetic pathway mutants studied by time-resolved optical, EPR and electrometric techniques. The Journal of Biological Chemistry. 275, 31, 2000.

20) I Sieckmann, K Brettel, C. Bock, A. van der Est & D. Stehlik. Transient Electron Paramagnetic Resonance of the Triplet State of P700 in Photosystem I: Evidence for Triplet Delocalization at Room Temperature. Biochemistry, 1993, 32, 18, 4842-4847.

21)N. Krauss, W. Hinrichs, I Witt, P. Fromme, W. Pritzkow, Z. Dauter, C. Betzel, K. Wilson, H. Witt, & W. Saenger. Three-dimensional structure of system I of photosynthesis at 6 Å resolution. Nature 361 1993.

23) www.chemistry.adelaide.edu.au/external/Soc-Rel/Content/epr.htm EPR

24) K. A. McLauchlin. Magnetic Resonance. Clarendon Press, Oxford. 1972.

25) www.chem.queensu.ca/eprnmr/EPR_summary.htm EPR

26) T. Brown, H. Lemay and B. Bursten. Chemistry: The Central Science 6th edition. Prentice Hall, Englewood Cliffs 1994.

27)Y. Pushkar, S. Zech, D. Stehlik, S. Brown, A. van der Est & H. Zimmermann. Orientation and Protein-Cofactor Interactions of Monosubstituted n-Alkyl Naphthoquinones in the A1 Binding Site of Photosystem I. J. Phys. Chem. B 2002, 106, 12052-12058.

28) Y. Sakuragi, B. Zybailov, G. Shen, A. Jones, P. R. Chitnis, A. van der Est, R. Bittl, S. Zech, D. Stehlik, J.H. Golbeck & D.A. Bryant. Insertional Inactivation of the *menG* Gene, Encoding 2-Phytyl-1,4-napthoquinone methyltransferase of *Synechocystis* sp PCC 6803, Results in the incorporation of 2-phytyl-1,4-napthoquinone into the A1 site and Alteration of the Equilibrium constant between A1 and Fx in Photosystem I. Biochemistry 2002, 41, 394-405.

29) A. van der Est. Light Induced Radical Pairs in Natural and Synthetic Photosystems studied by Transient EPR at Several Microwave Frequencies. Habilitationsschrift, 1999.

30) A. van der Est & D. Stehlik. Structural and Functional Properties of the State P+Q- from Transient EPR Spectroscopy. Springer Series in Biophysics, (1995) Springer, Berlin.

31) J. McMurry. Organic Chemistry 4th Edition. Brooks/Cole Publishing Company Pacific Grove. 1996.

32) A. van der Est, I. Sieckmann, W. Lubitz & D. Stehlik. Differences in the binding of the primary quinone acceptor in Photosystem I and reaction centres of Rhodobacter sphaeroides-R26 studied with transient EPR spectroscopy. Chemical Physics 194 (1995) 349-359.

33) J. Barber. Book Review: Throwing light on photosynthesis. Trends in Biochemical Sciences vol 27, No 8 August 2002 page 433.

34) www.csulb.edu/~bruss/courses/biol447_547/MPPlect15.htm Midpoint potential

35) R. Rustandi, S. Snyder, J. Biggins, J. Norris & M. Thurnauer. Reconstitution and exchange of quinones in the A1 site of Photosystem I. An electron spin polarization electron paramagnetic resonance study. Biochimica et Biophysica Acta, 1101 (1992) 311-320.

36) J. Biggins. Evaluation of Selected Benzoquinones, Naphthoquinones and Anthraquinones as Replacements for Phylloquinone in the A1 Acceptor Site of the Photosystem I Reaction Centre. Biochemistry 1990, 29, 7259-7264.

37) www.geocities.com/bioelectrochemistry/marcus.htm Marcus theory

38) www.life.uiuc.edu/crofts/bioph354/lect19.html Marcus theory

39) P. Joliot & A. Joliot. In Vivo Analysis of the Electron Transfer within Photosystem I: Are the Two Phylloquinones Involved? Biochemistry 1999, 38, 11130-11136.

40) www.sigmaaldrich.com Structures of Quinones used

41) E. Schlodder, K. Falkenberg, M. Gergeleit & K. Brettel. Temperature Dependence of Forward and Reverse Electron Transfer from A_1^-, the Reduced Secondary Electron Acceptor in Photosystem I. Biochemistry 1998, 37, 9466-9476.

42) R. Macomber. A Complete Introduction to Modern NMR Spectroscopy. John Wiley & Sons, Inc. New York, 1998.

43) www.shu.ac.uk/schools/sci/chem/tutorials/molspec/luminl.htm

44) G. Füchsle, R. Bittl, A. van der Est, W. Lubitz & D. Stehlik. Transient EPR spectroscopy of the charge separated state P+Q- in photosynthetic reaction centres. Comparison of Zn-substituted Rhodobacter sphaeroides R-26 and Photosystem I. Biochimica et Biophysica Acta, 1142 (1993) 23-35.

45) http://coenzymeq10.sun-cell.com

46) www.oceansonline.com/origins.htm

47) J. Golbeck. Structure and Function of Photosystem I. Annu. Rev. Plant Physiol. Plant Mol. Biol. 1992 43: 293-324.

48) A. van der Est, T. Prisner, R. Bittl, P. Fromme, W. Lubitz, K. Mobius, D. Stehlik. Time Resolved X- K- and W- Band EPR of the Radical Pair State P700+A1- of Photosystem I in Comparison with P865+QA- in Bacterial Reaction Centres. J Phys. Chem. B 1997, 101, 1437-1443.

49) S. Zech, A. van der Est, R. Bittl. Measurement of Cofactor Distances Between P700+ and A1- in Native and Quinone Substituted Photosystem I using Pulsed Electron Paramagnetic Resonance Spectroscopy. Biochemistry 1997, 36 9774-9779.

50) S. Purton, D. Stevens, I. Muhiuddin, M. Evans, S. Carter, S. Rigby, Heathcote, P. Site-Directed Mutagenesis of PsaA Residue W693 Affects Phylloquinone Binding and Function in the Photosystem I Reaction Centre of Chlamydomonas reinhardtii. Biochemistry 2001, 40, 2167-2175.

51) S. Snyder, R. Rustandi, J. Biggins, J. Norris, M. Thurnauer. Direct Assignment of vitamin K1 as the secondary acceptor A1 in photosystem I. Proc. Natl. Acad. Sci. USA. 88 pp 9895-9896, 1991.

52) A. van der Est, C. Boch, J. Golbeck, K. Brettel, P. Setif, D. Stehlik. Electron Transfer From the acceptor A1 to the Iron Sulfur Centres in Photosystem I As Studied by Transient EPR Spectroscopy. Biochemistry, 1994 33.

53) Diaz-Quinatan, A, Lielb, W, Bottin, H and Setif, P. Electron Transfer in Photosystem Reaction Centres Follows a Linear Pathway in Which Iron-Sulfur Cluster FB is the Immediate Electron Donor to Soluble Ferredoxin. Biochemistry 1998, 37, 3429-3439.

54) M. Guergova-Kuras, B. Boudreaux, A. Joliot, P, Joliot, K. Redding. Evidence for two active braches for electron in photosystem I. PNAS 2001, 98, 8 4437-4442.

55) G. Hastings, V Sivakumar. A Fourier Transform Infrared Absorption Difference Spectrum Associated with the Reduction of A1 in Photosystem I: Are Both Phylloquinones Involved in Electron Transfer? Biochemistry 2001, 40, 3681-3689.

56) C.C. Moser & P.L. Dutton. Engineering protein structure for electron transfer function in photosynthetic reaction centres. Biochimica et Biophysica Acta 1992, 1101, 171.

57) I. Sieckmann, A. van der Est, H. Bottin, P. Setif, & D. Stehlik. Nanosecond electron transfer kinetics in photosystem I following substitution of quinones for vitamin K1 as studied by time resolved EPR. FEBS Letters, 284 1 98-102.

58) M. Iwaki & S. Itoh. Reaction of Reconstituted Acceptor Quinone and Dynamic Equilibration of Electron Transfer in the Photosystem I Reaction Center. Plant Cell Physiol. 35 (7) 983-993 (1994)

59) M. Iwaki, S. Kumazaki, K. Yoshihara, T. Erabi, S. Itoh. ΔG° Dependence of the Electron Transfer Rate in the Photosynthetic Reaction Center of Plant Photosystem I: Natural Optimization of the Reaction between Chlorophyll a (A0) and Quinone. J. Phys. Chem. 1996, 100, 10802-10809.

60) M. Iwaki, S. Itoh, H. Hara, A. Kawamori. Spin-Polarized Radical Pair in Photosystem I Reaction Center that Contains Different Quinones and Fluorenones as the Secondary Electron Acceptor. J. Phys. Chem. B 1998, 102, 10440-10445.

61) A. Morris, S. Snyder, Y. Zhang, J. Tang, M. Thurnauer, P. Dutton, D. Robertson, M. Gunner. Electron Spin Polarization Model Applied to Sequential Electron Transfer in Iron-Containing Photosynthetic Bacterial Reaction Centres with Different Quinones as QA. J. Phys. Chem. 1995, 99, 3854-3866.

62) R. Silbey & R. Alberty. Physical Chemistry 3rd Edition. John Wiley & Sons Inc New York 2001.

63) R. Rustandi, S. Snyder, L. Feezel, T. Michalski, J. Norris, M. Thurnauer & J. Biggins. Contribution of Vitamin K1 to the Electron Spin Polarization in Spinach Photosystem I. Biochemistry 1990, 29, 8030-8032.

64) G. Rodgers. Introduction to Coordination, Solid State, and Descriptive Inorganic Chemistry. McGraw-Hill, Inc. New York, 1994.

Appendix 1: Optical Spectra of Extraction Supernatant

ATI UNICAM - UV/VISIBLE VISION SOFTWARE V3.00

Operator Name	(None Entered)		
Department	Chemistry	Date of Report	6/23/96
Organisation	Brock University	Time of Report	14:58:03
Information	(None Entered)		

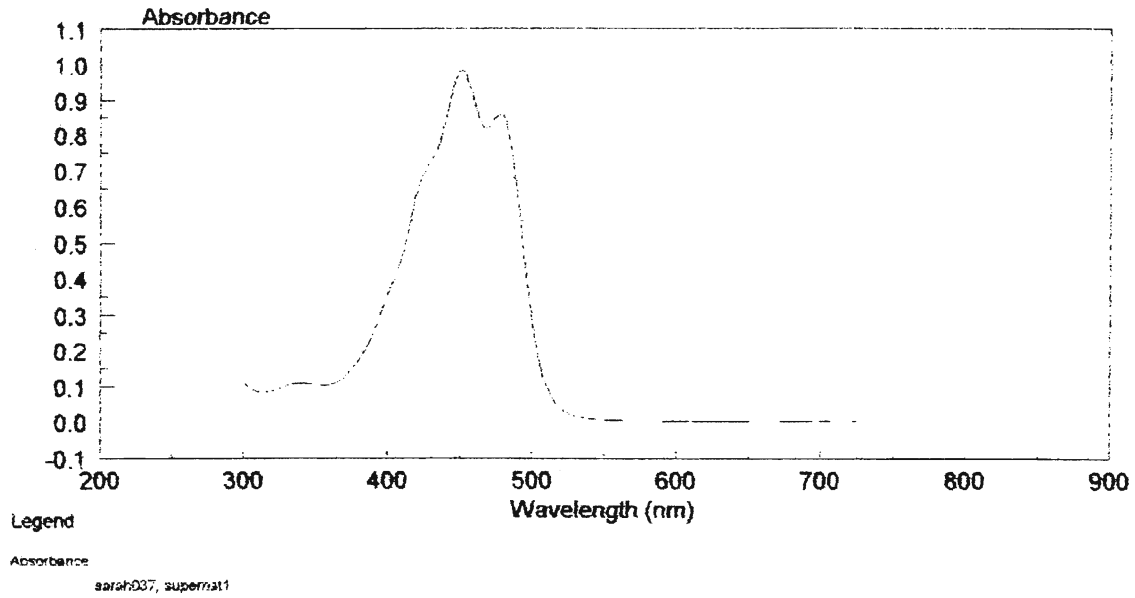

Optical Spectrum of the supernatant of PSI extracted with hexane

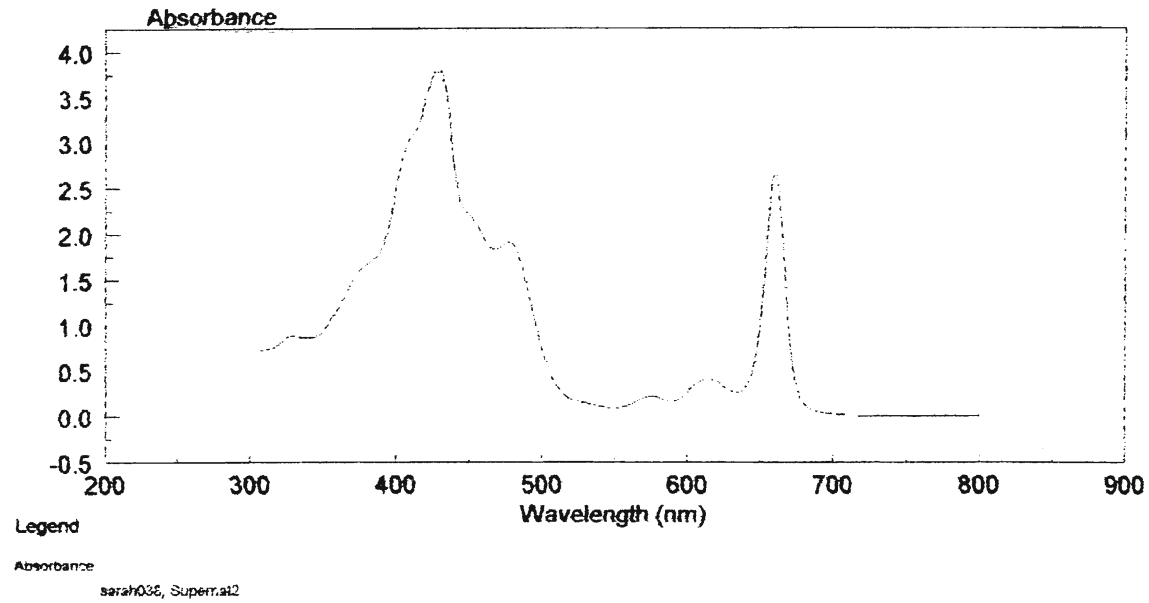

Optical spectrum of supernatant from the first Hexane-Methanol extraction

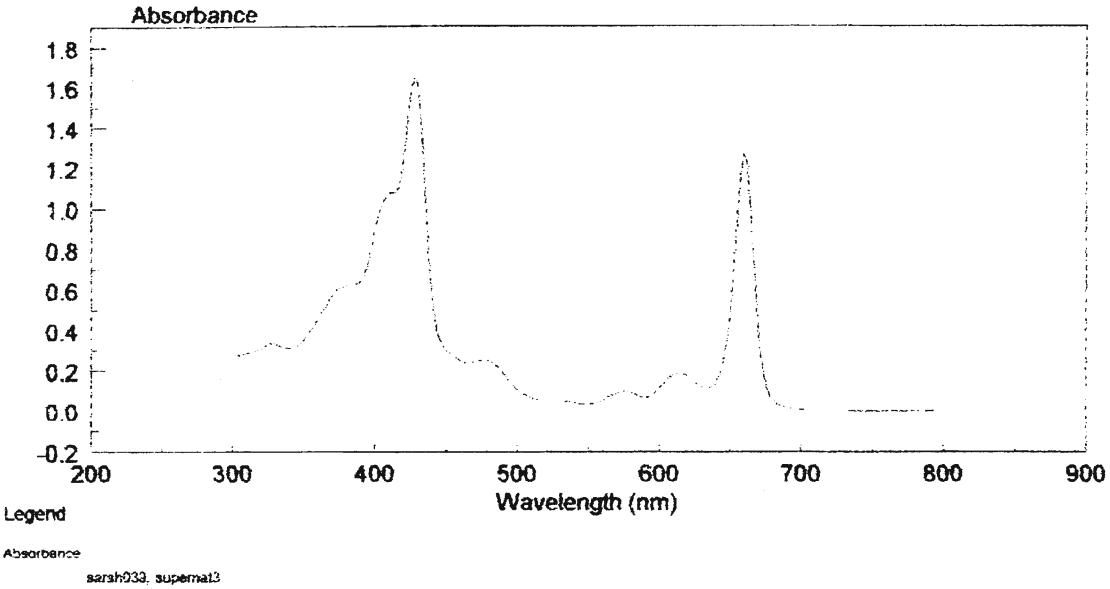

Optical spectrum of supernatant from the second Hexane-Methanol extraction

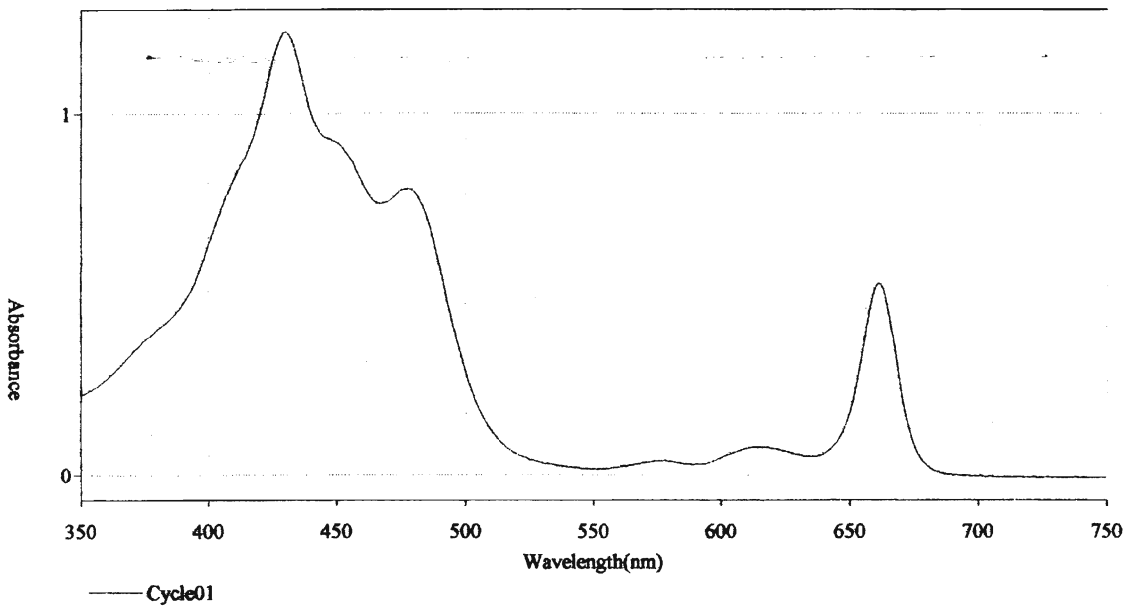

scan001,SN2,Cycle01
Description PSI Extraction supernatant in hexane with 0.5% Methanol (2nd extraction)
Date Collected 9/24/02 Time Collected 12:10:01

Optical spectrum from first extraction with Hexane-Methanol

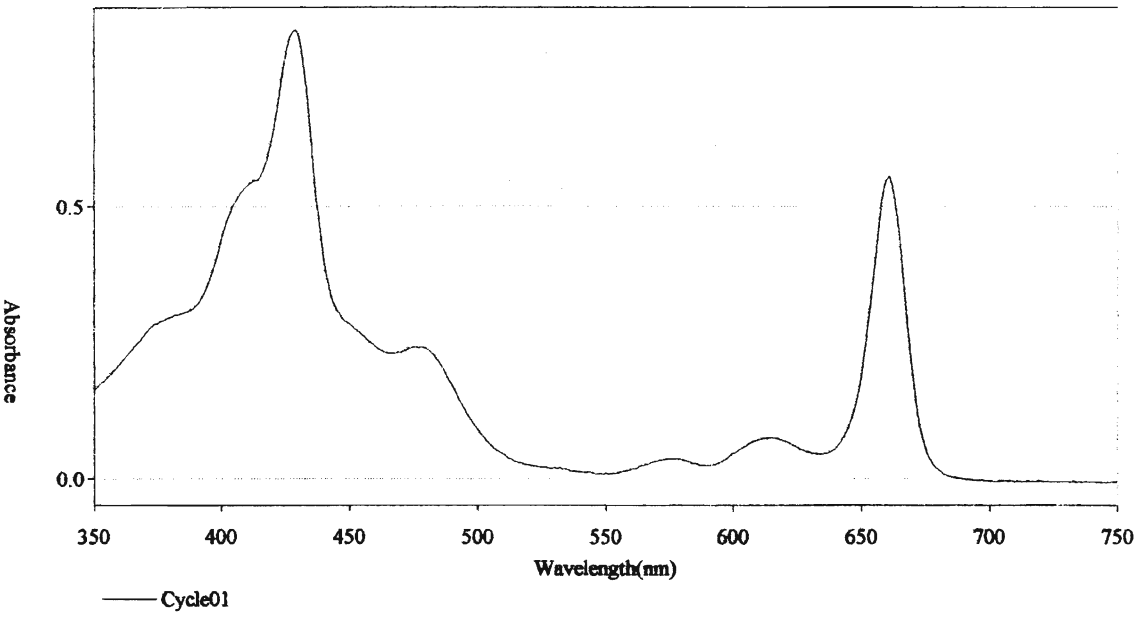

scan002,SN3,Cycle01
Description PSI 3rd extraction using hexane with 0.5% methanol
Date Collected 9/24/02 Time Collected 12:18:02

Optical spectrum from second extraction with Hexane-Methanol